Tissue specificity of MMP gene expression and secretion in Tuberculosis

Sara Sofia dos Santos Brilha

Imperial College London

Department of Medicine

2015

"(...) All our science, measured against reality, is primitive and childlike and yet it is the most precious thing we have."

Albert Einstein (1879-1955)

Abstract

In tuberculosis (TB), matrix metalloproteinases (MMPs) have a major role in tissue destruction and cavitation. The composition of each extracellular matrix (ECM) gives specificity to tissues and is important in control of local immune responses by acting as a "molecular postcode". Hence, it is likely to have important implications in TB. During central nervous system (CNS) infection, the effect of TB on blood-brain barrier (BBB) function is unknown. I hypothesised that the ECM environment may determine the MMP response during innate immune activation in pulmonary and CNS TB. I aimed to investigate the effect of adhesion to the lung's ECM in regulation of MMP expression and activity. I also aimed to develop a BBB cellular model and investigate the role of *Mycobacterium tuberculosis* (Mtb)-driven MMP secretion on BBB function. In a model of pulmonary TB, human bronchial epithelial cells (NHBEs) and monocytes were exposed to ECM components and stimulated with conditioned medium from Mtb-infected monocytes (CoMtb) or infected with Mtb. Type I collagen (Coll-I) matrix was shown to decrease MMP-1 mRNA accumulation by 48% and collagenolytic activity compared to NHBEs in the absence of matrix. MMP-1 co-localised with integrin α2β1 resulting in enhanced cell migration in wound healing assays. In contrast, soluble Coll-I led to integrin α2β1 occupancy without clustering and caused a 7-fold increase in collagenolytic activity but decreased migration. In Mtb-infected monocytes, adhesion to ECM components increased MMP-1 secretion by over 60%. Fibronectin and Coll-I also increased MMP-10 by 55% and 90% respectively. Surface expression of integrin αVβ3 was upregulated by Mtb-infection and adhesion to Coll-I. Activation of integrin αVβ3 mimicked the effect of Coll-I MMP secretion, while its inhibition impaired monocyte migration.

CoMtb-stimulation of the BBB model decreased trans-endothelial electrical resistance from 154 ± 1.2ohm.cm^2 to 111.6 ± 4.7ohm.cm^2, while Papp increased 3-fold. Coll-IV and tight junction proteins (TJPs) degradation was also detected. MMP concentrations increased 125-fold for MMP-1 (0.35 ± 2 to 43.8 ± 5.1ng/mL) and 619-fold for MMP-9 (0.072 ± 0.014 to 44.6 ± 8.9ng/ml). Treatment with the MMP inhibitor Ro32-3555 prevented BBB disruption. Neutrophil and monocyte transmigration increased 60% and 80% respectively and returned to control levels with MMP blockade. MMP-9 was shown to be responsible for BBB disruption and its inhibition by antibodies prevented BBB disruption. The Hedgehog pathway was downregulated during infection, resulting in decrease TJPs gene expression, which contributes to BBB dysfunction.

In summary, the ECM regulates both epithelial and monocyte expression of MMP-1 via integrins signalling. In the CNS, MMP-9 drives tissue destruction and BBB disruption which may be a potential reversible event in CNS TB immunopathology.

Table of Contents

CHAPTER III: ECM MODULATION OF MTB-DRIVEN MMP EXPRESSION BY BRONCHIAL EPITHELIAL CELLS   93

List of Figures

List of Tables

List of Abbreviations

Ab   Antibody

AM   Astrocyte medium

AP-1   Activator protein 1

BBB   Blood-brain barrier

BEGM   Bronchial epithelial cell growth medium

BSA   Bovine serum albumin

CNS   Central Nervous System

Coll-I   Type I collagen

Coll-IV   Type IV collagen

CoMtb   Conditioned medium from *M.tuberculosis* infected monocytes

Cy5   Cyanine 5

CTL   Cytotoxic T lymphocyte

DAPI   4',6'-diamidino-2-phenylindole

DMEM   Dulbecco's Modified Eagle's Medium

DMSO   Dimethyl Sulfoxide

EBM-2   Endothelial basal medium 2

ECM   Extracellular matrix

EDTA   Ethylenediaminetetraacetic acid

ELISA   Enzyme-linked immunosorbent assay

ERK   Extracellular signal-related kinase

F-actin   Filamentous actin

FAK   Focal adhesion kinase

FACS	Fluorescence activated cell sorting
FBS	Fetal bovine serum
FITC	Fluorescein isothiocyanate
Fn	Fibronectin
GM-CSF	Granulocyte-macrophage colony-stimulating factor
HA	Human astrocytes
HAT	Histone acetyltransferase
HBMEC	Human brain microvascular endothelial cells
HBSS	Hank's balanced salt solution
hCMEC/D3	Immortalised Human brain microvascular endothelial cell line
HDAC	Histone deacetyl transferases
hdBSA	Heat denatured BSA
HEPES	N-2-hydroxyethylpiperazine-N'-2-ethanesulfonic acid
Hh	Hedgehog
HRP	Horseradish peroxidase
ICAM	Intercellular adhesion molecule
IL	Interleukine
IFN-γ	Interferon gamma
JAM	Junctional adhesion molecule
JNK	c-Jun N-terminal kinase
Lam	Laminin
LPS	Lipopolysaccharide
MACS	Magnetic-activated cell sorting
MAPK	Mitogen-activated protein kinase
MCP-1	Monocyte chemotactic protein-1

MDM	Monocyte derived macrophage
MDR-TB	Multidrug resistant tuberculosis
MFI	Mean fluorescence intensity
MMP	Matrix metalloproteinase
MOI	Multiplicity of infection
Mtb	*Mycobacterium tuberculosis*
MT-MMP	Membrane-type matrix metalloproteinase
NHBE	Normal human bronchial epithelial cells
NF-κB	Nuclear factor kappaB
P$_{app}$	Apparent permeability
PAR-1	Proteinase activated receptor 1
PBMCs	Peripheral blood mononuclear cells
PBS	Phosphate buffered saline
PCR	Polymerase chain reaction
Ptched	Patched-1 receptor
rhMMP	Recombinant human matrix metalloproteinase
SCUBE2	Signal peptide-CUB-EGF domain-containing protein 2
Shh	Sonic hedgehog homolog
Smo	Smoothened receptor
STAT 3	Signal transducer and activator of transcription 3
TB	Tuberculosis
TBM	Tuberculous meningitis
TEER	Transendothelial electrical resistance
TEM	Transmission electron microscopy
TIMP	Tissue inhibitor of metalloproteinases

TJ	Tight junctions
TJP	Tight junction protein
TNF	Tumour necrosis factor
VCAM	Vascular cell adhesion molecule
v/v	Volume to volume ratio (%)
v/w	Volume to weight ratio (%)
XDR-TB	Extensive drug resistant tuberculosis

Acknowledgements

A warm thanks to my beloved family and dearest friends. Thank you for the everlasting support and understanding. Here I express my deepest gratitude to my mother, who is my reference of strength and conduct. Thank you for always being present and, more than anybody, for always believing in me.

I wish to express my sincere gratitude to my supervisor, Professor Jon Friedland, for all the support and guidance, all the given opportunities and also for the important life lessons during these four years at the Department of Infectious Diseases and Immunity. And I also thank Professor Joanna Porter, who gave a crucial input into the project.

A kind thanks to all my colleagues. Thank you for your support, friendship and for the many conversations and meals we had together. You also had an important contribution to this moment.

Chapter I: Introduction

1. Tuberculosis: a global health emergency

Tuberculosis (TB) was declared a global health emergency by the World Health Organization in 1993 [1] and still remains the second leading cause of death by an infectious agent. Annually, it is estimated that there are 8.6 million new cases and 1.3 million deaths caused by TB[1]. In the 90s, the first cases of multidrug resistant TB (MDR-TB) and, later, extensive drug resistant TB (XDR-TB) were reported [2], and we still continue to witness a rise in these cases, with 94,000 cases of MDR-TB cases reported in 2012 and 92 countries reporting XDR-TB [1].

The majority of TB cases occur in Africa, South/ South-East Asia, Eastern Europe and Central/ South America [1]. In these resource challenged settings, it is difficult to comply with the long treatment regimen due to lack of availability of all drugs and also limited availability of drug sensitivity testing. Furthermore, treating drug resistant TB is expensive and complicated, involving drugs with serious side effects and limited efficacy [3].

Although only accounting for 1% of all cases, TB of the central nervous system (CNS) is a highly devastating form of the disease and is associated with high mortality and neurological morbidity [4]. CNS TB has a higher incidence in children and human immunodeficiency virus-infected individuals [5,6]. CNS TB manifests itself primarily as tuberculous meningitis (TBM) and less commonly as tubercular encephalitis, intracranial tuberculoma, or a tuberculous brain abscess [6].

New therapeutic approaches which shorten treatment duration of TB and limit tissue destruction are clearly needed, as well as new approaches for vaccine development that allow the creation of a vaccine that confers long-term protection to *Mycobacterium tuberculosis* (Mtb) infection.

2. Pathogenesis of tuberculosis

The Mtb infection cycle is usually initiated with inhalation of mycobacteria aerosilised by a patient with active pulmonary disease. Mtb reaches lower sections of the lung and is phagocytosed by resident alveolar macrophages, which in turn will release cytokines (IL-6, TNF-α, IL-1β) to recruit and activate blood monocytes, neutrophils and dendritic cells, forming the *Ghon* focus (primary lesion). At this initial stage, the destruction of Mtb will depend on the microbicidal capacity of host macrophages and virulence factors of the engulfed mycobacteria [7]. If macrophages fail to clear the infection, mycobacteria will grow exponentially and blood-derived macrophages will accumulate. Neutrophils also have the capacity to kill internalised mycobacteria and may also have an important role at this stage [8]. Although not well understood, during this process, mycobacteria may disseminate, either freely or inside infected phagocytes, to local lymph nodes and the bloodstream, most frequently to highly oxygenated regions such as the brain.

After adaptive immunity recruitment and activation, CD4+ T lymphocytes proliferate within the early lesion and secrete cytokines, mainly INF-γ, which stimulates macrophages to destroy the intracellular mycobacteria (Fig. 1). Nevertheless, the adaptive immune response is not able to induce sterilizing immunity [9]. These events lead to the cessation of Mtb exponential growth, both intracellularly and extracellularly, due to the formation of central solid necrosis, rich in lipids and derived from dead macrophages, which inhibits Mtb extracellular growth. At this stage, infection may become stationary or dormant, depending on a complexity of host immune and Mtb virulence factors, which dictate whether infection is contained or if dessimination leads to clinical disease [7].
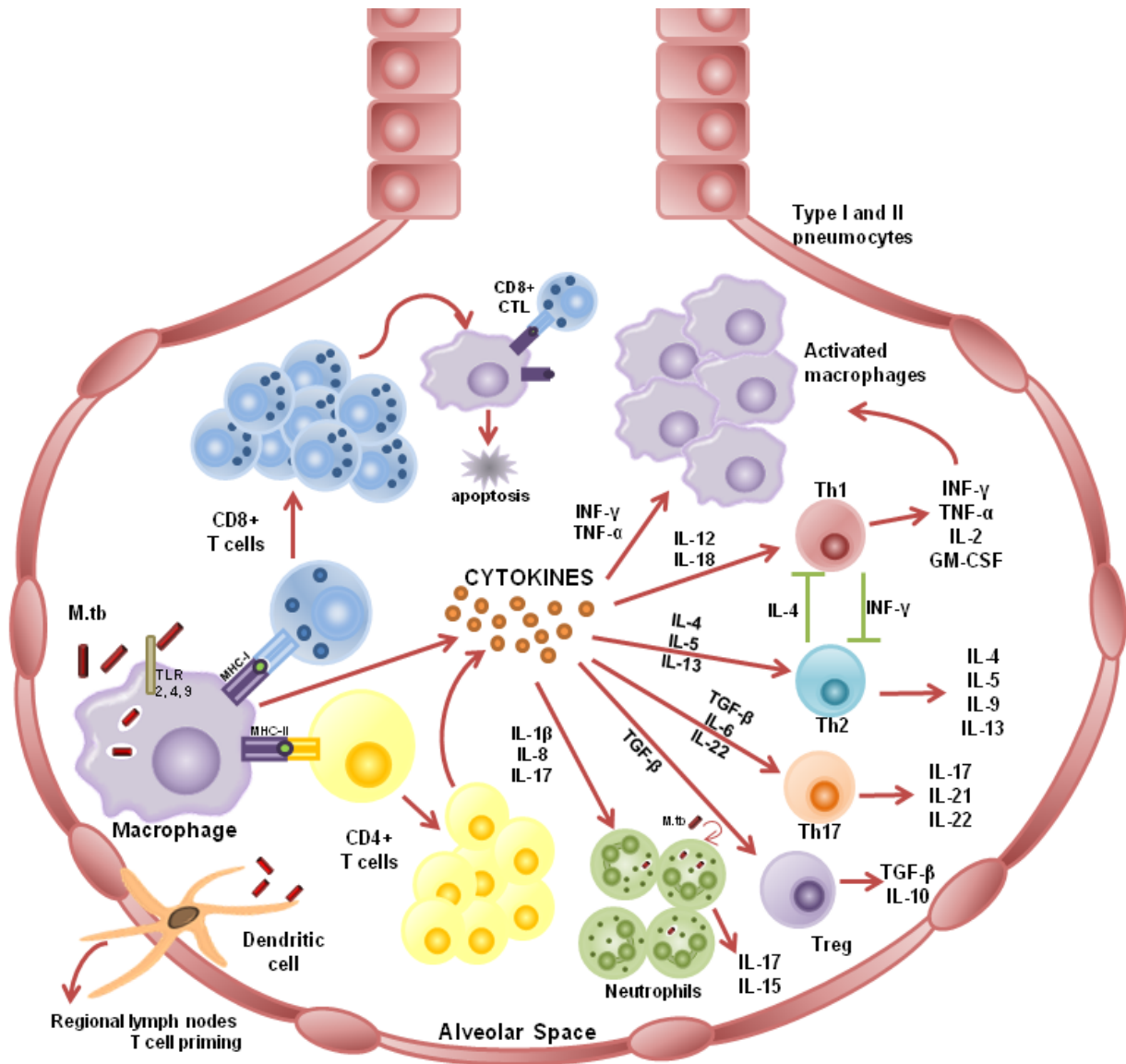
Figure 1. Representation of innate and adaptive immunity response to *Mycobacterium tuberculosis* infection.

CTL= cytotoxic T lymphocyte; GM-CSF= granulocyte-macrophage colony-stimulating factor; IL= interleukin; IFN-γ= interferon gamma; Mtb= *Mycobacterium tuberculosis*; Th1, 2, 17= T helper cell type 1, 2, 17; TGF-β= transforming growth factor-beta; TNF-α= tumour necrosis factor-alpha; TLR= toll-like receptor; Treg= regulatory T cell.

A complex interplay of host immune factors and Mtb virulence factors in the end determines whether or not the infection is contained and whether, or to what extent, the dissemination of the bacilli leads to clinical disease

When Mtb disseminates from the lung bases to the apices), it engages the host immune response to drive ECM destruction, resulting in cavities within which it proliferates exponentially. The pathogen is then transmitted to new hosts by cough aerosol generation.Cavity formation must involve the action of proteases, specifically MMPs, which are able to degrade the ECM.

In CNS TB, small tuberculous foci can form in the brain, spinal cord or meninges and the location and capacity to control these foci determines which form of CNS TB occurs. CNS tuberculosis manifests mainly as TB meningitis and less commonly as tubercular encephalitis, intracranial tuberculoma or tuberculous brain abscess [4].

The role of MMPs in pulmonary and CNS TB will be discussed in more detail in the chapters 3.3 and 3.4.

3. Matrix metalloproteinases

Humans have 23 MMPs, and their activity under basal conditions is considered low in most tissues. However, MMP expression can be upregulated by inflammatory cytokines, growth factors, hormones or cell to cell interactions [11]. Generally an MMP is composed of a pro-peptide domain (around 80 amino acids), a catalytic domain (around 170 amino acids), a linker peptide of variable length and a hemopexin domain (approximately 200 amino acids) (Fig. 2). Exceptions to this structure are MMP-7, -26 and -23, which lack the linker and hemopexin domains [11].
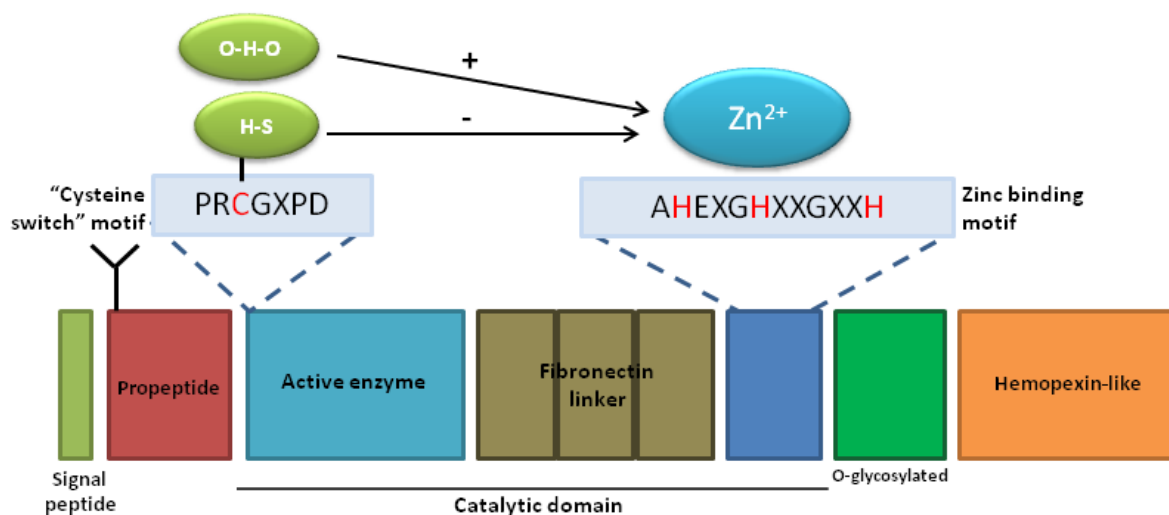
Figure 2. Matrix Metalloproteinases general structure.

Matrix metalloproteinases are generally composed of a pro-peptide domain, a catalytic domain, a linker peptide and a hemopexin domain. The pro-peptide domain is part of the "cysteine switch." It contains a conserved cysteine residue (sequence PRCGXPD) that interacts with the zinc in the active site and keeps the enzyme in an inactive form. In the catalytic domain forming the active site there is a catalytically important Zn^{2+} ion, which is bound by three histidine residues found in the conserved sequence HExxHxxGxxH. Gelatinases have fibronectin type II modules linking the zinc-binding motif to the catalytic domain. The catalytic domain is connected to the C-terminal domain by a flexible hinge or linker region. The hemopexin-like domain is thought to be involved in protein-protein interactions. In the inactive form, the SH group bound to the conserved cysteine and Zn^{2+} prevents binding of H_2O molecule to the zinc cation, which is essential for catalysis.

The "cysteine switch" in the catalytic domain and the zinc binding motif are essential structures in MMP activation. The coordination between the cystein and the zinc cation keeps pro-MMPs inactive by preventing the binding of a H_2O molecule to the zinc cation, which is essential for catalysis. The catalytic domain also contains a conserved methionine ("Met-turn"), located eight residues downstream of the zinc binding motif which forms a base to support the structure around the catalytic zinc [12].

Based on domain organization and substrate preference, MMPs have been classically grouped into collagenases, gelatinases, stromeolysins, matrilysins and membrane-type (MT-MMPs) which and are summarised in table 1. MMPs are involved in several physiological functions including tissue homeostasis, host defence and tissue repair [13]. Proteolysis of the extracellular matrix (ECM) is an important feature of tissue repair and remodelling. Cells involved in wound repair express MMPs and regulate their activity, e.g. MMP-1, -3 and -9 are involved in repair of skin and lung tissues [14,15].

Table 1- Matrix Metalloproteinases classification.

Traditional classification	Matrix Metalloproteinase	Substrates
Collagenases	MMP-1 MMP-8 MMP-13 MMP-18	Type I, II and III collagen Other ECM molecules and soluble proteins
Gelatinases	MMP-2 MMP-9	Gelatin Type IV, V and XI collagen Laminin, hyaluronan
Stromeolysins	MMP-3 MMP-10 MMP-11	Pro-MMP activation Several ECM substrates
Matrilysins	MMP-7 MMP-26	Elastin Cell surface molecules (e.g. pro-α-defensin or pro-TNF-α Other ECM substrates
MT-MMPs	MMP-14 MMP-15 MMP-16 MMP-17 MMP-24 MMP-25	Activated on the cell surface Collagenolitic activity (types I, II and III).

References: 17-22. ECM- extracellular matrix; MMP- matrix metalloproteinases, MT-MMPs- membrane-type metalloproteinases; TNF-α- tumour necrosis factor-α

3.1. Regulation of Matrix metalloproteinase expression

Since these enzymes are so efficient at breaking down tissue, MMP activity is tightly regulated. In addition to transcriptional regulation, MMPs are secreted as pro-enzymes, in which the catalytic site is occupied by a pro-peptide domain that can be enzymatically removed by cleavage by other MMPs or modified by interactions with reactive oxygen species or plasmin. They are also co-secreted with endogenous antagonists – Tissue inhibitors of Metalloproteinases (TIMPs), a family of four proteins that bind MMPs in a 1:1 stochiometry to prevent proteolytic activity [11,16]. MMP activity is also regulated by compartmentalisation, for example MMP-1 binds to integrin α2β1 restricting its activity to the pericellular space [17].

There are three groups of MMP gene promoters. The first group, which includes MMP-1, -3 and -9, is composed of a TATA box at -30 base pairs (bp) and an AP-1 binding site at -70bp. The second group, which includes MMP-8 and -11, also has a TATA box but no proximal AP-1 binding site. Finally, the third group, which includes MMP-2, has multiple transcriptional start sites, no TATA box and is constitutively expressed [18]. Therefore, MMP expression is cell, tissue and stimulus dependent.

Key transcriptional regulators of MMPs include nuclear factor-κB (NF-κB), AP-1 and signal transducer and activator of transcription 3 (STAT3) pathways [19,20]. Due to the AP-1 binding site, group 1 promoters are inducible by cytokines and growth factors, through extracellular signal-regulated kinase (ERK) 1/2, c-Jun N-terminal kinase (JNK), and p38-MAPK-signaling pathways [21-24]. Also, the MMP-9 promoter contains a consensus binding site for NF-κB at -600bp and therefore its expression is

inducible by TNF-α [25,26]. There are no NF-κB binding sites in the MMP-1 and -3 promoters and yet their expression is also inducible by NF-κB, either via other transcription factors or by non-canonical NF-κB sites [27,28].

Epigenetic mechanisms, including DNA methylation and covalent modification of histones, are also emerging as key regulators of MMP gene expression. Methylation and acetylation of histones can activate or repress transcriptional activation by regulating the access of transcriptional machinery to coding sequences [29]. Most studies in histone modifications on MMP gene expression were focused on histone acetylation, a process that is regulated by two enzymes: histone acetyltransferases (HATs) and histone deacetyl transferases (HDACs). The inhibition of HDACs by chemical inhibitors or siRNA to decrease methylation-associated gene silencing revealed that inhibition of HDACs induced MMP-1, -2, -9 and -13 gene expression [30-32]. However, in some cases HDAC inhibitors caused a decrease in MMP levels. HDAC inhibitors have been shown to block MMP-9 gene expression in several cancer cell lines (e.g. liver cancer cells, neuroblastoma, human gastric cancer cells, A549 lung adenocarcinoma cells), leading to a reduced invasive phenotype [33-36].

3.2. Matrix metalloproteinases in homeostasis and inflammation

3.1.1 Cell migration

Cell migration in the ECM requires MMP proteolytic activity which in turn is controlled by association with cell surface receptors, restricting MMP activity to the pericellular space. Secreted MMP-1 binds to integrin α2β1, while MMP-2 binds to integrin αVβ3 and MMP-9 to CD44 and β1 and β5 integrin subunits [17,37-40]. The localized ECM proteolysis occurs in specialized cell receptor-ECM contacts, (e.g. lamellipodia, filopodia, podosomes) where MMPs act in tight coordination with the cell migration machinery. MMPs also facilitate cell migration by generating chemokine gradients to direct cell migration. ECM fragments generated by MMP proteolysis have also been shown to have chemotactic properties [41].

MMP-1 is required for alveolar and keratinocyte cell migration and proliferation [17,42], while MMP-12 is required for macrophage influx in mouse models of emphysema [43] and MMP-14 is required for monocyte migration[44]. MMP-3 is required for neutrophil recruitment to the airways in mouse models of acute lung injury [45].

3.1.2. Cytokine and chemokine processing

Besides degrading components of the ECM, MMPs may act on a variety of non-matrix substrates. *In vitro*, MMP-1,-2, -3 and -9 are able to activate TNF-α [46], MMP-2, -3 and- 9 can activate pro-IL-1β, which in turn also degrades the active form IL-1β [47,48]. In addition to cytokines, MMPs also processes chemokines. MMP-9 processes CXCL8 (IL-8) to a fragment with enhanced chemotactic capacity [49]. Conversely, CCL7 (MCP-3) is cleaved into an inactive form by MMP-2, and the CCL7 fragment acts as a receptor antagonist [50]. Table 2 summarises chemokines that are known to be processed by MMPs (work reviewed in [51]).

Table 2- Proteolytic processing of human chemokines by MMPs.

Function	Chemokine	MMP
Activation	CXCL8/IL-8	MMP1, -8, -9, -13, - 14
	CXCL5	MMP-1, -8
Inactivation	CXCL1	MMP-9, -12
	CXCL2	MMP-12
	CXCL3	MMP-12
	IL-8	MMP-12
	CXCL4	MMP-9
	CXCL5	MMP-9, -12
	CXCL5	MMP-1, -9, -12
	CXCL7	MMP-9
	CXCL9	MMP-7, -8, -9, -12
	CXCL11	MMP-7, -9
	CXCL12	MMP-1, -2, -3, -9, - 13, -14
	IL10	MMP-7, -8, -9, -12
Antagonist	CCL2/MCP-1	MMP-1, -3, -8, -12
	CCL8/MCP-2	MMP-1, -3, -12
	CCL7/MCP-3	MMP-1, -2, -3, -12, - 13, -14
	CCL13/MCP-4	MMP-1, -12
	CXCL11	MMP-8, -12

Reviewed in Biochim Biophys Acta. 2010;1803(1):39-54 [51].

3.1.3. Regulation of intracellular signalling

MMPs can also mediate intracellular signalling. For example MMP-1 can cleave the extracellular domain of proteinase activated receptor 1 (PAR-1), which activates a G-protein dependent signalling cascade and calcium flux [52]. Furthermore, emerging evidence indicates that intracellular MMPs also have roles in cell signalling [53]. MMP-2 and MMP-3 have nuclear localisation sequences [54,55] and the presence of these MMPs in the nucleus has been associated with apoptosis [55,56]. A study on dopaminergic neurons also indicates a pro-apoptotic role for active intracellular MMP-3, by activation of caspase-3. In opposition, MMP-1 appears to prevent apoptosis [57]. MMP-1 association with the nucleus and mitochondria also appears to have a role in regulation of cell growth and may contribute to tumour cell survival [58].

Transcription factor-like properties have also been attributed to MMPs. MMP-3 has been shown to be a *trans* regulator of connective tissue growth factor (CCN2/CTGF) by interacting with heterochromatin protein-γ [59]. In a viral infection model, MMP-12 secreted by macrophages was transported to coxsackievirus type B3-infected HeLa cells and translocated to the nucleus, enhancing transcription of IκBα which in turn is necessary for export of IFN-α from virus-infected cells [60].

3.1.4 Activation of antimicrobial peptides

In mice, MMP-7 is key in activating α-defensins in the gut, which was demonstrated by the impaired bacterial clearance from the gut in MMP-7 deficient mice [61]. MMP-7 also appears to play a similar role in the airways, since its expression has been shown to be upregulated in respiratory epithelial cells in cystic fibrosis [62]. Also, bacterial products have been shown to drive MMP-7 secretion in respiratory epithelial cells [63].

3.1.5. Pathogenic functions of MMPs

Although MMPs are crucial for tissue homeostasis and inflammatory response, excess MMP activity is also involved in immunopathological conditions such as inflammatory diseases and cancer leading to marked tissue destruction as well as cancer progression. In myocardial infarction, activation of latent collagenases causes rapid degradation of the myocardial matrix, followed by *de novo* synthesis of MMP-1, -2 and -9 leading to extensive matrix breakdown [64]. The collagenases MMP-1 and -13 have predominant roles in rheumatoid arthritis (RA) and osteoarthritis. MMP-1 is secreted mainly by synovial cells that line the joints, while MMP-13 is produced by chondrocytes in the cartilage [65]. Extensive studies have been done on the role of MMPs in cancer cell invasion and metastasis [66-68]. Upregulation of MMP expression in benign cancer cells leads to acquisition of malignant properties, while blockade of MMP activity reduces the aggressiveness of malignant cells [66].

MMPs can also be upregulated in infection and can be either protective or deleterious to the host. For example, MMP-2 and 9 have a protective role in the immune response against *Streptococcus pneumoniae* infection [69], while MMP-9 was found to be essential for resistance to *Escherichia coli* peritonitis [70]. In contrast, in malaria, hemozoin induces MMP-9 by monocytes and endothelial cells [71-74] and serum MMP-8 and TIMP-1 have been associated with disease severity [75]. In human cytomegalovirus (HCMV) infection, MMP-9 expression by macrophages appears to be downregulated by an immediate-early or early viral gene product. HCMV was shown to decrease MMP-9 activity in infected cells, which was suggested to contribute to the development of vascular diseases [76].

3.3. Matrix metalloproteinases in pulmonary tuberculosis

In TB, ECM breakdown has been considered a part of the caseous necrosis process [77]. However caseation and ECM destruction are likely to be distinct processes since the collagen network can only be degraded by proteases [78]. ECM destruction is essential since it creates an immunoprivileged site within which mycobacteria can proliferate and spread to new hosts. Several studies have implicated MMP upregulation in TB tissue destruction. MMP expression (namely MMP-1, -3, -9 and -7) has been localized within TB granulomas [19,79,80] and is associated with disease severity [81]. Moreover, in mice models, Mtb infection upregulated MMP-9 [82,83] and one study performed with human MMP-1 expressing transgenic mice indicated that MMP-1 upregulation with Mtb infection is the main MMP responsible for tissue destruction in pulmonary granulomas [84]. In TB patients, including patients with TB/HIV co-infection, MMP-1 concentrations in plasma and sputum were increased compared with controls and associated with tissue destruction [85].

Direct Mtb infection of monocytes/macrophages or neutrophils induces MMP gene expression and secretion. However, these are not the only source of MMPs in TB. It is likely that cell-cell interactions, involving phagocytic and stromal cells such as respiratory epithelial cells, amplify this signal, constituting the main route that drives MMP secretion in TB (Fig. 3) [86].

Our group has an established *in vitro* model of pulmonary TB, where responses to Mtb by respiratory epithelium, monocytes, neutrophils and macrophages can be studied, as well as cell-cell networks. Primary human bronchial epithelial cells (NHBEs) and monocytes are stimulated with conditioned medium from Mtb-infected monocytes (CoMtb), to mimic the effect of Mtb infection on uninfected cells. Previous work from our group has demonstrated that CoMtb contains both host derived cytokines and chemokines (e.g. TNF-α, IL-1β, IL-6) and pathogen-derived antigens and lipids [80]. Also it was reported that TNF-α in CoMtb is the main inducer of MMP-9 by monocytes, while in NHBEs MMP-9 synergistic upregulation is observed with TNF-α and soluble Mtb antigens but not lipoarabinomannan [80]. However, in NHBEs, MMP-9 secretion is independent of IL-1 and IL-6 as well as the chemokines CCL2, 3 and 5 and CXCL 8 and 12 [80].
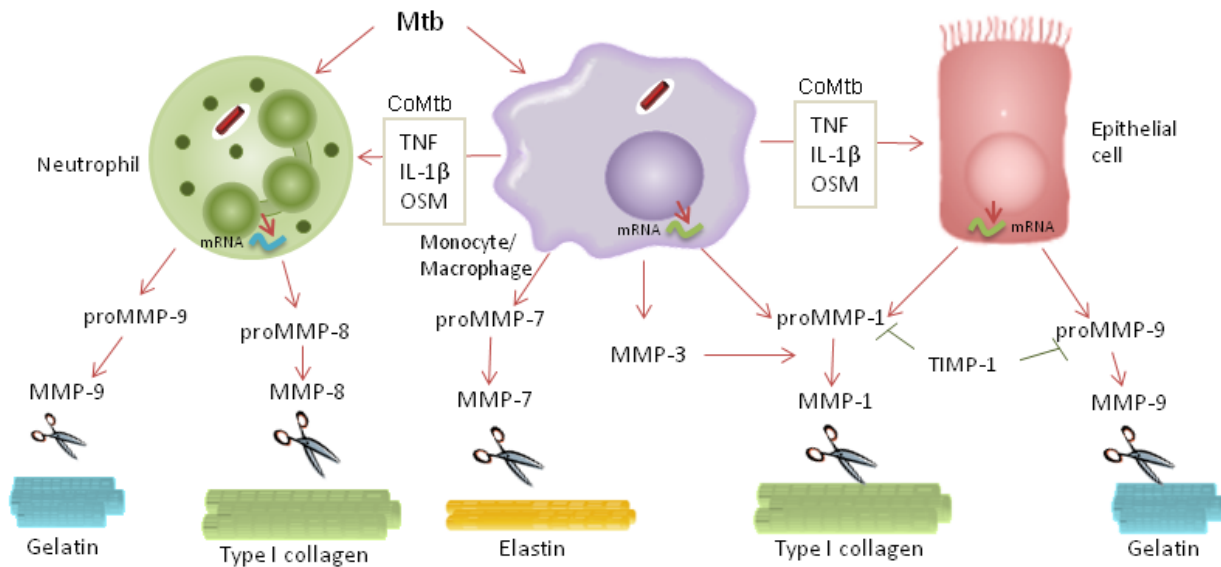
Figure 3. Cellular networks that drive matrix metalloproteinases gene expression and secretion in tuberculosis.

Leukocytes infected by Mtb will express MMPs but will also secrete cytokines and chemokines such as TNF-α, IL-1β and OSM which induce stroma and uninfected leukocytes to also express MMPs. When used in the laboratory context, the supernatant collected from infected monocytes/macrophages is denominated CoMtb. MMPs can be inhibited by specific tissue inhibitors such as TIMP-1.

CoMtb- conditioned medium from *Mycobacterium tuberculosis* infected monocytes; IL-1β- interleukin 1 beta; MMP- matrix metalloproteinase; Mtb- *Mycobacterium tuberculosis*; OSM- ocostatin M; TIMP- tissue inhibitor of metalloproteinases; TNF- tumour necrosis factor

3.4. Matrix metalloproteinases in central nervous system tuberculosis

In CNS tuberculosis, it is likely that MMPs also play a key role in immunopathology, and its pathological effect has been demonstrated in neurodegenerative disorders [87-90]. MMPs were shown to be upregulated in Mtb-infected microglial cells (MMP-1, -3 and -9) [19] and in CoMtb-stimulated astrocytoma cell lines U373-MG and U87-MG (MMP-9) [91]. MMP-2 is constitutively expressed by many cells and is regulated by pro-peptide activation [92,93]. In the CNS, MMP-2 drives neuronal apoptosis and breakdown of components of CNS ECM such as dystroglycan and laminin [94]. Due to substrate overlap, MMP-9 is also able to cleave the previous components, as well as type IV collagen, which is an important component of the basement membrane of the cerebral epithelium and endothelium and is important in maintenance of blood-brain barrier (BBB) integrity [95].

The use of steroids appear to have a beneficial effect in CNS TB which may be due in part to their influence on MMP secretion [96]. However, the link between MMP levels and the presence of BBB disruption in CNS TB has not yet been investigated.

4. The extracellular matrix

The ECM is present in a substantial part of the extracellular space. It provides a physical scaffold to the cells, segregates tissues from one another, regulates cellular communication and provides the biomechanical and biochemical properties of each organ. Therefore, the ECM plays a crucial role in tissue behaviour from morphogenesis and homeostasis to inflammation and fibrosis. The importance of the ECM became clearer with the knowledge that genetic abnormalities in matrix components results in a wide range of severe syndromes [97].

Collagens

Collagens are proteins composed of three polypeptide chains forming a triple helix, and can be divided in two classes: fibrillar (type I, II, III, V, VI, XI) and non-fibrillar collagens (type IV, VII, VIII, IX, X, XII and XIV). Other collagens have only been characterised at the genomic level and their structures remain unknown [98]. The main cell-binding site of fibrillar collagens is the triple-helical GFOGER sequence (Glycine-Phenylalanine-Hydroxiproline-Glycine-Glutamic acid-Arginine) and there is also the RGD sequence (Arginine-Glycine-Aspartic acid), which is a second integrin binding site.

The primary fibril of the lung is type I collagen (Coll-I), which provides tensile strength and is highly resistant to enzymatic degradation [13]. The alveolar wall is mainly composed of type III collagen while the basement membrane, which underlies the

alveolar epithelium and capillary endothelium, is composed of non-fibrillar type IV collagen (Coll-IV) interspersed with laminins, fibronectin, nidogen and proteoglycans [98,99].

Elastin

Elastin confers distensibility which is extremely important in several tissues such as the lung, arteries, tendons and skin [100]. Elastin is synthesised and secreted as the soluble precursor tropoelastin and cross-linked into an insoluble elastin fibre. The balance between elastin and collagen fibrils varies between tissues according to their mechanical properties.

Fibronectin

Fibronectin (Fn) is a dimeric glycoprotein that has two main forms: soluble plasma fibronectin (major component of plasma); and insoluble cellular fibronectin which binds to several ECM components and has biological effects in cell adhesion, migration and differentiation [101]. The most well characterised cell-binding domains of fibronectin are homologous polypeptide repeats –type III repeats- which contain an RGD sequence which is a cell binding site of fibronectin and also PHSRN sequence (Proline-Histdine-Serine-Arginine-Asparagine). The RGD and PHSRN sequences are both located in the molecular surface loop regions of the 9–10th type III repeat, but on opposite sides, suggesting interaction with different sites in the integrin receptor [102].

Laminins

Laminins (Lam) are trimeric proteins and form an insoluble network connected to Coll-IV, influencing cellular attachment, differentiation and migration [103]. There are five α chains (α1-α5), three β chains (β1-β3) and three γ chains (γ1-γ3) which combine to form the 18 different isoforms currently identified, but in the healthy adult lung only laminin-5 (α3β3γ2), laminin-10/11 (α5β1γ1/ α5β2γ1), laminin-2 (α2β1γ1) and laminin-8 (α4β1γ1) are present [104].

Proteoglycans

Proteoglycans are a diverse family of core proteins covalently linked to polysaccharides or glycosaminoglycans and are present in most ECMs and plasma membranes [105]. Proteoglycans can promote cell adhesion, can associate with other ECM molecules such as fibrillar collagen and fibronectin and a number can bind to a variety of growth factors, concentrating them in the local tissue. Examples of proteoglycans include aggrecan (highly present in cartilage tissue), lumican (forms a gel that aids transparency of the cornea), neurocan (surrounds nerves) and perlecan (forms gels in basement membranes).

Other components of the ECM include: glycoprotein such as nidogen (present in basement membranes) and tenascin. Hyaluronan (HA), a glycosaminoglycan, is present in connective, epithelial, and neural tissues.

4.1. Tissue specificity of the extracellular matrix

The matrix components and amounts of each component present in each ECM gives specificity to tissues. For example, the lung's ECM is rich in type I collagen, which provides tensile strength, while elastin provides distensibility [106], while the brain's ECM has a reduced number of fibrous matrix proteins [107] and is mainly composed of nets of proteoglycans, HA and tenascins, which stabilise neuronal synapses [108]. However, when cells are removed from their native matrix, differentiated cells may lose important characteristics when cultured without an adequate supportive microenvironment. Besides soluble molecular factors (e.g. growth factors or cytokines), cells are influenced by physical factors such as stress and strain and by the insoluble matrix microenvironment [109,110].

Increasing evidence indicates that, besides regulating tissue function and homeostasis, the tissue specific ECM microenvironment also plays a key role in the regulation of immune responses by acting as a "molecular postcode" that controls local immune function [111,112]. For example, specificity in chains composition of proteoglycan were seen between different tissues [113], which potentially may regulate the function of proteins, such as those that control angiogenesis and innate immunity [112].

4.2. The extracellular matrix and matrix metalloproteinases

MMPs are necessary for the normal maintenance of the ECM. In healthy tissues, the ECM is regularly remodelled and damaged proteins are removed, recycled and replaced by new proteins. However, in pathological conditions, this maintenance is disturbed and the composition and quality of the matrix is altered, which in turn may be sensed by adherent cells.

ECM remodelling is the result of multiple concurrent processes that vary according to the initiating stimulus. However the conserved key events of ECM remodelling are synthesis and deposition of matrix components and proteolytic breakdown [114]. Different proteases have been implicated in the proteolytic degradation of the ECM, with the vast majority belonging to the MMP family. MMPs can cleave practically all components of the ECM and although initially being divided into collagenases, gelatinases, stromelysins, and matrilysins, there is a high degree of overlap among MMP substrate specificity. Also, MMPs can also cleave numerous substrates that are not part of the ECM.

4.3. The extracellular matrix and integrin signalling

Cells adhere and sense the ECM environment mainly through the integrin receptors. Integrins are a family of heterodimeric transmembrane glycoproteins, with one α and one β subunit, that constitute cation-dependent receptors for components of the ECM (Fig. 4). In humans 18 α-subunits and 8 β subunits have been identified, which can form a total of 24 integrin heterodimers [115]. Important roles played by integrins have been identified in practically all aspects of cell behaviour such as migration, establishment of polarity, growth, survival, differentiation and also expression of other genes like cytokines [116-118].

Integrin adhesion to the ECM is highly dynamic with cells continuously "sampling" their pericellular environment and, therefore, integrin receptor activation is highly responsive. Integrin signalling is induced by assembly of adhesome complexes on the cytoplasmic side of the membrane. The formation of these complexes is achieved by receptor clustering, which increases avidity of molecular interactions and by induction of conformational changes in the receptors that expose effector binding sites [119]. Although models of integrin function suggest that integrin activation requires receptor extension, there is also evidence suggesting that ligand-bound integrin can adopt a bent conformation. Crystallized αVβ3 can bind a cyclic RGD peptide in the bent conformation [120] and complexes of bent αVβ3 integrin bound to fibronectin were also demonstrated [121]. In opposition, FRET-FLIM analysis of α5β1 in adherent cells showed that α5β1 integrins are extended in focal adhesions and

bent elsewhere [122]. This suggests that the mechanism of integrin activation might differ between receptor and cell type.

The binding of individual or clusters of integrins to a ligand drives an initial talin-mediated interaction between the cytoskeleton and the ECM, leading to recruitment of additional cytoskeletal and signalling proteins. Multiprotein complexes then assemble at the cytoplasmic side of the integrin cluster and these connect integrins to the actin cytoskeleton and activate signalling cascades [123]. The processes of outside-in signalling are still poorly understood. The mechanisms that trigger signalling and allow a cell to interpret the binding of different ligands are still unclear, along with those regulating the sensing of the microenvironment at the molecular level. The mechanisms of integrin-ligand engagement and signalling mediators will be further discussed in Chapter III.
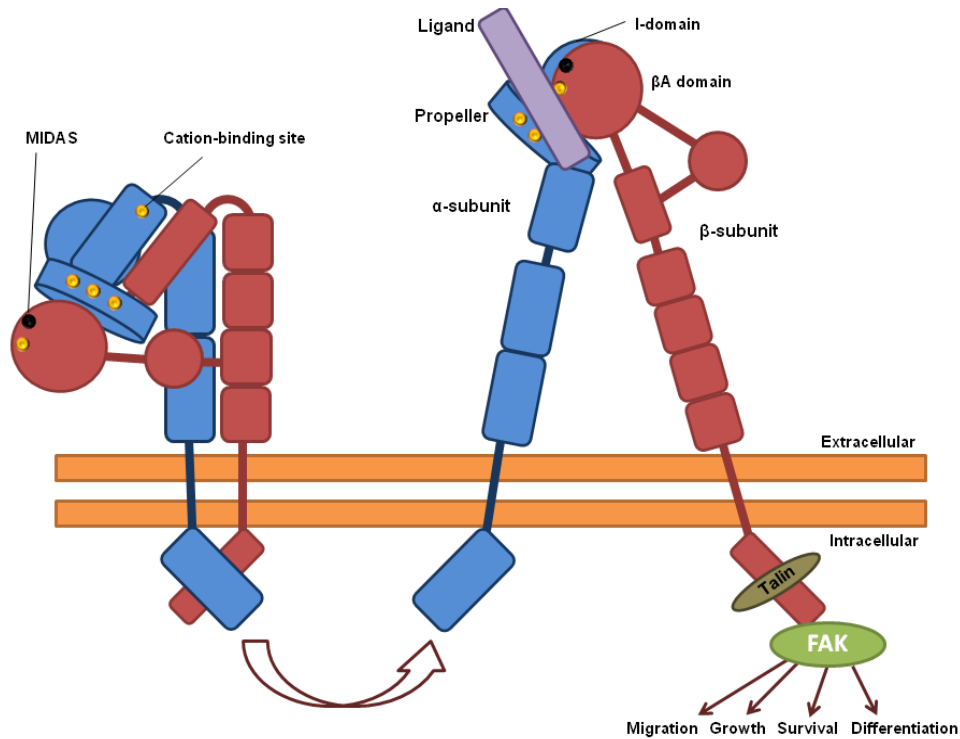
Figure 4. Integrin basic structure.

Integrins are composed of one α and one β subunit, each constructed from several domains with flexible linkers. Each subunit has a single membrane-spanning helix and a short cytoplasmic tail. The last blades of the propeller contain cation-binding domains facing away from the ligand-binding surface. Integrin ligand binding also requires an Mg^{2+} ion, which binds to the MIDAS located in the αI-domain. Integrins have a bent and a high-affinity extended conformation.

FAK= focal adhesion kinase; MIDAS= metal ion-dependent adhesion site;

There are at least seven different integrin heterodimers expressed on respiratory epithelial cells of adults: α2β1, α3β1, α6β4, α9β1, αvβ5, αvβ6 and αvβ8 (Table 3) [124-126]. The only integrins for ligands present in basement membranes are α3β1 and α6β4 (Coll-IV, Fn and Lam) [127,128]. The fibronectin receptor α5β1 is generally not seen on the respiratory epithelium but is rapidly induced by injury [129]. Since pulmonary epithelial cells express integrins for ligands which are absent in resting healthy airways, these integrins are probably used to detect, coordinate and spatially organize responses to airway injuries.

Leukocytes also display particular patterns of integrins that can change in a signal- and time-dependent manner (Table 3). For example, freshly isolated human monocytes express β1 and β2 integrins, but their culture changes the pattern and induces αvβ3 integrin [130].

In the brain different groups of integrins are expressed by the endothelium and parenchyma (Table 4). For example, brain endothelial cells express β1, β3, β5, β6, while astrocytes express only β1 and β5.

Different integrins can adhere to similar substrates, e.g. integrin α2β1 adheres to the GFOGER region of Coll-I while integrin α3β1 can adhere to Coll-I through the RGD sequence [131]. Also, a specific integrin can adhere to different substrates with different affinities (Table 3).

Table 3- Ligands of integrins in the lung.

Integrin		Ligands	Cells
β1	**α1**	Collagens (++type IV, GFOGER), laminin	Monocytes
	α2	Collagens (++type I, GFOGER), laminin	Lung epithelial cells, fibroblasts, lymphocytes
	α3	Laminins, fibronectin, collagens (RGD)	Lung epithelial cells
	α4	Fibronectin (RGD), VCAM-1	Monocytes, lymphocytes
	α5	Fibronectin (PHSRN)	Lung epithelial cells, monocytes, fibroblasts
	α6	Laminin	Monocytes
	α9	Tenascin	Lung epithelial cells
β2	**αM**	ICAM-1, collagens	Monocytes/ macrophages
	αX	Fibrinogen, collagens	Monocytes/ macrophages
β3	**αV**	Collagens, fibronectin, fibrinogen, vitronectin (RGD)	Monocytes
β4	**α6**	Laminins	Lung epithelial cells, fibroblasts
β5	**αV**	Fibronectin	Lung epithelial cells, fibroblasts
β6	**αV**	Fibronectin (RGD)	Lung epithelial cells
β8	**αV**	Fibronectin (RGD), laminin	Lung epithelial cells

ICAM-1- intercellular Adhesion Molecule 1; VCAM- vascular cell adhesion protein 1; PHSRN- proline-histdine-serine-arginine-asparagine; RGD sequence- arginine-glycine-aspartic acid; GFOGER sequence- glycine-phenylalanine-hydroxiproline-glycine-glutamic acid-arginine

Table 4- Integrins in the brain.

Integrin		Ligand	Cells
β1	α1	Collagens, laminin	Endothelial cells, astrocytes, neurons, radial glia, pericytes
	α2	Collagens, laminin	Endothelial cells, pericytes
	α3	Collagens, fibronectin, laminin	Endothelial cells, neurons
	α4	Fibronectin	Neurons
	α5	Fibronectin	Endothelial cells, neurons, astrocytes, pericytes
	α6	Laminin	Endothelial cells, neurons, astrocytes, oligodendroglia, pericytes
	αV	Fibronectin, vitronectin	Neurons
β3	αV	Collagens, laminin	Endothelial cells
β5	αV	Fibronectin, vitronectin	Endothelial cells, neurons, astrocytes, oligodendroglia
β6	αV	Fibronectin, tenascin	Endothelial cells, neurons, oligodendroglia
β8	αV	Fibronectin, laminin	Neurons, astrocytes, oligodendroglia

Reviewed in: Schmid RS et al. Cereb. Cortex 2003;13 (3): 219-24; Tigges U et al. JNI 2013; 10:33; Mobley AKJ Cell Sci. 2009;122(11):1842–51.

4.4. Extracellular matrix regulation of the immune response

4.4.1.   ECM regulation of innate immunity

The inflammatory response requires emigration and maturation of leukocytes from the circulation into affected tissues, while peripheral dendritic cells (DC) mature into antigen presenting cells and migrate to lymphoid organs to recruit cells of acquired immunity. It has been shown that discoidin domain receptor tyrosine kinase 2 mediated DC adhesion to Coll-I, leading to mouse bone marrow DC activation and functional upregulation [132]. This was recently confirmed to also occur in human DC cells [133]. During inflammation, secretion of cytokines and chemokines induces a protease-rich environment leading to degradation of the ECM [64] and formation of a provisional matrix. Besides contributing to leukocyte infiltration, these early changes in matrix composition also regulate inflammatory pathways. Emerging evidence suggests that release of ECM fragments occurs during inflammation and may play an important role in leukocyte recruitment [41] and activation of the Toll-like receptor (TLR) family, in particular TLR2 and 4 [134,135]. Fragments of Coll-I, Coll-IV and elastin-derived peptides have been shown to be bioactive and to induce monocyte and neutrophil chemotaxis [41]. The best studied Coll-I derived peptide is acetylated proline-glycine-proline (AcPGP), which acts as a neutrophil chemoattractant in endotoxin-induced pulmonary inflammation by signalling through the chemokine receptors CXCR1/2 [136] and is generated in a multi-step process involving MMP-8, -9 and a prolyl-endopeptidase [137]. MMP-9 appears to be essential for PGP formation, since MMP-9 deficient mice have shown lower PGP levels and fewer

neutrophils in bronchoalveolar fluid of *Francisella tularensis* pulmonary infection [138]. We have demonstrated that in the immune response to TB, procollagen III N-terminal propeptide and desmosine are released by MMP-mediated ECM destruction and can be detected in the plasma and sputum of infected patients [85]. Elastin peptides have been shown to dampen lipopolysaccharide (LPS)-stimulated monocytes immune response and it was suggested this may be due to negative trans-regulation of CD14 and TLR4 [139]. Tenascin C, which is upregulated in synovial fluid and cartilage from individuals with RA, interacts with TLR4 of synovial fibroblasts and macrophages leading to pro-inflammatory cytokine production, which is distinct from the cytokine pattern induced by bacterial LPS and contributes to perpetuating inflammation in the joint [134]. In renal inflammation, soluble biglycan, a small proteoglycan induced during reperfusion, also functions as endogenous agonist of TLR-2/4. It activates the inflammatory response with secretion of TNF-α, CXCL1, CCL2 and CCL5 and influx of leukocytes, leading to worsened renal function in a murine model of renal ischemia–reperfusion injury [140].

Bacteria can also bind to the ECM through microbial surface components recognising adhesive matrix molecules (MSCRAMMs) and use these in early steps of colonisation and subsequent infection [141-144]. For example, in infection by enterohaemorrhagic *Escherichia coli*, bacterial binding to the ECM components, particularly Fn, Lam and Coll-IV, contributes to bacterial colonisation of the gastrointestinal tract [145]. However, components of the matrix generally activate the immune response by recruiting/activating immune cells.

Adhesion of phagocytes to diverse matrix components such as Fn, collagens, laminin-111 or fibrinogen enhances phagocytic functions and oxidative burst [41]. Furthermore, the presence of cytokines within the ECM enhances cell adhesion and bacterial activities of phagocytes [146]. Tissue macrophages are extremely important in initiating inflammatory responses and their depletion was shown to affect chemokine production and neutrophil influx in models of inflammation [147]. They express a wide range of receptors for the recognition of pathogen-associated molecular patterns (PAMPs) and danger-associated molecular patterns (DAMPs); however the usage of these receptors as well as other functional and morphological properties are directed by the tissue, which creates unique phenotypes in distinct microenvironments [147]. For example, inflammation increases breakdown of HA into low molecular weight HA, which was shown to activate monocytes and macrophages and to polarise human macrophages toward an M1 phenotype [148]. However, even after initial polarisation (M1/M2), macrophages remain very sensitive to changes in the local tissue environment, which suggest they might serve as potential targets for therapeutic interventions [149].

4.4.2.   ECM regulation in fibrosis

After initial wound response, recruited fibroblasts begin to synthesise large quantities of ECM proteins. Myofibroblasts, which may have different progenitors in different organs, constitute the primary ECM-secreting cells (mainly collagens) during wound healing. They are also the main cells responsible for the stiffening and contraction of scar tissue [150]. This microenvironment disrupts the basement membrane of

surrounding epithelium and promotes epithelial cell migration towards the wound site. In a healthy response, once the wound healing is completed, feedback mechanisms are initiated, inducing apoptosis of myofibroblasts, repression of cytokines that drive ECM deposition and resolution of fibrosis. However, under certain conditions, these normal feedback mechanisms are compromised and ECM synthesis and deposition is perpetuated, as well as the imbalance of TIMP prevailing MMP production [151]. This altered wound healing is characterised by scar tissue, which is rich in fibrillar collagens and which has altered architecture, mechanical stability and reduced elasticity. Fibrosis may originate in response to various acute or chronic stimuli, from infection and autoimmune responses to mechanical injury [152], and is believed to be driven by a series of cellular and molecular events. The importance of the ECM in directing cellular processes and maintaining tissue integrity is known; however, the extent to which a fibrotic ECM can drive pathological cellular phenotypes is not well defined. Idiopathic pulmonary fibrosis, which often leads to patient death, is characterised by increased Coll-I deposition which forms a fibrotic reticulum that impairs gas exchange [153,154]. Evidence shows that this fibrotic ECM drives a positive feedback loop which may redirect fibroblast ECM expression by reducing negative regulators of ECM genes, such as miR-29 [153]. Also, adhesion to monomeric Coll-I was shown to activate alveolar macrophages via CD201, causing a shift towards the profibrotic M2 type [155]. Proliferative vitreoretinopathy results from a failure of surgical repair of rhegmatogenous retinal detachment and is driven by plasma fibronectin present in the sub-retinal space, which act as a chemoattractant of retinal pigment epithelial cells which in turn synthesise excessive fibrillar collagens [156]. In fact, a recent study shows that usage of a fragment antibody termed Fn52RGDS, which interacts with specific sites necessary for fibronectin

polymerisation and with integrins through an attached arginine-glycine-aspartic acid (RGD) sequence tag, reduces fibrotic features [157]. Therefore, innate immune responses induced by a pathogenic ECM might perpetuate fibrosis.

4.4.3. ECM regulation of acquired immunity

After T cell activation and transendothelial migration, cells need to migrate within the inflamed tissue environment and locate the affected area. The site and extent of lymphocyte extravasation appears to be defined by the composition of the endothelial basement membrane and laminins were suggested to be essential for leukocytes to penetrate the vessel wall [158,159]. Although it was recently demonstrated that T cells can migrate in 3D ECM independently of integrins by actin-myosin protrusion and contraction [160,161], the exact mechanisms for directed cell migration in inflammation remain unclear. One study identified the key role of integrins containing the αV subunit in T cell migration in inflamed dermis [162]. It verified increased fibronectin content and condensation of collagen fibres into thicker bundles in inflamed dermis. T cells then migrated around this network of ECM fibres via integrin αV binding to fibronectin RGD sequences. This indicated that the "context" given by the ECM directs T cell migration in inflamed tissues and might be crucial for protective immunity. Also, the density and orientation of stromal ECM around lung tumours controls T cell motility, thereby affecting the anti-tumour immune response by impairing T cell migration to these regions [163].

The ECM has also been implicated in peripheral immune tolerance. Intact HA, characteristic of healing tissues, promotes CD44-dependent induction of IL-10

producing regulatory T-cells (TR1) which are crucial in maintenance of immune tolerance. On the other hand, fragmentary HA, typical of inflamed tissues, was unable to promote TR1 induction and IL-10 production [164], indicating a role for tissue integrity in this immunotolerance system. Aggrecan is present in the cartilage matrix and has recently been identified as a candidate auto-antigen in RA [165]. B cells are capable of efficiently extracting components of the ECM for subsequent presentation and one study demonstrated that B cells specific for aggrecan can present it to CD4+ T cells, leading to activation and effector functions. This may be key for the development of autoimmunity [166]. Elastin-derived peptides may also impact adaptive immunity. For example, they promote Th1 cell differentiation and enhance Th1 cytokines with phytohemagglutinin stimulation [167]. One study demonstrated that stimulation of T cells with elastin peptides resulted in IFN-γ release and high levels of circulating anti-elastin antibodies correlated with pulmonary emphysema in smokers [168].

Once regarded as simply a cellular scaffold, the ECM is now acknowledged as a key regulator of cell and tissue function and may be both an inhibitor and a driver of pathogenesis. The matrix environment affects cell and tissue behaviour by providing a context to the information sensed from soluble factors and helps fine-tune inflammation. Hence, the ECM should not be disregarded when establishing cellular models, since the absence or presence of the ECM and its nature can cause different responses by the cells in inflammatory conditions. Although much has been accomplished regarding the understanding of cell function regulation by the ECM, we still have a simplistic view about the effects of cell adhesion on its behaviour. Purified ECM proteins in 2D monolayers or 3D gels cross-linked with ECM proteins (e.g.

Matrigel) do not accurately reproduce the biophysical characteristics of native ECM. However new developments in the biomaterials field, such as electrospun scaffolds (collagen, gelatin, poly-caprolactone; PCL or poly-L-lactide-co-glycolide; PLGA) [169] and anisotropically nanostructured substrates formed from polyethylene glycol (PEG) or polyurethane acrylate (PUA) polymers [170,171] are promising. However, more work with different cells and tissues is necessary to conclude if these new biomaterials are indeed relevant in matrix biology and can overcome the shortcomings of previous models.

5. The blood-brain barrier

The CNS has three barriers that regulate molecular exchange between blood and the brain tissue or the cerebrospinal fluid (CSF): the BBB, the choroid plexus epithelium between blood and ventricular CSF and the arachnoid epithelium between blood and subarachnoid CSF. Since neurons are rarely more than 20µm from a brain capillary but can be millimetres to centimetres from a CSF compartment, it is believed that the BBB has the main control over the immediate microenvironment of brain cells [172].

The BBB separates the circulating blood from the brain extracellular fluid and constitutes both a structural and functional barrier. It maintains the homeostasis of the microenvironment by blocking the passage of large and hydrophilic molecules but allowing the diffusion of water, some gases (e.g. O_2 and CO_2) and small hydrophobic molecules. Other important molecules such as amino acids or glucose are actively transported across the barrier by specific transporters and receptors, such as excitatory amino acid transporters 1–3 (EAAT1–3), glucose transporter 1 (GLUT1) or L-system for large neutral amino acids (LAT1) (Fig. 5) [172].

Figure 5. Cellular constituents of the blood–brain barrier.

The blood-brain barrier is composed of capillary endothelial cells, surrounded by basement membranes, astrocytes and pericytes. Important molecules such as amino acids or glucose are actively transported across the barrier by specific transporters and receptors, such as EAAT1–3, GLUT1 or LAT1.

EAAT1-3- excitatory amino acid transporters 1–3; GLUT1- glucose transporter 1; LAT1- l-system for large neutral amino acids.

From: Abbot NJ et al. Nature Reviews Neuroscience 2006;7:41-53

The BBB is formed of capillary endothelial cells, surrounded by basement membranes composed mainly of Coll-IV and Lam, and astrocytic perivascular end-feet (Fig. 6). Astrocytes, besides providing biochemical support to endothelial cells, provide a cellular link to neurons. Pericytes are contractile cells that are wrapped around the endothelial cells and embedded in basement membranes. They help the maturation of endothelial cells and establishment of the BBB by inhibiting the effects of CNS immune cells (which can damage the formation of the barrier) and by reducing the expression of molecules that increase vascular permeability. Finally, microglial cells constitute the resident macrophages.
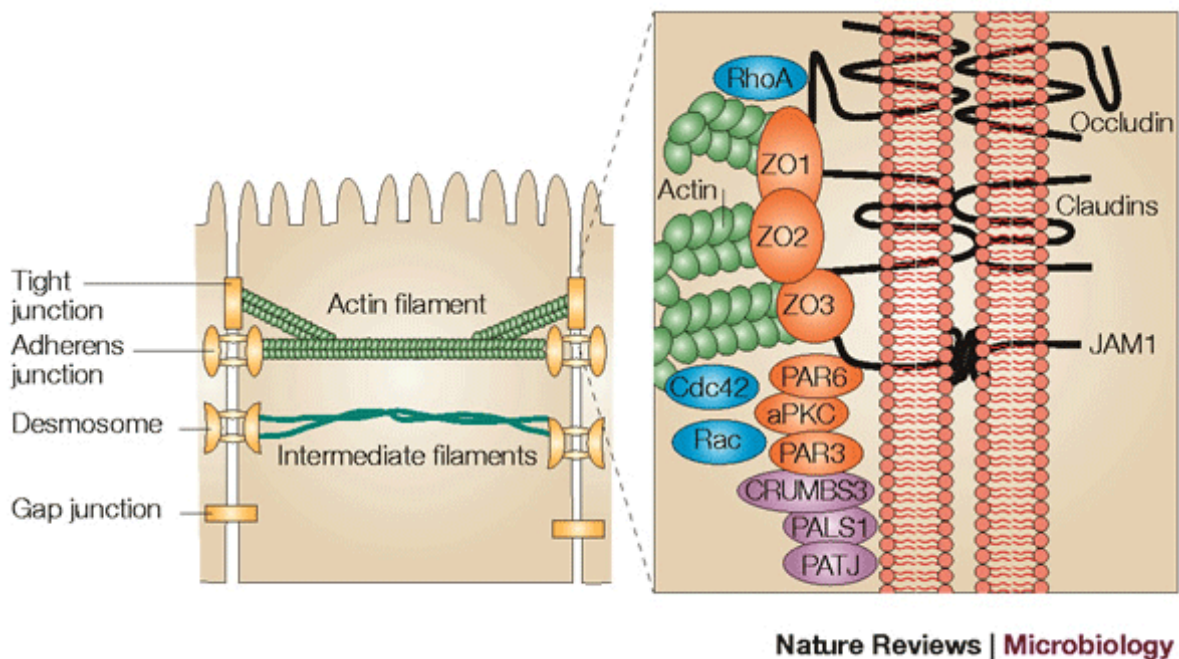
Figure 6. Model of the tight junctions found in the epithelial and endothelial barriers.

JAM-junctional adhesion molecule; ZO- Zonula occludens; PAR- Partitioning defective protein; aPKC- Diacylglycerol-independent protein kinase C.
From: K Aktories & JT Barbieri. Nature Reviews Microbiology 2005;3:397-410

The barrier functions of the brain endothelium are dependent on tight junctions (TJs). These are the most apical intercellular junctional complex, composed of several transmembrane tight junction proteins (TJPs) such as occludin, claudins and adaptor proteins which connect them to the actin cytoskeleton, allowing TJ to form a seal (Fig. 6).

Occludin

Occludin is a 60KDa protein composed of four transmembrane helices and a coiled-coil cytosolic C-terminus (Fig. 7) which mediates its lateral oligomerisation [173,174]. Occludin oligomerisation appears to be redox-sensitive, since studies have demonstrated that normoxic conditions promote occludin oligomerisation and TJ assembly, while oxidative stress associated with hypoxia [175] or inflammation [176,177] results in TJ disruption. The second extracellular domain has been shown to be required for stable assembly of TJs [178], and occludin degradation is associated
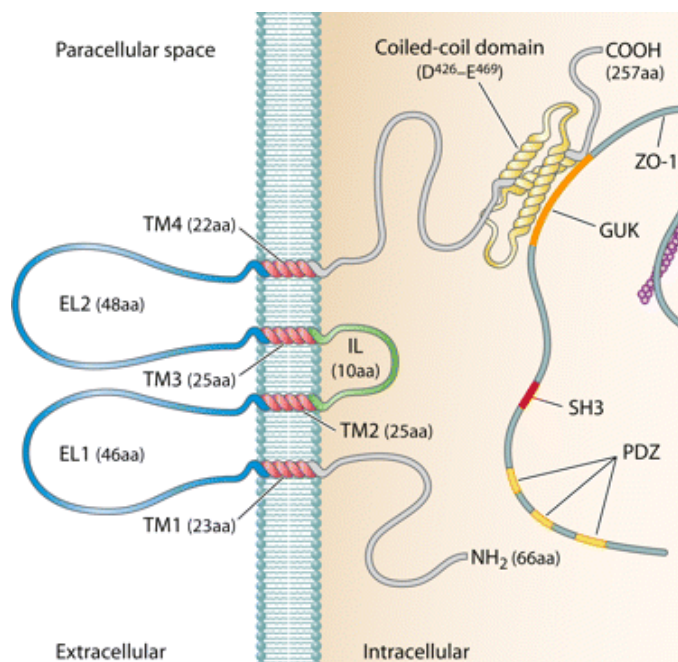
Figure 7. Human occludin.

Occludin domains (and amino acid lengths) are indicated, as well as the C-terminal occludin interaction with the ZO-1 GUK domain.

EL1/2- extracellular loops 1/2; GUK- guanylate kinase domain; IL- intracellular loop; SH3- src homology 3 domain; TM1-4- transmembrane domains 1 to 4.

From: Mol Cell Biol 2012 vol. 32 no. 2 242-250.

with increased permeability of primary and immortalized human brain microvascular

endothelial cells [179,180]. However, well-developed TJs were reported in cells lacking occludin [181]. Also, occludin deficient-mice are viable, exhibiting normal TJs morphology, as well as intestinal epithelium barrier function [182,183]. This indicates that occludin is important, but not essential, for TJ formation.

Claudins

Claudins are a family of 20-27kDa proteins with four transmembrane domains that are expressed in TJs of various cell types (Fig. 8). Brain endothelial cells express mainly claudin-3 and claudin-5 [184,185], whereas claudin-12 is likely to be expressed in minor amounts [186]. Claudin-3 and -5 have a key role in TJ formation and BBB integrity, due to their capacity to homodimerise as well as

Figure 8. General structure of human claudins.
EL1/2- extracellular loops 1/2; TM1-4-transmembrane domains 1 to 4.

heterodimerise through their second extracellular loop [187-189]. Exogenous expression of claudin-5 was shown to strengthen BBB properties in rat brain endothelial cells [186], while depletion of claudin-5 induces disruption of the BBB in claudin-5 deficient mice [190].

Junctional adhesion molecules

Junctional adhesion molecules (JAMs) belong to the immunoglobulin superfamily. JAM-1/JAM-A, a 32kDa glycoprotein composed of two immunoglobulin loops in the extracellular domains, is expressed in the TJ of human endothelial and epithelial cells [191] but also in circulating neutrophils, monocytes and lymphocytes [192]. Although JAMs are not essential for TJ formation in brain endothelial cells, they may be involved in facilitating the assembly of TJPs and the establishment of cell polarity [193].

Cytoplasmic adaptor proteins

A number of cytoplasmic proteins are known to associate with TJ transmembrane proteins and contribute to TJ integrity. Among these are the PDZ domain-containing family: zonula occludens-1 (ZO-1), -2 (ZO-2) and -3 (ZO-3) [194,195]. ZO-1 forms heterodimers with ZO-2 and -3 and these interact with the C-terminal domain of claudins via the PDZ domain 1[196] and with occludin via the GUK domain [197]. It has been shown that ZO proteins are essential for assembly of claudins, occludin and JAM-1[198-200] and for anchoring of this complex to the actin cytoskeleton [201].

5.1. Regulation of TJ assembly by perivascular cells

Astrocyte and pericyte derived Wnt and hedgehog proteins have been shown to control BBB formation during development, but also maintain TJ integrity in adult tissues.

5.1.1. The Wnt/ β-catenin pathway

This pathway has been recently discovered as a key regulator of the BBB. Wnt ligation to its membrane receptors, Frizzled4 (Fz4) and LRP5/6 expressed by brain endothelial cells, inhibits the β-catenin repressor complex, allowing β-catenin cytoplasmic accumulation, nuclear translocation and transcription of various genes, including claudin-3 and -5 [202].

5.1.2. The Hedgehog pathway

The Hedgehog pathway (Hh) is involved in morphogenesis, neuronal guidance and angiogenesis [203,204] and in adult tissues it is associated with vascular differentiation and tissue repair [205]. The Hh pathway has also been linked to inhibition of endothelial production of chemokines and expression of adhesion proteins, which supports extravasation of leukocytes to the brain [206]. In the CNS, Shh is produced by astrocytes (Fig. 9). Mammals have three Drosophila Hedgehog homologs: Indian Hedgehog (Ihh), Desert Hedgehog (Dhh) and Sonic Hedgehog

(Shh) however, CNS morphogenic events are mainly associated with Shh signalling [207].
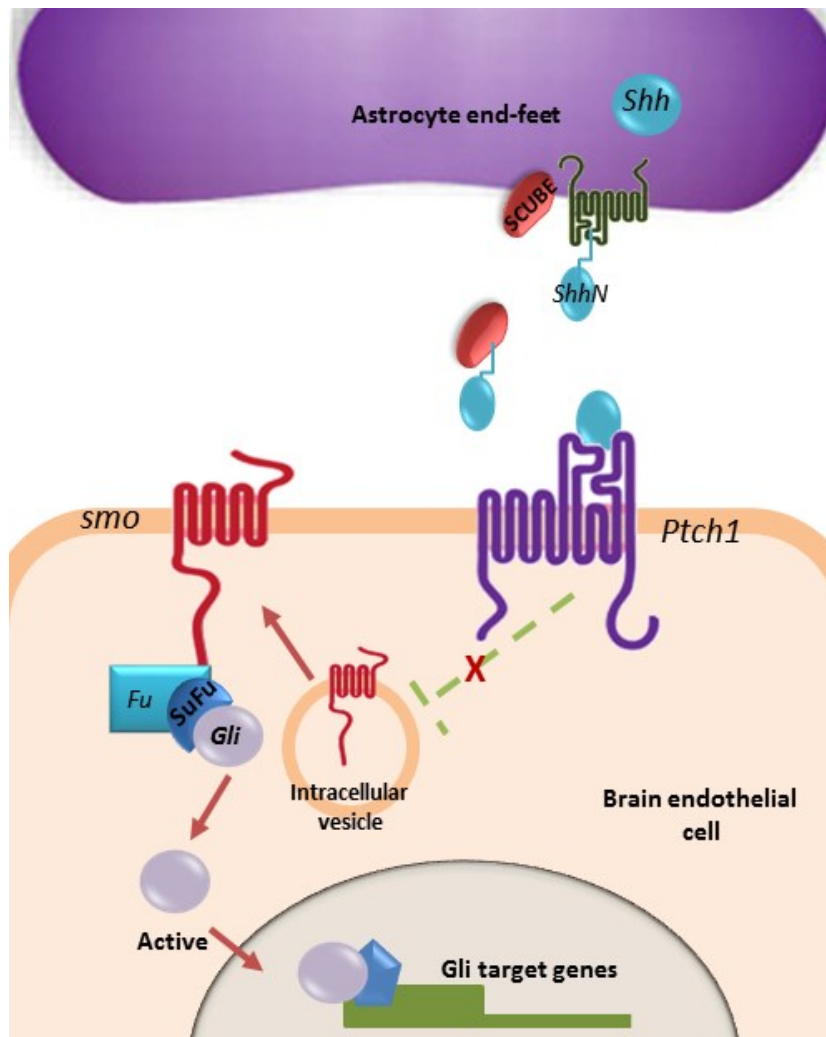
Figure 9. Representation of the Sonic Hedgehog signalling pathway in the blood-brain barrier.

In the CNS, Shh is produced by astrocytes, where SCUBE appears to be necessary for efficient Shh processing and delivery to endothelial cells. Shh bound to Ptch1 inhibits its repressor abilities and Smo is translocated to the membrane, leading to inhibition of SuFu and activation of Gli transcription factors. Gli-1/2 accumulates in the nucleus and controls transcription of Hh target gene.

Gli- GLI family zinc finger; Hh-Hedgehog; Ptch1- patched-1 receptor; Shh- sonic hedgehog homolog; Smo- smoothened receptor; SuFu- suppressor of Fused

5.2. BBB in infection and inflammation

The CNS inflammatory response has been associated with enhanced BBB permeability and disturbance of brain function in multiple sclerosis [208], lymphocytic choriomeningitis [209], rabies virus infection [210], West Nile virus encephalitis [211] and neuroAIDS [212].

Disruption of brain endothelial functions is often associated with development of oedema [213]. The resultant raised intracranial pressure leads to impaired tissue perfusion and risk of herniation, severe neurological morbidity or death.

Several host mediators have been shown to affect BBB permeability, e.g. nitric oxide, TNF-α, IL-1, TGF-β, proinflammatory neuropeptides, caspases and also MMPs [214]. These mediators also have direct toxic effects on neurons by activation of apoptotic and necrotic pathways causing neuronal loss and neurological sequelae [215-217]. The role of MMPs in BBB disruption in bacterial meningitis is becoming increasingly clear. MMP-2, -3 and -9 are produced by multiple cell types, including the endothelium, astrocytes, microglia and neurons [218]. MMPs can also be released from infiltrating leukocytes. Neutrophils predominantly carry MMP-8 and -9 [219], whereas monocytes can produce multiple MMPs [220].

MMP-8 and MMP-9 are upregulated in the CSF of children with bacterial meningitis, levels being 10 to 1000-fold higher than in viral meningitis [221]. MMP-8 is also upregulated upon *Neisseria meningitidis*, leading to human brain microvascular endothelial cell (HBMEC) detachment from the ECM and cleavage of occludin [179].

In a cellular model of BBB, virulent strains of Mtb were shown to tranverse the BBB independently of leukocytes [222] However, in this model human astrocytes were disregarded, hence it is unclear what their role is in preventing Mtb entry into the brain parenchyma. BBB integrity has never been accessed before and during Mtb infection.

6. Hypothesis and aims

As the composition of the ECM is tissue-specific and there is evidence that the ECM may be key in shaping local immune inflammatory responses, I hypothesise that the local tissue environment regulates MMP response, not only in pulmonary TB, but also in CNS TB.

- In a cellular model of pulmonary TB, addressed in Chapters III and IV, I aimed to study the effect of specific components of the lung ECM in regulation of MMP expression and activity. This was investigated in CoMtb-stimulated NHBE cells and monocytes and also in Mtb-infected monocytes, and the responses between inflammatory and epithelial cells were compared and contrasted.

- In a cellular model of the BBB, in which the normal composition of the ECM is different from the lung, I aimed to study the role of TB-driven MMP production in BBB disruption and leukocyte transmigration. I also aimed to compare the MMP response with the one seen in the lung.

Chapter II: Materials and Methods

2. Materials and Methods

2.1. Reagents and antibodies

All chemical inhibitors, agonists and antagonists used are summarised in table 4.

Table 4- Chemical inhibitors

Name	Target	Supplier
FAK inhibitor II	Focal adhesion kinase (FAK)	Calbiochem, Millipore
Wortmanin	PI3K activity	Calbiochem, Millipore
PD169316	Erk-1/2 activity	Calbiochem, Millipore
Cytochalasin D	actin polymerization	Sigma-Aldrich
Ro32-3555	Collagenases & gelatinases	Calbiochem, Millipore
GM6001	MMP inhibitor	Calbiochem, Millipore
EDTA	Integrin activity (non-specific)	Sigma-Aldrich
Cyclopamine	smo receptor antagonist	Calbiochem, Millipore
Purophamine	smo receptor agonist	Calbiochem, Millipore
GANT61	Gli1/2 transcription factor	Calbiochem, Millipore
GM6001	MMP inhibitor	Calbiochem, Millipore

All recombinant human proteins used are summarized in table 5 and primary and secondary antibodies are in tables 6 and 7.

Table 5- Recombinant human proteins

Name	Supplier
rhMMP-1	R&D
rhMMP-9	R&D
rhSHH	eBiosciences
rhMCP-1	Peprotech
rhIL-8	Peprotech

Table 6- Primary antibodies

Target	Host	Clone / Isotype	Supplier
Human integrin α2β1 (FUNC/ Co-IP)	Mouse	IgG1/ BHA2.1	Millipore
Human integrin α3β1 (FUNC)	Mouse	IgG1/M-KID2	Millipore
human ICAM-1 (IF)	Mouse	IgG1	Abcam
Isotype control (IF/ FUNC)	Mouse	IgG1	BD Biosciences
human integrin β1 (IF, FUNC)	Mouse	IgG1/ P4C10	Millipore
human integrin β2 (IF, FUNC)	Mouse	IgG1/ MEM48	Millipore
human integrin β3 (IF, FUNC)	Mouse	IgG1/25E11	Millipore
human integrin αV (IF, FUNC)	Mouse	IgG1/272-17E6	Millipore
human ZO-1 (WB/ IF)	Mouse	IgG1/1A12	Life Technologies
human Occludin (WB/ IF)	Rabbit	Polyclonal	Life Technologies
human Claudin-5 (WB/ IF)	Rabbit	Polyclonal	Life Technologies
human Claudin-3 (WB/ IF)	Rabbit	Polyclonal	Life Technologies
p-Akt (Ser 473; WB)	Rabbit	Polyclonal	Cell Signalling
Total Akt (WB)	Rabbit	Polyclonal	Cell Signalling
p-Erk1/2 (Thr 202/ Tyr204; WB)	Rabbit	Polyclonal	Cell Signalling
Total Erk1/2	Rabbit	Polyclonal	Cell Signalling
p-p38 (Thr180/Tyr182; WB)	Rabbit	Polyclonal	Cell Signalling
Total p38 (WB)	Rabbit	Polyclonal	Cell Signalling
p-JNK (WB)	Rabbit	Polyclonal	Cell Signalling
Total JNK (WB)	Rabbit	Polyclonal	Cell Signalling
β-actin (WB)	Mouse	IgG	Sigma-Aldrich
Human SHH (WB/IF)	Rabbit	Polyclonal	Millipore
Human SCUBE2 (WB)	Rabbit	Polyclonal	Abcam
Human smo (WB)	Rabbit	Polyclonal	Abcam
human Gli-1 (WB/ IF)	mouse	IgG	Abcam

Applications: FUNC- Functional; IF- Immunofluorescence; WB- Western blotting

Table 6- Primary antibodies (Cont.)

Target	Host	Clone / Isotype	Supplier
Human MMP-1 (FUNC)	Rabbit	Polyclonal	R&D
Human MMP-9 (FUNC/ IF)	Rabbit	Polyclonal	R&D
Human MMP-1 (IF/WB)	Rabbit	Polyclonal	Millipore
Human MMP-10 (IF/WB)	Rabbit	Polyclonal	Millipore

Applications: FUNC- Functional; IF- Immunofluorescence; WB- Western blotting

Table 7- Secondary and conjugated antibodies

Target / conjugation	Host	Clone / Isotype	Supplier
CD64-FITC (IF)	Mouse	IgG1	BD
CD66c-FITC	Mouse	IgG1	BD
Human integrin α2-FITC (IF)	Mouse	AK7/ IgG1	Abcam
Human integrin α3-FITC (IF)	Mouse	17C6/ IgG1	Abcam
Human CD16-FITC (IF)	Mouse	IgG1	BD Biosciences
Mouse IgG H+L –FITC (IF)	Goat	polyclonal	Sigma-Aldrich
Mouse IgG H+L - DyLight 549 (IF)	Goat	polyclonal	Abcam
Mouse IgG-alexa fluor 488 (IF)	Goat	polyclonal	Life Technologies
Rabbit IgG H+L –Cy5 (IF)	Goat	polyclonal	Abcam
Rabbit IgG H+L-HRP (WB)	Goat	polyclonal	New England Biolabs
Mouse IgG H+L-HRP (WB)	Goat	polyclonal	Sigma-Aldrich

Applications: IF- Immunofluorescence; WB- Western blotting

2.2. *Mycobacterium tuberculosis* culture

Mtb strain H37Rv was cultured in Middlebrook 7H9 medium (BD Diagnostics) supplemented with 10% ADC enrichment medium (BD Diagnostics), 0.2% glycerol (Sigma-Aldrich) and 0.02% Tween 80 (Sigma-Aldrich) with agitation at 100rpm. Culture growth was monitored with a Biowave cell density meter (WPA, Cambridge, UK) and was subcultured when the optical density was 1.00.

For colony forming units (CFU) counting, supernatants and/or cell lysates were seeded in 7H11 agar plates (BD Diagnostics) supplemented with 10% OADC enrichment medium and 0.2% glycerol (Sigma-Aldrich). Plates were incubated at $37^{o}C$ for 3-4 weeks.

2.3. Conditioned media preparation (CoMtb)

Monocytes from single-donor leukocyte cones (National Blood Transfusion Service, London, UK) were isolated by gradient centrifugation with Ficoll-Plaque (GE Healthcare, Buckinghamshire, UK) and adhesion purification. Monocytes were counted in peripheral blood mononuclear cell (PBMC) solution by adhesion to haemocytometer slides and seeded at a density of 2.5×10^5 cells/cm^2 in 60mm petri dishes. Non-adherent cells were removed by washing with Hank's balanced salt solution (HBSS; Life Technologies, Paisley, UK). Fresh RPMI 1640 medium (Life Technologies) supplemented with 2mM glutamine and 10 mg/ml ampicillin added before infecting cells with Mtb strain H37Rv at a multiplicity of infection (MOI) of and incubating for 24h at $37^{o}C$ and 5% CO_2. Control medium from uninfected cells

(CoMCont) was prepared in a similar manner but with the addition of an equal volume of 7H9 medium without Mtb. Supernatants were collected, filtered through a 0.2µM polypropylene filter (Whatman Anotop 25, Buckinghamshire, UK) to remove Mtb and MMPs from the supernatants [223], aliquoted and stored at -20°C.

2.4. Cell culture

2.4.1. Coating of tissue culture plates and latex beads

Tissue culture plates were pre-coated with human Coll-I (VitroCol), Col-IV, fibronectin (Fn) (Advanced BioMatrix, USA) or laminin (Lam) (Life technologies, UK) according to the manufacturer instructions.

In brief, for Coll-I, wells were coated at a desired concentration of VitroCol diluted in sterile distilled water and incubated at room temperature for 1h, rinsed with sterile phosphate buffered saline (PBS). Coll-IV was diluted in a 0.25% acetic acid solution and coated plates incubated for one hour and rinsed with Hank's balanced salt solution (HBSS). Fn was diluted in HBSS, plates incubated for one hour and rinsed with sterile distilled water. Plates were stored at 4°C ensuring they remained sterile. Finally, Lam was slowly thawed to avoid formation of a gel, diluted in HBSS and incubated at room temperature for one hour. After incubation any excess material was aspirated and plates were blocked with sterile 1% heat denatured bovine serum albumin (hdBSA) and allowed to air dry for at least 45 minutes before introducing cell suspensions.

Latex beads (0.3µm, Sigma-Aldrich) were sterilised by tantalization (cycles alternating between 37°C and 60°C) and resuspended in 1mg/ml of Coll-I in 0.1M bicarbonate buffer and incubated with rotation for 1h at room temperature. After washing with PBS beads were blocked with 1% heat denatured BSA for 2h with rotation at room temperature. After the washing steps, beads were resuspended in culture medium and added to the wells in a 100:1 bead-to-cell ratio.

To mimic integrin engagement to Coll-I, plates were coated with goat anti-mouse IgG monoclonal antibodies (Ab) overnight at 4°C, washed with PBS, blocked with 1% hdBSA and coated for 2h at room temperature with either 20µg/ml of anti-integrin α2β1 Ab or anti-integrin α3β1 Ab.

2.4.2. Respiratory epithelial cell culture

Human alveolar adenocarcinoma epithelial cell line (A549 cells) were maintained in RPMI 1640 (Gibco, Life technologies) supplemented with 10% heat inactivated FBS (Biowest, UK), 2mM glutamine and 10 µg/ml ampicillin and were subcultured at 80%-90% confluence using 0.25% trypsin-EDTA for 2min and neutralised with growth medium. For experiments, cells were seeded at a density of 40,000 cells per cm^2 in serum free medium.

Primary Normal Human Bronchial epithelial cells (NHBE; Clonetics, Lonza, Basel, Switzerland) were grown in bronchial epithelial growth medium (BEGM; Clonetics, Lonza) and were subcultured at 80% confluence using trypsin-EDTA for 2min and

neutralised with trypsin neutralising solution (Clonetics, Lonza). For experiments, cells were seeded at a density of 50,000 cells per cm^2 and rested overnight.

For both cell types, CoMtb was added to wells in a 1:5 dilution. Cells were stimulated between 24-72h for secretion experiments and for 6h for gene expression. For secretion experiments, cells were incubated for 24h-72h and supernatants were collected, centrifuged at 11,000rpm for 2 min and stored at -20°C. For gene expression, cells were incubated for 6h, rinsed with sterile PBS and lysed with Tri-Reagent and stored at -80°C. For wells with soluble Coll-I or coated beads, 100µg/ml Coll-I or pre-coated beads in growth medium was added to the wells. Cell viability was determined by trypan blue exclusion.

2.4.3. Human primary astrocyte culture

Human astrocytes were maintained in T75 flasks pre-coated with poly-L-lysine (Sigma-Aldrich) in complete astrocyte medium (basal medium, astrocyte growth supplement and 2% FBS) with 1% penicillin-streptomycin (Sciencell Research Laboratories) until the culture was approximately 90% confluent. Cells were used between passages 4 and 10.

2.4.4. hCMEC/D3 cell line culture

The brain microvascular endothelial cell line hCMEC/D3 was maintained in T75 flasks pre-coated with rat tail Coll-I (Sigma-Aldrich) in EBM-2 medium (Lonza) supplemented with 1.4µM hydrocortisone (Sigma-Aldrich), 5µg/mL ascorbic acid

(Sigma-Aldrich), 1% chemical defined lipid concentrate (Life technologies), 1ng/mL of basic fibroblast growth factor (Sigma-Aldrich), 10 mM HEPES (Life technologies), 5% FBS (Sciencell Research Laboratories) and 1% penicillin-streptomycin (Sciencell Research Laboratories) until the culture was 100% confluent. Cells were used between passages 25 and 32.

2.4.5. Co-cultivation of hCMEC/D3 cells and human astrocytes

67,000 astrocytes were seeded in inverted transwell permeable inserts, 5.0µm pore size (Millipore) pre-coated with 150µg/mL of Coll-IV in 250µL of growth medium and let to adhere for 1h at 37°C and 5% CO_2. Transwells were inserted in 12-well receiver plates containing 1.2mL astrocyte growth medium and 50,000 hCMEC/D3 cells were seeded in the apical side in 400µL endothelial cell growth medium.

The BBB was left to mature between 6 and 11 days. When the BBB was matured (accessed by trans-endothelial resistance), cells were stimulated with CoMtb (1:5 dilution) or infected with Mtb (MOI 20). For experiments using direct Mtb infection, antibiotics were removed from the culture medium.

2.4.6. Monocyte purification and culture

Monocytes from fresh blood volunteers (JSF research group donors list) were isolated by gradient centrifugation with Ficoll-Plaque PLUS (GE Healthcare) and CD16-monocytes were purified from PBMCs by negative magnetic-activated cell sorting (MACS monocyte isolation kit II; Miltenyi Biotec Ltd., UK) according to the

manufacturer's instructions. Purity was confirmed by CD64 staining and FACS analysis. Monocyte purity was over 96% (Fig. 10). Viability was accessed by trypan blue exclusion and viability was ≥98%.
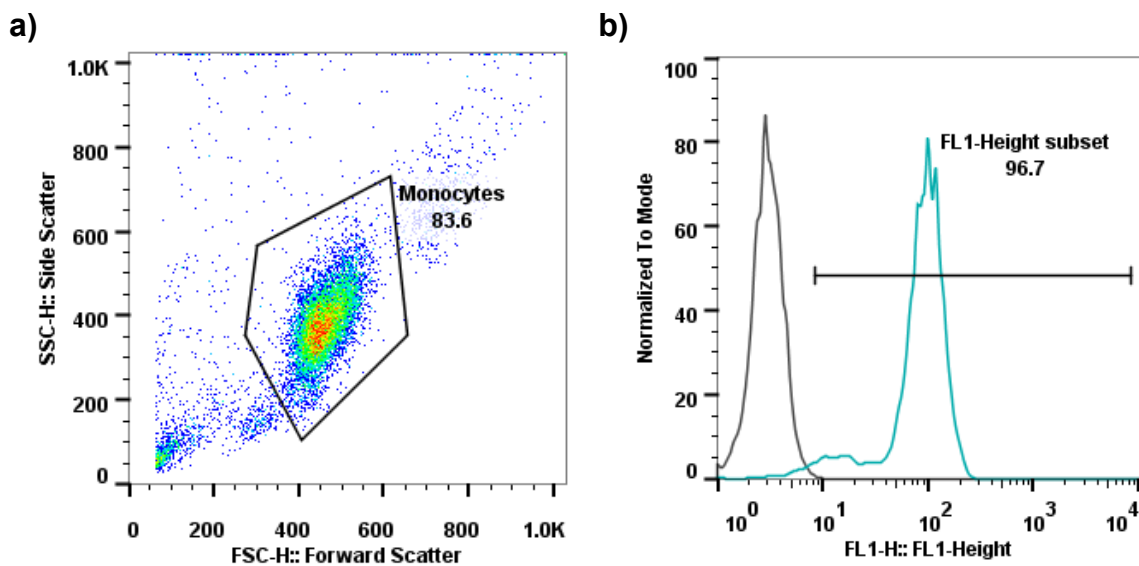
Figure 10. FACS analysis of monocyte purity.

Monocytes were isolated from peripheral blood by gradient centrifugation and negative magnetic-activated cell sorting and labelled with FITC-conjugated CD64 antibody or isotype control and 10 000 events were gated.

Monocytes were seeded at a density of 2.5×10^5 cells per cm^2 in RPMI 1640, supplemented with 2mM glutamine and 10µg/ml ampicillin and 10% heat inactivated FBS. Monocytes were left to rest for 1h before adding 1:5 diluted CoMtb (diluted in RPMI with 10% heat inactivated FBS) or infecting with Mtb H37Rv at a MOI of 1. For

secretion experiments, cells were incubated for 24h and supernatants were collected, centrifuged at 11,000rpm for 2 min and stored at -20°C and for gene expression, cells were incubated for 6h, rinsed with sterile PBS and lised with Tri-Reagent and stored at -80°C.

2.4.7. Neutrophil purification and culture

Neutrophils from fresh blood volunteers (JSF research group donors list) were isolated by dextran/ saline erythrocyte lysis, followed by gradient centrifugation with Ficoll-Plaque PLUS (GE Healthcare) and 3 steps of erythrocyte hypotonic lysis, each consisting of 30 sec cell incubation wilth 20mL of ice cold 0.2% NaCl followed by 20ml in ice cold 1.6% NaCl and centrifugation at 250g at 4°C for 4 min without brake. The neutrophil pellet was resuspended in RPMI 1640 with 10% FBS and used in experiments.

Purity was confirmed by CD66c staining and FACS analysis. Neutophil purity by this melhod was over 98%. Viability was accessed by trypan blue exclusion and viability was ≥99% (Fig. 11).

a)

b)
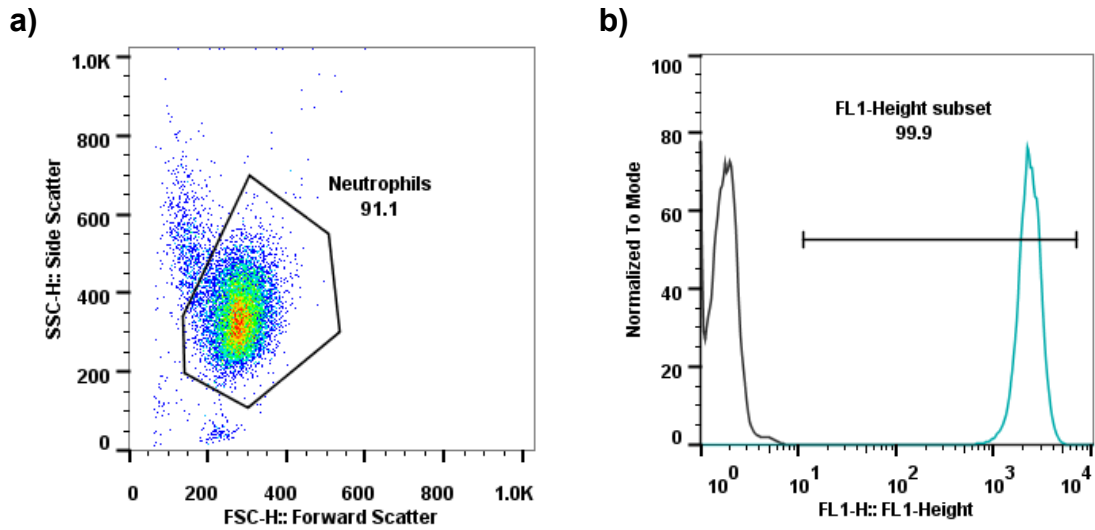
Figure 11. FACS analysis of neutrophil purity.

Monocytes were isolated from peripheral blood by gradient centrifugation and negative magnetic-activated cell sorting and labelled with FITC-conjugated CD66c antibody or isotype control and 10 000 events were gated.

2.5.   Enzyme-linked immunosorbent assay (ELISA)

Secretion levels of MMPs and TIMPs were analysed by ELISA (Duoset, R&D Systems, Abdingdon, UK) according to the manufacturer's instructions. The 96-well micoplate (Costar) was read at 450nm with a reference wavelength of 540nm on a µQuant plate reader (Biotek Instruments Inc). The lower limit of sensitivity for the Duoset kits were: 21.2pg/ml for TIMP-1, 31.2pg/ml for TIMP-2, 156pg/mL for MMP-1and and 31.2pg/ml for MMP-10.

2.6. Luminex bead Array

Microparticle based multiplex immunoassays were used to analyse total secretion levels of MMPs, cytokines and soluble adhesion molecules. Specific antibodies are pre-coated onto colour-coded microparticles or beads. Microparticles, standards, and samples were pipetted into a Luminex plate and agitated at 500rpm for 2h allowing immobilised antibodies to capture the analyte of interest. Biotinylated antibodies specific to the analyte were added and agitated for 1h. Next, streptavidin phycoerythrin (PE) was added with agitation for 30min to generate a signal. Washes are performed between each step. Finally, the beads were resuspended and read using the Luminex dual laser analyser (Bio-Rad Bio-Plex 200 System). One laser classifies the bead and determined the analyte which is being detected, the second laser determined the magnitude of the PE derived signal, which is in direct proportion to the analyte bound.

MMPs were analysed using the Fluorokine MAP kit (R&D Systems) according to the manufacturer's instructions. The lower limits of sensitivity were: 1.1pg/ml for MMP-1, 12.6pg/ml for MMP-2, 7.3pg/ml for MMP-3, 6.6pg/ml for MMP-7, 16.6pg/ml for MMP-8, 13.7pg/ml for MMP-9 and 3.2pg/mL for MMP-10. All samples were run with appropriate controls and were within the linear range of detection as indicated by the manufacturer. Adhesion molecules were analysed using the 4-plex human adhesion molecule performance kit (R&D Systems) with the following lower limits of sensitivity: 303pg/mL for ICAM-1, 7.4pg/mL for E-Selectin, 12.2pg/mL for P-Selectin and 529pg/mL for ICAM-1.

2.7. EnzChek DQ collagen type I assay

Collagenolytic activity was measured using EnzChek DQ collagen type I assay (Life technologies) and performed as indicated in the manufacturer's instructions. Briefly, a standard curve was originated from known concentrations of collagenase from *Clostridium histolyticum* and standards and cell supernatants were incubated with DQ type I collagen for 24h. Collagenase activity was measured by gain of fluorescence originating from DQ type I collagen degradation.

2.8. Gelatin and casein zymogram

Samples were diluted in SDS loading buffer and proteins were separated by electrophoresis in 0.05% casein gels (Life technologies) or 0.12% gelatin gel (made in-house) and incubated in collagenase buffer overnight at 37°C. All gels were run with a recombinant human MMP-1 or MMP-9 standard (Calbiochem, Merck Biosciences, UK). Caseinolytic/gelatinolytic activity was revealed by Coomassie blue staining (Pharmacia) and methanol: acetic acid: water distaining.

2.9. RNA extraction and cDNA synthesis

Total RNA was extracted using DirectZol™ RNA MiniPrep Kit (Cambridge Biosciences, UK) according to the manufacturer's instructions. 1µg RNA was reverse transcribed using QuantiTect Reverse Transcriptase Kit (Qiagen, Manchester, UK) and qPCR reactions were performed in the ABI Prism 7700 (Applied Biosystems, Paisley, UK). For low quantities of RNA (monocyte experiments), 15ng RNA were

reverse transcribed using the OneStep RT-PCR kit (Quiagen) according to the manufacturer's instructions.

2.10. Plasmid standards

Plasmid standards were kindly engineered by Dr Catherine Ong using the TOPO vector (Life technologies)**.** 80ng of plasmids containing MMPs and/or housekeeping genes were used to transform chemically competent *E. coli* TOP10 (Life technologies) according to the manufacturer's instructions. Bacteria were incubated in SOC medium (Life technologies) overnight at 37°C with agitation. Transformed bacteria were selected by plating into LB/Amp agar plates. Positive isolated clones were picked from plates and grown in LB/Amp broth. Successful transformation was tested by real-time PCR. Part of the transformed bacteria was frozen in 50% glycerol at -80°C and the rest was used to purify the grown plasmids, using GenElute GP plasmid miniprep (Qiagen) according to the manufacturer's instructions.

Serial dilutions of the linearised plasmids were used to generate a standard curve with a known number of gene copies.

2.11. Real-time polymerase chain reaction (PCR)

RT-PCR was performed in a Framestar 96 well PCR plate (4titude, Wotton, UK) on the Stratagene Mx3000Pro machine (Agilent Technologies Inc.) with a thermal profile of: 10min at 95˚C (Taq polymerase activation) followed by 40 cycles at 95˚C for 30 sec (cDNA denaturation) then 60˚C for 1 min (annealing of primers and probes/extension). When using the OneStep RT-PCR kit, the thermal profile was: 30 min at 50˚C (reverse transcription) and 15 min at 95˚C (Taq polymerase activation), followed by 40 cycles of 30 sec at 94˚C (cDNA denaturation), 30 sec at 60˚C (annealing of primers and probes) and 1min at 72˚C (extension). Primers and probes used are summarised in table 8 and 9.

MMP-1/10 cycle thresholds were quantified by comparison to an MMP-1/10 standard curve generated using known MMP-1 concentrations and then standardised to 18S rRNA.

When standards were not available (e.g. claudin-5, occludin), the Pfaffl comparative Ct method was used applying the following equation:

$$\text{Ratio} = \frac{E_{target}{}^{\wedge\Delta Ct\ (control-target)}}{E_{reference}{}^{\wedge\Delta Ct\ (control-target)}}$$

where E is the real-time PCR efficiency of one cycle in the exponential phase, calculated according to the equation: $E = 10^{[-1/slope]}$ and the reference gene is β-actin.

Table 8- TaqMan custom Primers and Probes used (spp. Homo)

Target gene		Sequence
MMP-1	Forward	5'- AAGATGAAAGGTGGACCAACAATT -3'
	Reverse	5' -CCAAGAGAATGGCCGAGTTC -3'
	Probe	5'- FAM-CAGAGAGTACAACTTACATCGTGTTGCGGCTC-TAMRA -3'
MMP-14	Forward	5'-AAGGCCAATGTTCGAAGGAA -3'
	Reverse	5'-GGCCTCGTATGTGGCATACTC -3'
	Probe	5'- FAM-CAACATAATGAAATCACTTTCTGCATCCAGAATTACA - TAMRA -3'
MMP-10	Forward	5'- GGACCTGGGCTTTATGGAGATAT -3'
	Reverse	5'- CCCAGGGAGTGGCCAAGT -3'
	Probe	5'- FAM- CATCAGGCACCAATTTATTCCTCGTTGCT-TAMRA -3'

Table 9-TaqMan Primer and probe mix (Life technologies)

Target gene	Reference
18S	4308329
β-actin	431088E
Occludin	Hs00170162_m1
Claudin-5	Hs00533949_s1
Shh	Hs00179843_m1

2.12. Wound healing assay

96-well ImageLock plates (Essen Biosciences Ltd, Hertfordshire, UK) were coated with either Coll-I or poly-L-lysin (Sigma-Aldrich) and 20,000 NHBE cells were seeded in each well. A standard wound was created in the cell monolayer of each well using a WoundMaker (Essen Bioscience Ltd) according to the manufacturer's protocol. Cells were stimulated as previously described and plate was incubated in the IncuCyte Zoom (Essen Biosciences Ltd). Images were taken at 2h intervals for a maximum of 18h.

2.13. Laser scanning cytometry

4-well glass slides were pre-coated and NHBE cells were seeded, incubated and stained for F-actin as previously described. Fluorescence was determined by quantitative imaging cytometry using an iCys Research Imaging Cytometer (CompuCyte, Cambridge, USA) with iNovator software (CompuCyte). A scanning protocol for quantification was configured with two channels; 405nm diode laser excitation and blue channel detection (445nm-485nm) for DAPI and HeNe 633 nm laser excitation and long red channel detection (650nm LP) for F-actin. High resolution scans were acquired using the 60x objective and 0.5mm x-step size. Watershed filters were applied to separate closely spaced events, size constraints to exclude artefacts and border objects were removed. Cells were contoured on the blue channel to identify events (>4000 cells per well). A peripheral contour was set 14 pixels outside the nuclear contour to sample the cytoplasmic staining and long red channel peripheral measurements were used to quantify F-actin fluorescence, which was expressed as levels per cell. A confirmatory analysis was performed to verify the results obtained from the iCys software analysis. Image files acquired from the iCys scans were imported into the Columbus analysis software (Perkin Elmer). An analysis protocol was set up to identify nuclei (size constraints were added to exclude artefacts and partial image border objects were also removed) and to identify the total cytoplasmic F-actin staining associated with each nucleus in the far red channel. A batch analysis was run for each well and the measurements determined and expressed as fluorescence per cell.

2.14. Co-immunoprecipitation

After 24h incubation, supernatants were removed and cells were washed three times with ice-cold phosphate-buffered saline (PBS) and then lysed on ice with 500µL of 1.5% (v/v) Triton X-100, 10mM Tris (pH 7.5), 150mM NaCl, 1mM MgCl$_2$, 1mM MnCl$_2$, 2mM phenylmethylsulfonyl fluoride, 20 µg/ml aprotinin, and 12.5µg/ml leupeptin. Cell lysates were centrifuged at 20,000g for 10min at 4°C and supernatants removed to a fresh tube. Co-immunoprecipitation was performed using the Dynabeads Protein G kit (Life technologies), according to the manufacturer's instructions. The following antibodies were used for immunoprecipitation: mouse anti-human MMP-1 (R&D systems), mouse anti-human integrin α2β1 Ab (clone BHA2.1, Millipore) and mouse IgG isotype control (BD biosciences).

2.15. Trans-endothelial electrical resistance (TEER)

TEER measurements were conducted to monitor BBB maturation and integrity, by using STX2 electrode and EVOM2 meter (World Precision Instruments). STX2 electrode was equilibrated in HBSS buffer and black measurement was registered. The chopstick STX2 electrode was placed vertically in the wells, allowing the longer (external) electrode to touch the bottom of the dish containing the external culture media while preventing the shorter (internal electrode) from reaching the monolayer at bottom of the tissue culture insert. TEER values were obtained by a 4 point measurement system on transwell inserts. Coll-IV coated insert without cells was used as a control.

2.16. Apparent permeability (Papp)

BBB integrity was also analysed by assessing the permeability to 100µg/mL solution of fluorescein conjugated sodium salt (306Da, Sigma-Aldrich) or 1mg/mL fluorescein-dextran solution (3KDa, Life technologies). Briefly, 500µL of fluorescein conjugated molecules was loaded into the apical side of the insert, while the basolateral side contained 2mL of PBS. Solutions were let to permeate the BBB for 45min to 3h at 37°C and 5% CO_2 and 100µL samples were collected from the basolateral side for fluorimetric analysis (FLUOROstar galaxy, BMG Laboratories) using 485nm excitation and emission filters and 590nm emission filter.

Concentrations were obtained by creating a 6-point standard curve with serial dilutions of the permeation solution. Papp was obtained using the equation:

$$Papp \ (cm/s) = (dQ/dt)/C0*A)$$

where dQ/dt is the rate of permeation (µg/sec), C0 is the initial concentration and A is surface area of the monolayer.

2.17. Transmigration assay

Co-culture of hCMEC/D3 and HA and cell stimulation were performed as previously described. Isolated neutrophils or monocytes were gently resuspended in 0.5µM CellTracker green dye (Life technologies) working solution and incubated for 20min on ice. An aliquote of $2x10^6$ neutrophils/monocytes was left unstrained in RPMI with FBS, on ice. Cells were centrifuged and resuspended in DMEM (with 1%FCS, 2%glutamine and 25mM HEPES) to a final concentration of $5.5x10^6$ cells/mL.

Transwells were rinsed and 150ng/mL of IL-8 or MCP-1 (chemoattractants for neutrophils and monocytes respectively) in DMEM (with 1%FBS, 2%glutamine and 25mM HEPES) were added in the lower chamber and 200µl cell suspension ($1.1x10^6$ cells) in the upper chamber. Cells were incubated between 90-120 min at 37^oC, with $5\%CO_2$. Transmigrated cells were collected from the bottom well and gently scraped from the bottom of the transwell, transferred to FACS tubes, centrifuged at 1200rpm for 5min at 4^oC and resuspended in 400µL PBS.

2.18. Immunoblotting

Western blotting was used for chemiluminescent detection of phosphorylated and total proteins. Proteins were separated by electrophoresis, using NuPAGE® 4-12% Bis-Tris Gel (Life technologies) in an XCell SureLock Mini-Cell (Life technologies), filled with the appropriate running buffer (MES buffer for proteins <60kDa, MOPS buffer for proteins >60kDa, Life technologies). A full range rainbow protein molecular weight marker (GE Healthcare Life Sciences) was also loaded. Transfer to a nitrocellulose membrane (Amersham Hyobond – ECL, GE Healthcare Life Sciences) was performed, using the X-Cell II Blot Module (Life technologies) soaked in Transfer Buffer (Life technologies) with 20% methanol (Sigma-Aldrich)/0.6% SDS (Sigma-Aldrich). Membranes were blocked with 0.1% Tween-20, 5% non-fat milk in Tris-buffered saline (Sigma-Aldrich) or 0.1% Tween-20, 5% BSA in Tris-buffered saline prior to staining with primary antibodies overnight. Membranes were then stained with HRP conjugated secondary antibodies for 1h. Washes with 0.1% Tween-20 in Tris- buffered saline were performed between each step. Finally, membranes were

placed in chemiluminescent substrate (Amersham ECL Plus/ Prime Western Blotting Detection System, GE Healthcare Life Sciences) for 1 to 2 min, and exposed to chemiluminescence film (Amersham 70 Hyperfilm ECL, GE Healthcare Life Sciences) and this was developed.

2.19. Flow cytometry

Cells were detached with 5mM EDTA, washed with PBS, fixed with 4% paraformaldehyde (v/w) and blocked with 1% BSA/ 5% human serum (v/v) buffer. Cells were incubated for 1h at room temperature with FITC conjugated anti-human integrin Ab or mouse IgG1 isotype or secondary antibody alone as controls. Flow cytometry was performed on a FACSCalibur (BD Biosciences) cytometer which was calibrated using FACS CaliBRITE (BD Biosciences) beads. The baseline Forward Scatter, Side Scatter and FL1H settings were adjusted using an unstained, unstimulated cell sample. Median fluorescence intensities (MFI) were compared after normalisation to the isotype control. Data was analysed using FlowJo vX.0.6 (Tree star, USA).

For transmigration assays, cells were resuspended in 400µL PBS and 50µL of CountBright Absolute Counting Beads (Life technologies) was added to each tube. 5.5×10^6 unstimulated and unlabelled cells were used to adjust baseline Forward Scatter, Side Scatter and FL1H settings and gate cells of interest. The number of

FL1H positive cells in each condition was assessed by comparing the ratio of bead events to cell events.

2.20. Confocal microscopy

4-well glass slides were pre-coated with human Coll-I and cells seeded and incubated as previously described. For BBB co-cultures, all steps were performed directly in the transwells.

Cells were fixed with 4% paraformaldehyde, blocked with 1% BSA/ 5% human serum buffer and stained. For intracellular targets and F-actin staining, cells were permeabilised with 0.5% saponin (v/v) and stained with phalloidin conjugated with Alexa fluor 594 or Alexa fluor 488 (Life technologies). DAPI was used as a nuclear counterstain and a borosilicate glass cover slip (Fisher Scientific, UK) mounted.

ECM degradation was observed by pre-coating 4-well glass slides with DQ type I or type IV collagen. Cells were fixed with 4% paraformaldehyde and DAPI was used as a nuclear counterstain.

Confocal microscopy was performed on a Leica TCS SP5 Confocal equipped with 405nm diode laser, 488nm argon laser, 543nm and 633nm HeNe lasers and using the Leica Application Suite 2.6.2 software (Milton Keynes, UK). Images were edited using ImageJ software v1.46r (NIH, Maryland, USA).

2.21. Transmission electron microscopy (TEM)

Transwells were rinsed with ice cold PBS and fixed with 0.5% glutaraldehyde in 200mM sodium cacodylate for 30min. Transwells were washed with sodium cacodylate buffer, then sealed and stored in buffer at 4^oC until ready to process. Trans-wells were incubated with rabbit anti-human IgG for 1h and labelled with 6nM protein A gold particles for 2h. Samples were washed in cacodylate buffer and post-fixed in 1% osmium tetroxide and 1.5% potassium ferrocyanide for 1h. After washing in water, transwells were incubated in 0.5% magnesium uranyl acetate overnight at 4^oC, dehydrated in ethanol and propylene oxide, and embedded in EPON resin. Transwells were cut into ultrathin sections and collected on TEM grids, and lead citrate was added as a contrast agent. Sections were analysed using an FEI Tecnai G2 transmission electron microscope, and digital images were captured using Soft Imaging Software.

2.22. Statistical Analysis

Statistical analysis was performed using GraphPad Prism® v5.02 (GraphPad Software Inc, USA). Data are presented as mean ± standard deviation (SD) of three replicate samples per condition and are representative of at least three independent experiments, unless otherwise stated. Statistical analysis was performed using one-way ANOVA and Tukey's range test. For data from repeated measurements a two-way ANOVA and Bonferroni correction were used. Differences between variables were considered statistically significant for p-values lower than 0.05.

Chapter III: ECM modulation of Mtb-driven MMP expression by bronchial epithelial cells

3.1. Introduction

Pulmonary ECM is composed of a network of molecules including type I, III and IV collagen, fibronectin, laminin, elastin and proteoglycans. Coll-I, which is the primary structural fibril of the lung, provides tensile strength and is highly resistant to enzymatic degradation. MMPs are key in TB-associated tissue destruction and the collagenases, particularly MMP-1, are able to degrade fibrillar Coll-I. MMP expression is driven by infected phagocytes and the matrix destruction phenotype is amplified by stromal cells, such as respiratory epithelial cells in pulmonary TB.

Although responsible for tissue destruction, MMPs (particularly MMP-1 and 9) are also involved in lung epithelial repair. Mechanisms involving soluble factors (cytokines, chemokines and growth factors), ECM components, MMPs, focal adhesions and cytoskeletal structures promote cell spreading and migration during re-epithelisation [224]. Cell adhesion to the ECM is mediated by the integrin family of cell surface molecules. Diverse integrin heterodimers are expressed on adult human respiratory epithelial cells [115,225,226]. Of these, integrin α2β1 and α3β1 are constitutively expressed and bind to collagens [227], with integrin α2β1 having a high affinity to Coll-I [228], while α3β1 is also able to bind to other components such as laminins and fibronectin [229]. Integrin engagement to the ECM triggers assembly of an adhesome network, composed of scaffolding molecules (including adhesion receptors, adaptor proteins and actin cytoskeleton) and signalling molecules (including diverse kinases, phosphatases and GTPases) [230]. One of the key signalling molecules is FAK, a multidomain protein displaying docking and signalling functions [231]. FAK signals to several downstream molecules such as the Ras-ERK and the PI3K/Akt-signalling pathways [232]. Integrins can adhere to multivalent

immobilised ligands of the ECM resulting in their clustering on the cell surface at sites of adhesion; cell spreading then strengthens this adhesion. Integrins may also bind soluble monovalent forms of matrix that have been released from the ECM. This requires a high affinity form of the integrin and results in ligand binding without receptor clustering.   In normal lung, the vast majority of Coll-I, a ligand for integrin α2β1, is found in the ECM. However, fragments of Coll-I are released to the airway space and the circulation in TB [85]. It is, therefore, not just the integrin ligand that may be important, but the way in which it is presented to the adherent cell, either as immobilised multivalent protein or in soluble ligand form. Thus, the cell responds specifically to changes in the matrix environment following airway injury. It is likely that an appropriate epithelial-derived MMP-1 activity is required for respiratory tissue repair, while overexpression in later stages of disease may lead to unwanted proteolysis and impede tissue repair and this responses may be regulated by the tissue environment via integrin signalling.

Little is known about the interaction between MMP-1 and the local tissue environment although much evidence indicates that this is key in the inflammatory response. Therefore, in this chapter, the role of individual components of the ECM on Mtb-driven MMP expression will be dissected, as well as the integrin receptors involved in this response.

3.2. Specific aims

Hypothesis: In pulmonary TB, the local ECM environment regulates bronchial epithelial cell-derived MMP-1 gene expression and secretion, affecting tissue repair in later stages of TB disease.

Using primary Normal Human Bronchial Epithelial (NHBE) cells stimulated with conditioned medium from *Mycobacterium tuberculosis* -infected monocytes (CoMtb) I aimed to:

- Test if cell adhesion to ECM components (Collagen I-IV, Fibronectin and Laminin) regulates CoMtb-driven MMP expression and secretion and/or their inhibitors (TIMP-1/2);

- Verify if integrin engagement to the above ECM components regulates CoMtb-driven MMP expression;

- Dissect the pathways involved in MMP modulation by integrin engagement to ECM components.

- Verify how ECM and integrin signalling regulation of CoMtb-driven MMP-1 expression affects cell migration and tissue repair.

3.3. Results

3.3.1. Effect of pulmonary ECM components on MMP secretion by CoMtb stimulated epithelial cells

Our group has demonstrated in the past that Mtb upregulates epithelial cell MMP-1 secretion via a monocyte-dependent network. The monocyte-epithelial signal is transmitted by TNF-synergy with a GPCR ligand. Therefore, to mimic these monocyte-epithelial network, I have used CoMtb has a stimulus in this model instead of direct infecton with Mtb.

First, the kinetics of MMP-1 secretion by respiratory epithelial cells grown in the ECM components Coll-I (100 µg/mL), Coll-IV (250 µg/mL), Fn (20 µg/mL) and Lam (20 µg/mL) were studied using A549 cells (Fig. 12). In CoMtb stimulated samples, MMP-1 levels were shown to reduce in the presence of Coll-I and Lam for all time-points when compared with samples from uncoated wells ($p<0.01$), and showed a 2-fold downregulation at 72h for Coll-I and a 4-fold downregulation in the presence of Lam (Fig. 12a, d). However, no statistically significant difference was shown, between the cells in the absence of matrix and adherent to Coll-IV and Fn ($p>0.05$) (Fig. 12b, c). Subsequent experiments cells were only incubated for 24h since statistically significant differences for MMP-1secretion were found to be already present after 24h.
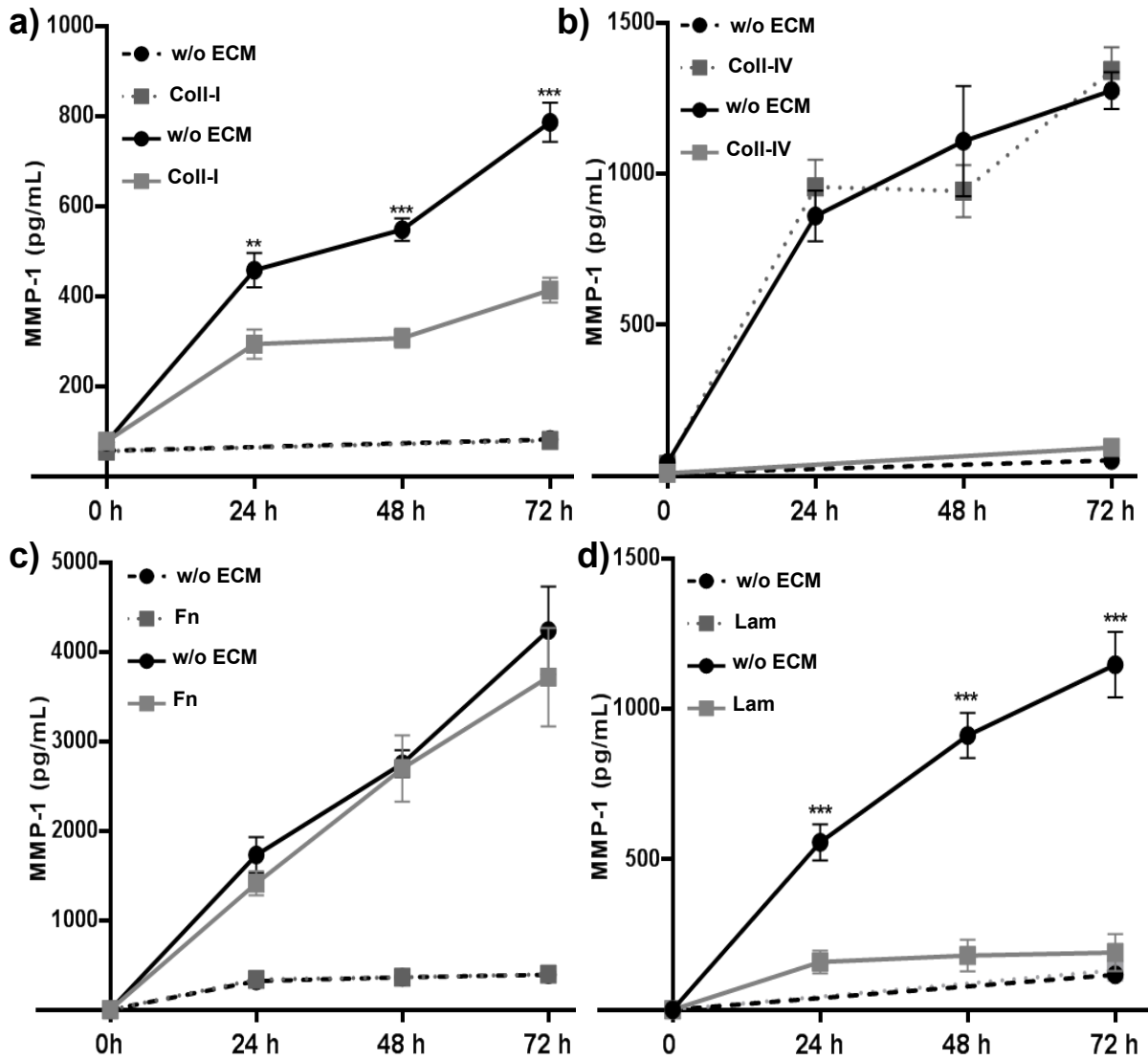
Figure 12. Kinetics of MMP-1 secretion with adhesion to ECM components.

A549 cells were seeded in the presence or absence of human Coll-I (a), Coll-IV (b) Fn (c) or Lam (d), stimulated with 1:5 CoMtb or control medium and incubated between 24-72h. Figures representative of three independent experiments performed in triplicate.

CC- conditioned medium from uninfected monocytes; Coll-I- type I collagen; Coll IV- type IV collagen; Fn- fibronectin; Lam- laminin; CT- conditioned medium from *Mycobacterium tuberculosis* infected monocytes;

To test if this MMP-1 downregulation seen with the presence of Coll-I and Lam is due to cell adhesion to these substrates, dose-response experiments were performed with A549 cells as well as primary NHBE cells (Fig. 13). For both, MMP-1 levels with CoMtb stimulation were lower in the presence of Coll-I in a concentration dependent manner. However, in the dose-response experiments performed with primary NHBE cells, no significant difference was seen in MMP-1 secretion levels with the presence Lam, despite the concentration dependent downregulation seen in A549 cells (Fig. 13 c, d). This might be due to the fact that A549 cells are a carcinoma cell line and hence have modifications in terms of receptors expression and activation of signalling cascades compared with NHBE cells.
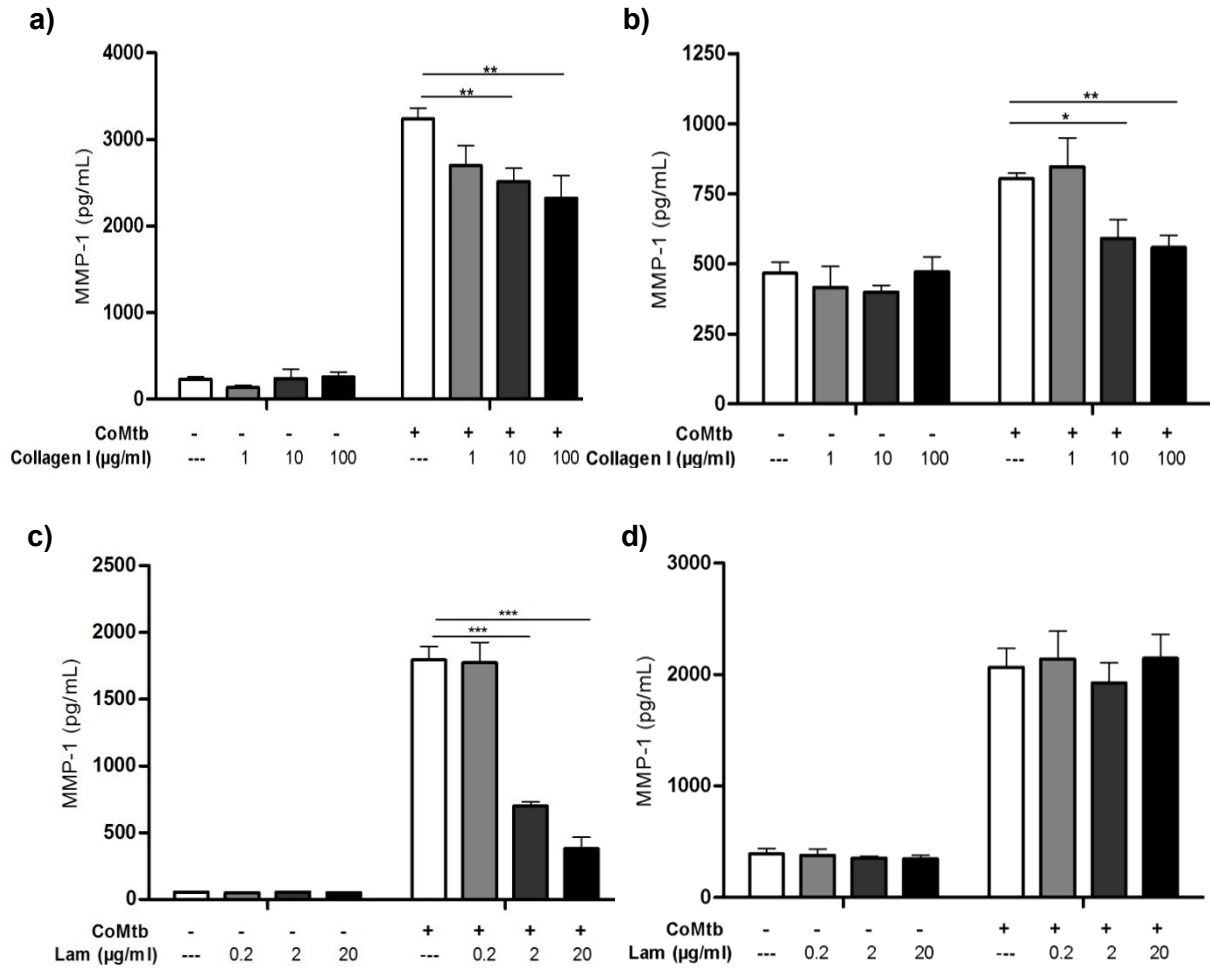
Figure 13. Dose-response of MMP-1 secretion with adhesion to Coll-I and Lam.

A549 (a and c) and NHBE (b and d) cells were seeded in the presence or absence of human Coll-I or Lam, stimulated with 1:5 CoMtb or control medium and incubated for 24h. Figures representative of three independent experiments performed in triplicate.

Collagen I- type I collagen; CoMtb- conditioned medium from *Mycobacterium tuberculosis* infected monocytes; Lam- laminin; NHBE- Normal Human bronchial epithelial cells.

3.3.2. Type I collagen modulates MMP-1 gene expression in CoMtb-stimulated NHBE cells

In normal lung tissue the vast majority of Coll-I is found in the ECM. However, fragments of Coll-I are released to the airway space and the circulation in TB [85], therefore cell adhesion to soluble Coll-I (sColl-I) was also analysed in primary respiratory epithelial cells and compared with MMP-1 in stimulated cells adherent to Coll-I matrix (mColl-I) and in the absence of matrix. NHBE cells grown on plastic or Coll-I produce low MMP-1 concentrations even in the presence of sColl-I, but MMP-1 concentrations are dramatically increased on stimulation with CoMtb. CoMtb-stimulated NHBE cells cultured in the absence of ECM had high levels of MMP-1 secretion which was down-regulated 32% (from 3198.4±238.1 to 2176.5±158.2 pg/ml) when CoMtb-stimulated NHBE cells were adherent to mColl-I, (Fig.14a; $p < 0.001$). Addition of sColl-I increased MMP-1 secretion by 48% (4176.9±245.5 pg/ml). At a transcriptional level, MMP-1 mRNA accumulation decreased 48% in the presence of mColl-I and increased 40% with sColl-I (Fig. 14b). Next, functional MMP collagenolytic activity was investigated and was 4-fold higher from cells adherent to plastic, compared to those adherent to mColl-I ($p < 0.05$) and was 7-fold higher in the presence of sColl-I ($p < 0.001$; Fig. 14c). Since matrix degradation is critically regulated by MMP:TIMP ratios, we investigated the effect of adhesion to ECM on secretion of TIMP-1/2, the main secreted inhibitors of MMP-1. Addition of CoMtb did not affect TIMP-1/2 secretion compared with un-stimulated controls ($p > 0.05$). However, in the presence of sColl-I, TIMP-1 secretion by CoMtb-stimulated NHBE cells was downregulated by 31% (from 22.4±0.7 to 15.3±0.6 ng/ml) and TIMP-2 by 30% (from

108.3±7.4 to 75.3±9.2 pg/ml) (Fig. 14d, e). Adhesion to mColl-I had no significant effect on TIMP-1/2 concentrations.

3.3.3. Effect of adhesion to type I collagen matrix on other MMPs

The effect of adhesion to Coll-I on other MMPs was investigated. Secretion of MMP-3, a stromelysin which may activate MMP-1 and -9, was upregulated from 327.2±24.5 pg/ml to 523.3±61.8 pg/ml in CoMtb-stimulated NHBE cells adherent to mColl-I ($p < 0.001$) but was unaffected by sColl-I (Fig. 15a). MMP-9 concentrations were upregulated by 46% in NHBE cells adherent to mColl-I (50.3±2.2ng/ml) and by 81% in cells adherent to sColl-I (142.5±4.7 ng/ml) compared with controls (27.2±2.2 ng/ml; Fig. 15b). Increased MMP-9 secretion was also seen in unstimulated NHBE adherent to plastic on addition of sColl-I. No differences were detected in MMP-9 secretion after adhesion to Coll-IV or to Fn. MMP-2 secretion from NHBE cells was not altered in the presence of Coll-I (Fig. 15e).
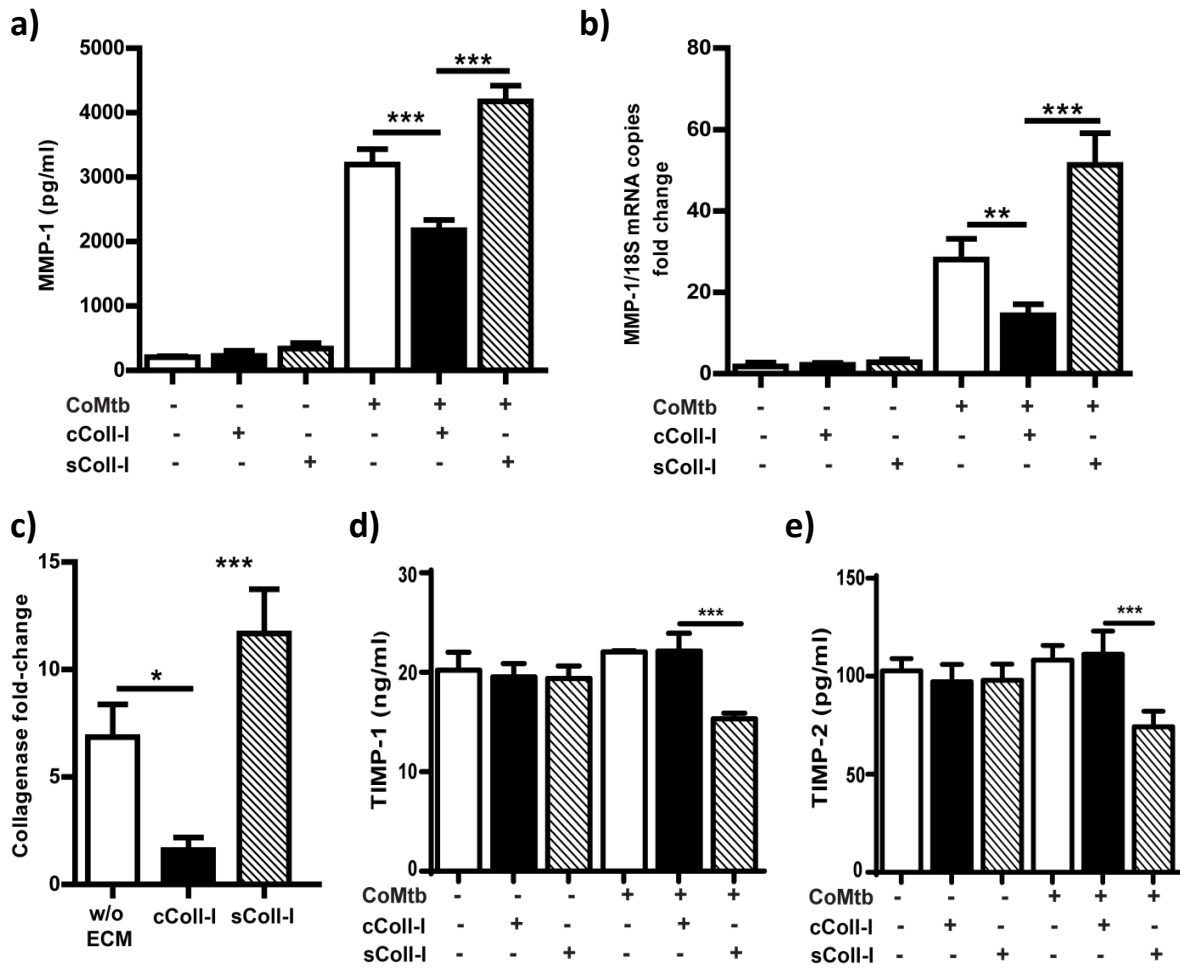
Figure 14. Type I collagen regulation of MMP-1 gene expression and secretion by CoMtb-stimulated NHBE cells.

NHBE cells were cultured in the absence or presence of 100µg/ml of coated or soluble human type I collagen and stimulated with CoMtb in a 1:5 dilution or control medium. (a) MMP-1 secretion, (b) MMP-1 gene expression, (c) collagenolytic activity and (d, e) TIMP-1/2 secretion. Samples were collected at 24h post-stimulation for secretion analysis and at 6h post-stimulation for gene expression. Figure representative of 3 independent experiments performed in triplicate. *p<0.05; **p<0.01; ***p<0.001. mColl-I- matrix type I collagen; sColl-I soluble type I collagen; CoMtb- conditioned medium of *Mycobacterium tuberculosis* infected monocytes; w/o ECM- without extracellular matrix. MMP-1- matrix metalloproteinase I; TIMP- tissue inhibitor of metalloproteinases.
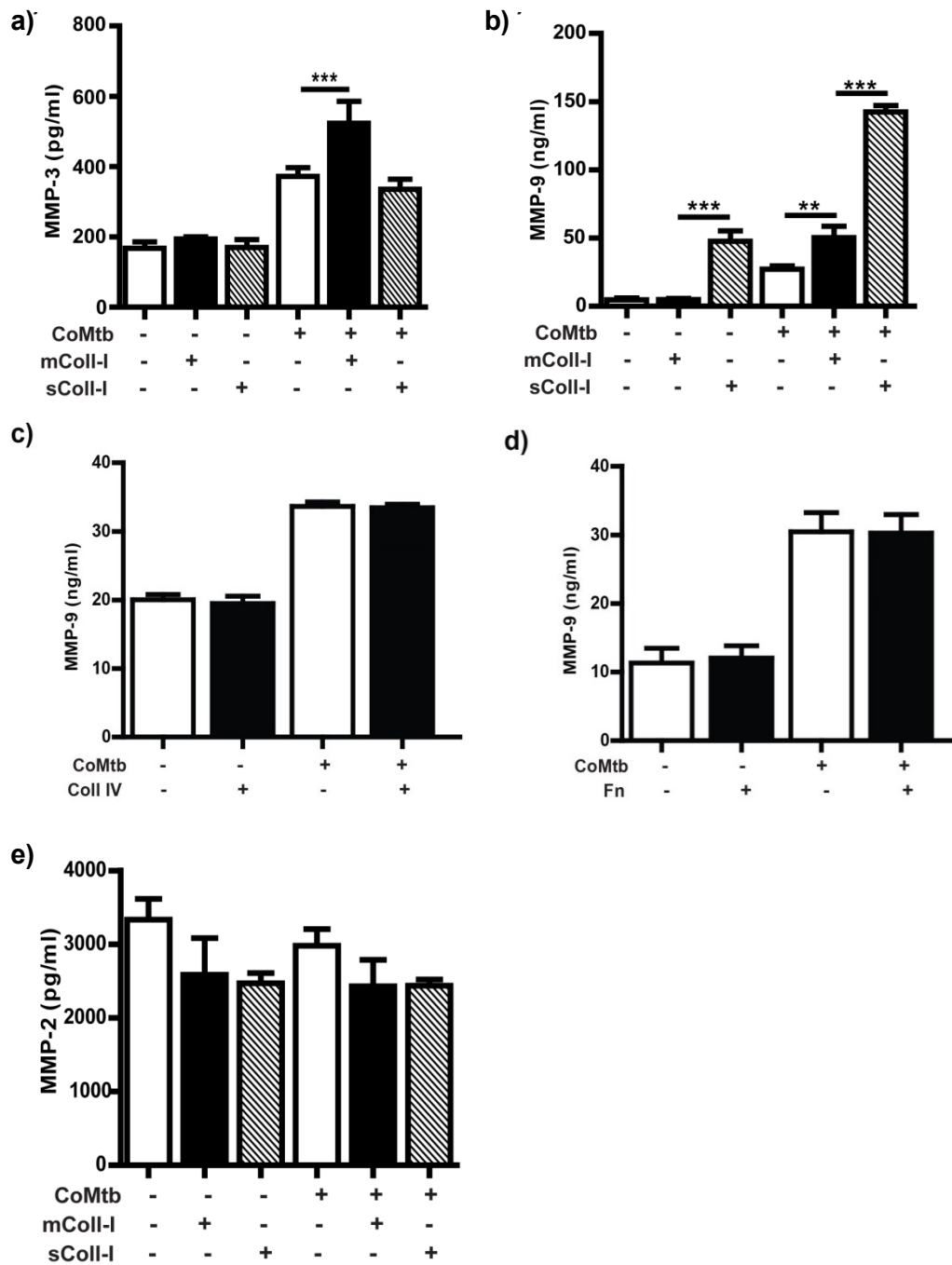
Figure 15. MMP-3, -9 and -2 secretion by NHBE cells adherent to type I collagen.

NHBE cells were cultured in the absence of ECM or in the presence of coated or soluble human Coll-I, -IV or Fn and stimulated with CoMtb in a 1:5 dilution or control medium. Concentrations of secreted (a) MMP-3, (b-d) MMP-9 and (e) MMP-2. Samples were collected at 24h post-stimulation and analysed by Luminex assay. Figure is representative of 3 independent experiments performed in triplicate. **p<0.01; ***p<0.001. mColl-I- matrix type I collagen; sColl-I soluble type I collagen; Coll-IV-type IV collagen; CoMtb- conditioned medium of *Mycobacterium tuberculosis* infected monocytes; ECM- extracellular matrix; Fn-fibronectin; MMP- matrix metalloproteinase.

3.3.4. Integrin α2β1 but not α3β1 regulates MMP-1 expression in NHBE cells

Next, I investigated the mechanisms by which integrin subunits regulate the MMP-1 response to Coll-I. Integrin-mediated adhesion is divalent cation-dependent and can be abolished by chelation of Mg^{2+} and Ca^{2+} [233]. In NHBE cells, the MMP-1 suppression observed in the presence of mColl-I was abolished by 2mM EDTA (Fig. 16a). To investigate the nature of receptor engagement, NHBE cells were incubated with latex beads coated with Coll-I (Fig. 16b) to allow receptor occupancy and clustering with localised cell spreading. This resulted in MMP-1 suppression (from 1292.1 ± 68 pg/ml to 828.9 ± 33 pg/ml; $p < 0.001$) equivalent to that seen following adhesion to mColl-I (898 ± 72 pg/ml; $p > 0.05$).

To identify the specific collagen-binding integrins involved in the MMP response, plates were coated with anti-α2β1 or α3β1 integrin Abs, which can be used as integrin agonists [234-236]. CoMtb-stimulated NHBE cells adherent to anti-α2β1 Abs had similar MMP-1 mRNA accumulation (5-fold change) and protein secretion (1223 pg/ml) to those observed in cells adherent to mColl-I (Fig. 16c, d). In contrast, adhesion to anti-α3β1 Abs did not cause a significant change in MMP-1 gene expression and secretion compared to cells cultured in the absence of ECM ($p > 0.05$). These results show that integrin α2β1 mediates the decrease in MMP-1 gene expression and secretion, as a result of integrin occupancy and clustering with localised cell spreading.
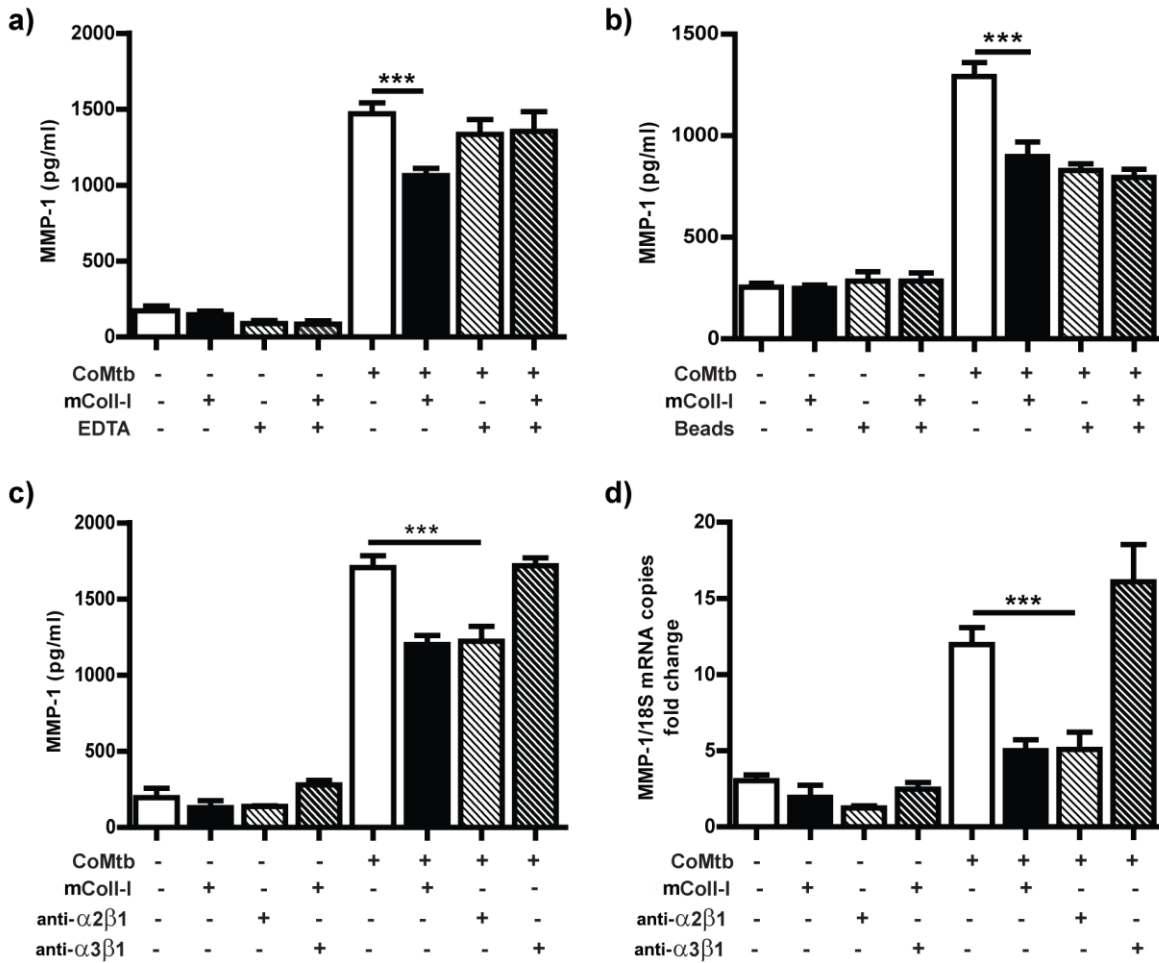
Figure 16. Integrin α2β1 regulation of MMP-1 gene expression and secretion with adhesion to type I collagen.

NHBE cells were cultured in the presence or absence of pre-coated human type I collagen and stimulated with CoMtb in a 1:5 dilution or control medium, in presence or absence of (a) 2mM EDTA; (b) type I collagen pre-coated latex beads and/or (c, d) anti-integrin α2β1 or anti-integrin α3β1 blocking monoclonal antibodies. Concentrations of secreted MMP-1 (a, b, c) were analysed from samples collected at 24h post-stimulation and for MMP-1 gene expression (d) at 6h post-stimulation. Figure is representative of 3 independent experiments performed in triplicate.***p<0.001; mColl-I- matrix type I collagen; CoMtb- conditioned medium of *Mycobacterium tuberculosis* infected monocytes; MMP- matrix metalloproteinase.

3.3.5. CoMtb-stimulated MMP-1 secretion is regulated by FAK and the actin cytoskeleton

I investigated whether CoMtb altered surface expression of collagen-binding integrins by flow cytometry (Fig. 17 a-c). No significant differences were seen in mean fluorescence intensities (MFIs) for the α2 or α3 integrin subunits between the different conditions ($p > 0.05$). Since integrin activation and clustering, may signal via the cytoskeleton, I measured the amount of polymerised F-actin inside the cells by laser scanning cytometry (Fig. 17d). Stimulation with CoMtb of NHBE cells grown on tissue culture plastic increased the amount of F-actin MFI per cell by 22% (from 1840.4±168 to 2359.5±143 MFI/cell; $p < 0.05$). In cells adherent to plastic, the addition of sColl-I increased F-actin to levels seen on adhesion to mColl-I (2287.8±193 MFI/cell) and further increased levels in CoMtb-stimulated cells (3040.8±69 MFI/cell; $p < 0.01$). In cells adherent to mColl-I the baseline level of F-actin was similar to that following CoMtb stimulation in cells adherent to plastic and no further increase was seen on the addition of CoMtb ($p > 0.05$). Confocal microscopy revealed that in CoMtb-stimulated NHBEs cultured on mColl-I, integrin α2β1 was mainly localized at the basal side of the cells, correspondent to the cell-matrix interface. In contrast, there was punctate integrin α2β1 staining in cells cultured in the presence of sColl-I, while no marked integrin staining was seen in the absence of Coll-I (Fig. 17e). Thus, CoMtb stimulation and α2β1 integrin occupancy act thorough distinct signalling pathways, and are additive in their effects on actin polymerisation; α2β1 integrin occupancy and clustering with cell spreading increases baseline actin polymerization that is not increased further by CoMtb.
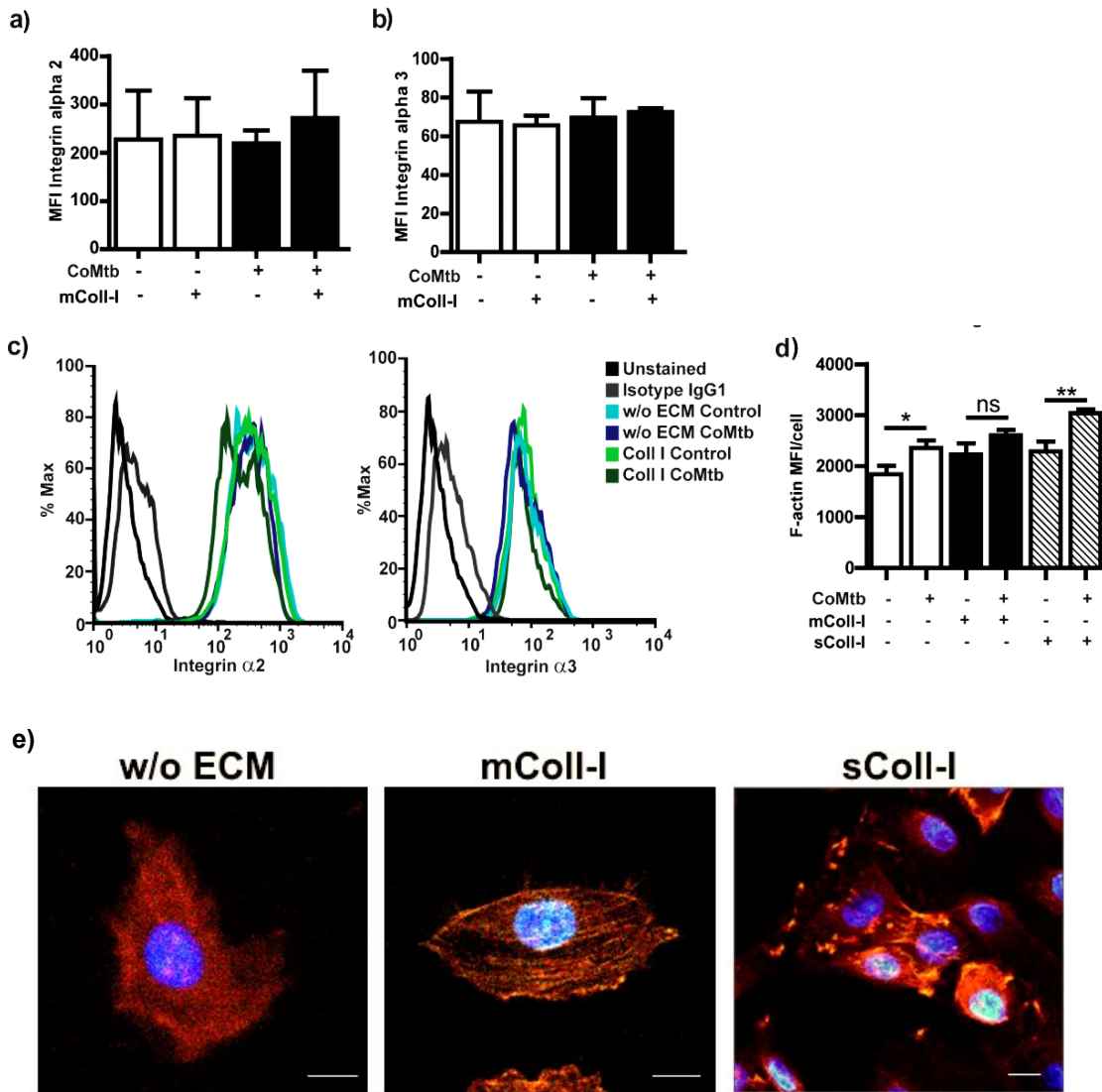
Figure 17. Integrin α2β1 surface expression and reorganisation and actin polymerisation with adhesion to type I collagen.

NHBE cells were seeded in the presence or absence of Coll-I and stimulated CoMtb. Cells were stained with FITC conjugated anti-integrin Abs, or IgG1 isotype control. Figures represent MFI for (a) integrin α2 and (b) integrin α3. (c) Flow cytometry histograms for integrin α2 and integrin α3 subunits. (d) Laser scanning cytometry analysis of NHBE cells stained for F-actin with phalloidin conjugated with Alexa Fluor 633 and nucleic acids with DAPI. e) cells stained with DAPI (blue) for nucleic acid, phalloidin conjugated with Alexa Fluor 594 (red) for F-actin and FITC conjugated anti-integrin α2 Abs (green) for integrin subunit α2. Yellow colour shows co-localization of F-actin and integrin α2β1. Scale bar: 10μm; *p<0.5; **p<0.01; ns-non significant; CoMtb-conditioned medium from *Mycobacterium tuberculosis* infected monocytes; Max- percentage of maximum; MFI- Median fluorescence intensity; mColl-I matrix type I collagen; sColl-I soluble type I collagen; w/o ECM-without extracellular matrix.

Inhibiting actin polymerisation with 4µg/ml cytochalasin D in control cells mimicked the effect of adhesion to mColl-I on MMP secretion in response to CoMtb reducing MMP-1 by 30% (from 3198.4±238 pg/ml to 2229.7±269 pg/ml; Fig. 18a). Cytochalasin D prevented the effect of sColl-I on the upregulation of MMP-1 (p<0.001). Cytochalasin D had no significant effect on MMP-1 secretion in cells adherent to mColl-I. 10µM FAK chemical inhibitor II has a similar effect as cytochalasin D and suppressed MMP-1 secretion by 41% (from 1536.5±75 pg/ml to 906.9±326 pg/ml) in cells on plastic and 64% (2969.2±136 pg/ml to1064.8±240 pg/ml) in cells exposed to soluble coll-I (Fig. 18b). Downstream of FAK, the PI3K and Erk-1/2 pathways were analysed since these are known regulators of MMP-1 expression. Blockade of Erk1/2 with 10µM PD169316 lead to a suppression of 33% for MMP-1 in stimulated cells adherent to plastic but did not cause any further downregulation in cells adherent to mColl-I (p>0.05, Fig. 18c), while blockade of PI3k lead to increased MMP-1 by cells both in presence and absence of mColl-I to similar levels (approximately 2250pg/ml, Fig. 18d).

When phosphorylated levels of Akt (p-Akt; a downstream effector of PI3k) and Erk-1/2 (p-Erk-1/2; p42/p44) were analysed, p-Erk-1/2 levels were increased in CoMtb-stimulated cells in the presence of sColl-I and decreased with mColl-I, compared with stimulated NHBEs in the absence of matrix (Fig. 18e).

These results demonstrate that dynamic changes in actin polymerization affect p-Erk-1/2 levels, which in turn affects CoMtb-driven MMP-1 secretion. Activation of FAK has a role in CoMtb stimulation of MMP-1 independent of the ECM.
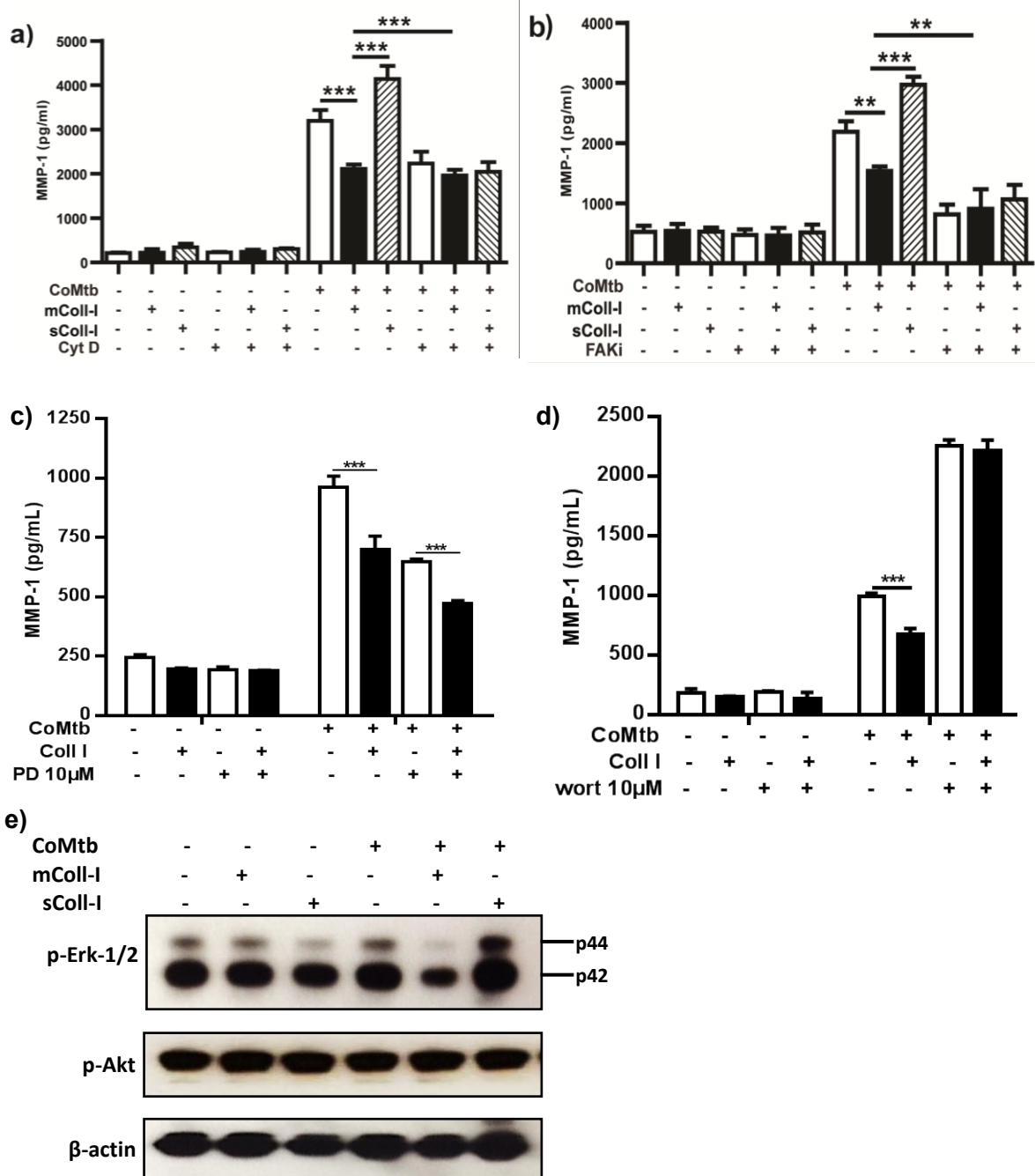
Figure 18. Effect of cytochalasin D and Focal Adhesion Kinase inhibition on CoMtb-driven MMP-1 secretion.

NHBE cells were seeded in the absence of matrix or in the presence of of coated or soluble type I collagen, and incubated for 2h with (a) 4µg/ml cytochalasin D, (b) 10µM FAKi (c)10µM PD169316 or d) 10µM wortmanin and stimulated with CoMtb or control medium. MMP-1 concentrations were measured at 24h post-stimulation. (e) western blot of phosphorylated Erk1/2 and Akt, using β-actin as loading control. Figures are representative of 3 independent experiments performed in triplicate. CoMtb- conditioned medium from *Mycobacterium tuberculosis* infected monocytes; MMP- matrix metalloproteinase; mColl- matrix type I collagen; sColl-2- soluble type I collagen; wort- wortmanin.

3.3.6. Adhesion to collagen matrix, MMPs and cell migration and repair.

Confocal microscopy demonstrated that MMP-1 staining in CoMtb stimulated cells cultured, in the absence of ECM, is distributed throughout the cell membrane. In cells cultured on mColl-I, MMP-1 expression was decreased compared to cells exposed to sColl-I and the distribution was focal instead of diffuse (Fig. 19a). This suggests that secreted MMP-1 is localised to ligand-occupied α2β1. To confirm the interaction between α2β1 integrin receptors and MMP-1, co-immunoprecipitation was performed using an antibody against α2 subunit and then western blot was performed for both α2 integrin and MMP-1. This suggested a degree of direct association between α2β1 integrin and MMP-1(Fig. 19b), which is consistent with the literature [17].
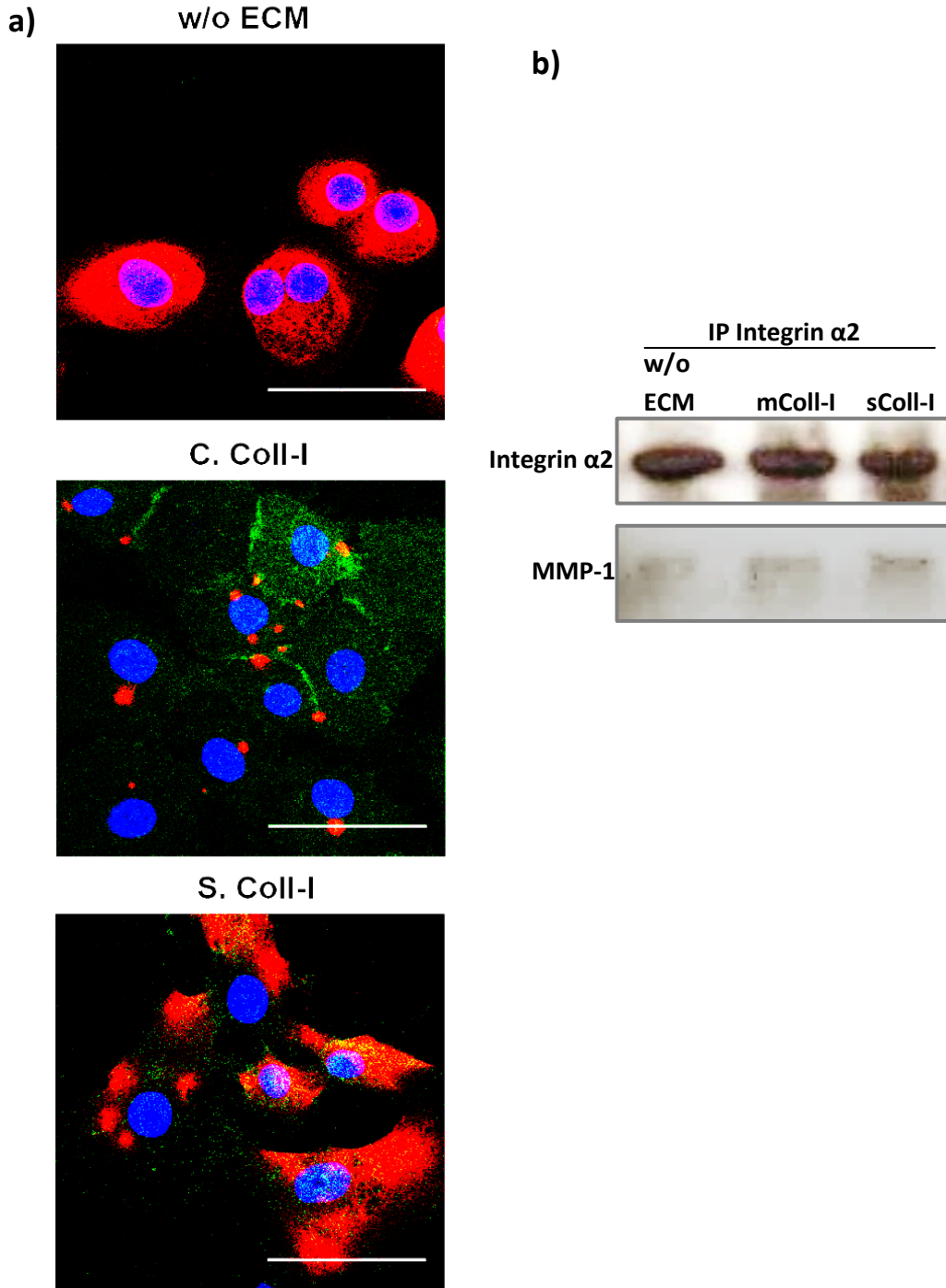
Figure 19. MMP-1 localization and interaction with integrin α2β1.

NHBE cells were seeded in 4-well glass slides or plates in the presence or absence of matrix or soluble Coll-I and stimulated with CoMtb in a 1:5 dilution. (a) Cells were fixed with 4% paraformaldehyde and stained with DAPI (blue) for nucleic acid, FITC conjugated anti-integrin α2 Ab, anti-human MMP-1 primary Ab and Cy5 conjugated goat anti-rabbit secondary Ab (red). (b) Cells were lysed on ice, imunoprecipitated with an anti-integrin α2 antibody and blotted for integrin α2 and MMP-1. Scale bar: 50μm. mColl-I- matrix type I collagen; sColl-I- soluble type I collagen; IP-immunoprecipitation; w/o ECM- without extracellular matrix.

To investigate the functional consequences of the collagen matrix on cellular migration and repair, wound healing assays were performed. CoMtb-stimulated NHBE cells on mColl-I migrated 28% (p<0.001) faster than cells in the absence of ECM (poly-L-lysine coated wells) and 60% faster than cells in the presence of sColl-I (Fig. 20b, c). In the absence of CoMtb, no statistically significant differences were seen in rates of migration between the different conditions (Fig. 20a). Following addition of CoMtb, cells cultured on mColl-I and in the absence of ECM, migrated significantly faster, taking approximately 2 hours less to reach similar relative wound density coverage compared with unstimulated controls (Fig. 20a, b). In contrast, NHBE cells cultured in the presence of sColl-I migrated slower than the corresponding controls with 21-49% lower relative wound density coverage at the corresponding time-point (p<0.01).
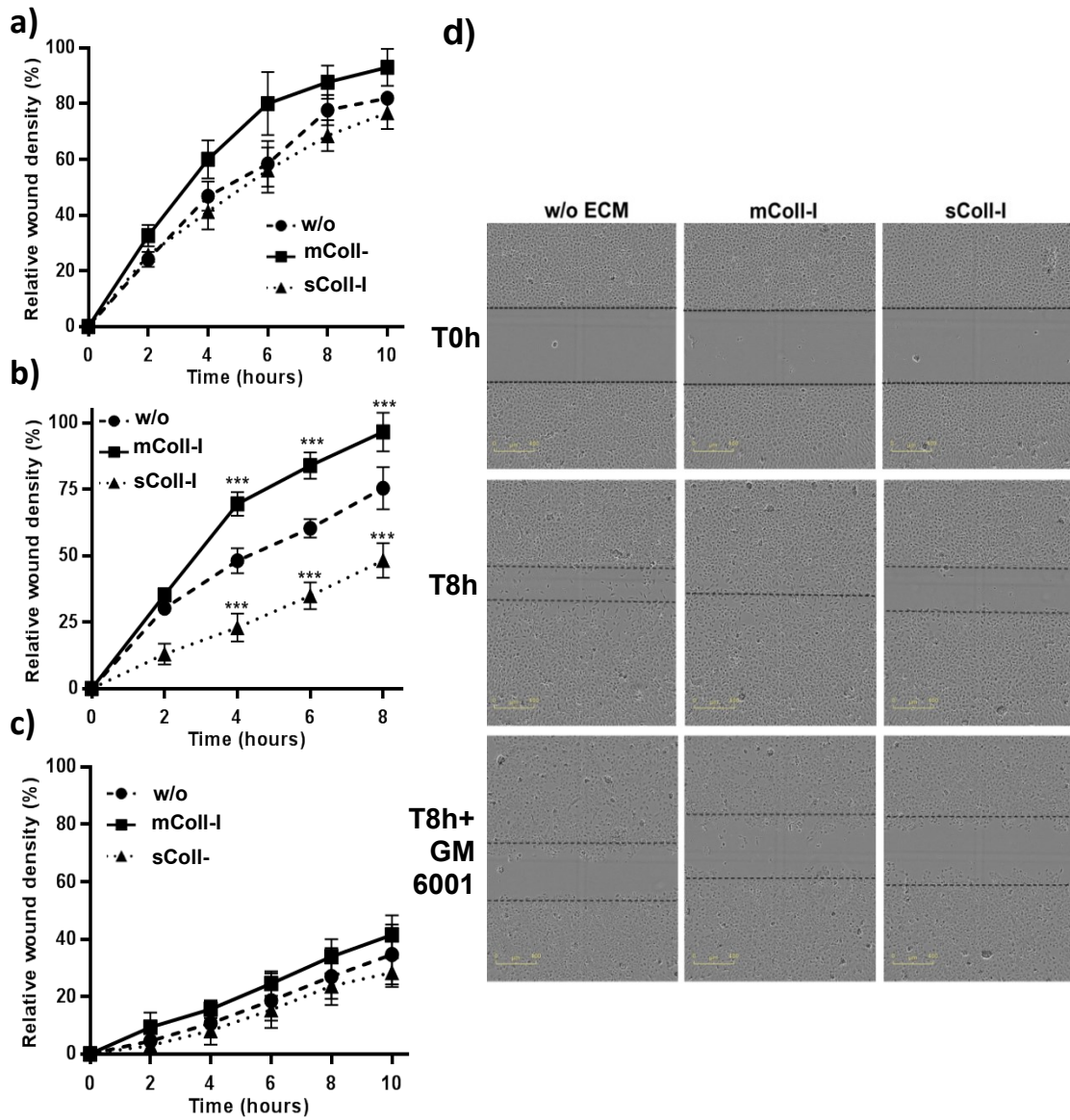
Figure 20. NHBE cell migration and wound healing following adhesion to type I collagen.

NHBE cells were seeded in 96-well plates in the presence or absence of coated or soluble type I collagen, a wound was created in the cell monolayer and wound closure was analysed for wells with control medium (a), CoMtb (b, d) or CoMtb+10µM GM6001 chemical inhibitor (c, d). Images were acquired at 2h intervals from wound creation (c). Relative wound density corresponds to the amount of wound coverage by migrating cells. Scale bar: 400µm. Figures are representative of 3 independent experiments performed in triplicate. ***p<0.001; mColl-I- matrix type I collagen; sColl-I- soluble type I collagen; w/o ECM- without extracellular matrix.

3.4. Discussion

It is increasingly evident that the ECM environment is at least as important in regulation of cellular function as soluble molecular factors [109]. In the present study I demonstrate that the matrix environment may also be a key factor in the respiratory epithelial response to Mtb infection. When NHBEs adherent to a Coll-I matrix were stimulated with CoMtb their migratory ability increased by almost 30% compared with cells in the absence of ECM, MMP-1 secretion and collagenolytic activity was decreased and MMP-1 was shown to cluster at cell edges. In contrast, adhesion to sColl-I, which is associated with extensive inflammation, decreased NHBEs migratory ability by more than 50% when compared with cells adherent to mColl-I. Cells also showed an increased collagenolytic activity, which is consistent with a tissue destruction phenotype.

Coll-I was shown to modulate gene expression and secretion of MMP-1 by NHBEs in response to CoMtb via integrin α2β1 engagement and signalling. MMP-1 gene expression and secretion by respiratory epithelial cells is increased by cell binding to sColl-I, while adhesion to Coll-I matrix suppresses MMP-1 secretion. TIMP-1/2 concentrations secreted by CoMtb-stimulated cells decreased approximately 30% in the presence of sColl-I, further contributing to increased matrix breakdown. The relative increase in MMP-1 to TIMP-1/2 activity was functionally important, causing a 7-fold increase in collagenase activity in CoMtb-stimulated NHBE cells in the presence of sColl-I compared with adhesion to mColl-I. NHBE cell adhesion to other components of the lung's ECM including Coll-IV and Fn, did not affect MMP-1 secretion, demonstrating that there is a tissue-specific response.

MMP-3 secretion was also upregulated in CoMtb-stimulated NHBEs adherent to coll-I matrix compared with sColl-I. MMP-3 is an activator of proMMP-1 and 9 [11,237], and is implicated in cell migration and wound healing, independently of protease activity [238]. MMP-9 was upregulated with adhesion to Coll-I even though MMP-9 is unable to cleave fibrillar collagens and so cannot cause Coll-I breakdown [13]. However, MMP-9 is involved in macrophage recruitment in murine and zebra fish models of TB [239,240], in repair of bronchial epithelial cells *in vivo* [14,15] and MMP-9 mRNA has been shown to be stabilised by integrin α3β1 in immortalised keratinocytes via Ras signalling [241].

The effect caused by adhesion to Coll-I was integrin-dependent and was disrupted by EDTA pre-treatment of cultures. MMP-1 secretion was regulated by integrin α2β1 but not by integrin α3β1, the other major collagen-binding integrin expressed on respiratory epithelial cells. The presence of Coll-I or CoMtb did not alter the surface expression of integrin α2β1 which indicates that the effects on MMP-1 expression are caused by events after ligand binding.

Our data demonstrates that in CoMtb-stimulated NHBE cells FAK has an important role in regulation of MMP-1 secretion. After integrin engagement, it is known that there is activation of FAK, followed by actin cytoskeleton reorganisation and activation of signalling cascades, (including PI3K, ERK and GTPases) [231]. Research in malignancy has highlighted the importance of FAK phosphorylation in dynamic regulation of focal adhesion and expression of MMPs [231,242]. Downstream of FAK, it has been demonstrated that Cdc42 decreases MMP-1

expression through Erk-1/2 inhibition in activated human keratinocytes and skin fibroblasts adherent to mColl-I [243,244]; Erk-1/2 is a key kinase involved in TB-mediated MMP-1 regulation in bronchial epithelial cells (data not published from Singh S.). FAK is also a positive regulator of PI3K, and our group has recently shown that PI3K is an important negative regulator of MMP-1 and its blockade leads to MMP-1 upregulation in CoMtb-stimulated NHBE cells [245].
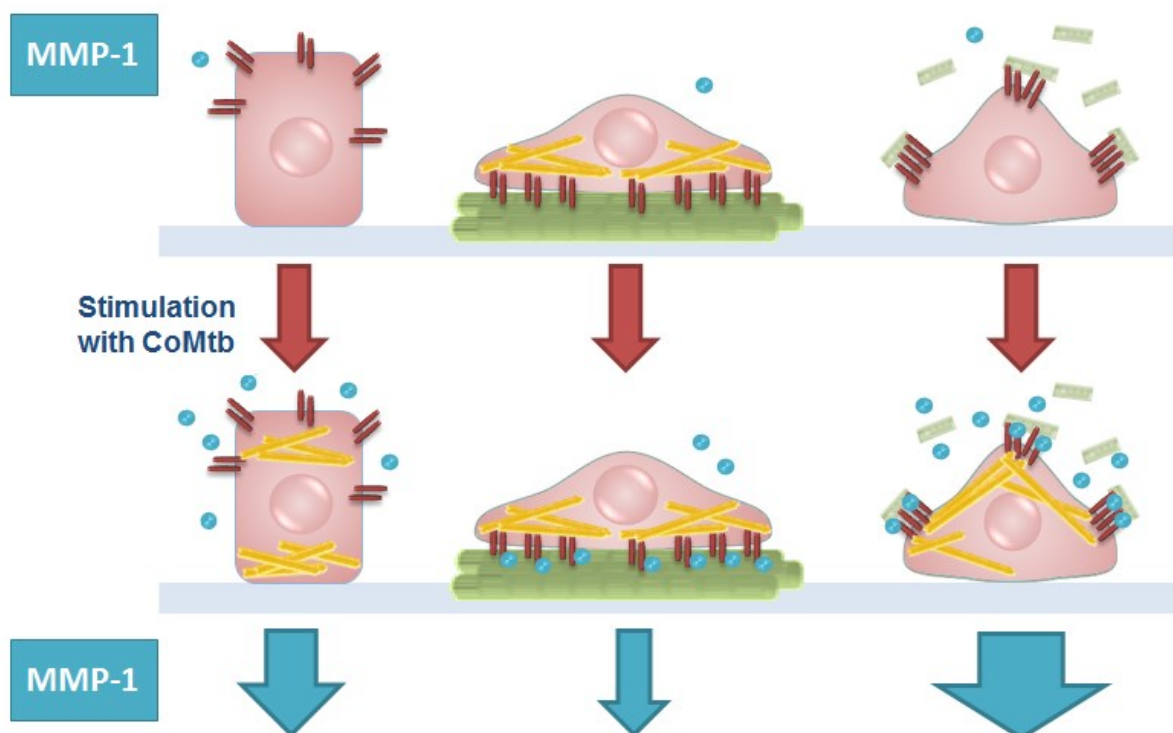
Figure 21. Dynamics of TB-associated MMP-1 expression in NHBE cells adherent to soluble and coated type I collagen.

Schematic summarization of the effects of adhesion to coated or soluble type I collagen (green) binding α2β1 integrin (red) and actin cytoskeleton (yellow) rearrangements on MMP-1 production (blue) in NHBE cells following stimulation with CoMtb. Thickness of blue arrows represents quantity of secreted MMP-1.

CoMtb- conditioned medium from *Mycobacterium tuberculosis* infected monocytes; MMP-1- matrix metalloproteinase 1; NHBE- normal human bronchial epithelial cells.

Differential effects on cell signalling events may depend on integrin occupancy and/or clustering (Fig. 21). I showed that increased MMP-1 expression on addition of sColl-I to NHBE cells attached to plastic, was due to integrin receptor occupancy without clustering. Decreased MMP-1 expression in cells grown on mColl-I is due to integrin receptor occupancy and clustering with cell spreading, and can be replicated with NHBE cell binding of Coll-I -coated beads. Such data indicate involvement of the actin cytoskeleton. CoMtb and adhesion of cells to soluble or immobilized Coll-I both increased F-actin levels by a similar amount, and the combination of CoMtb stimulation and sColl-I had an additive effect on F-actin levels. The data show that dynamic increases in actin polymerisation are responsible for upregulation of MMP-1 secretion by CoMtb and sColl-I from cells adherent to plastic in which polymerised actin levels are initially low. Conversely, if actin polymerisation and FAK activation are elevated in cells on mColl-I, the inability to increase these events further may underlie the inhibition of MMP-1 production when cells are adherent to mColl-I.

As well as affecting MMP-1 expression, the adhesion of NHBE to soluble and matrix Coll-I induced a reorganization of integrin α2β1 and a different localisation of MMP-1. Similarly, in migrating keratinocytes, there is direct binding of pro-MMP-1 to integrin α2β1 and the ternary complex formed between integrin α2β1, Coll-I and pro-MMP-1 spatially confines proteolysis to specific points of cell-matrix contacts which allow directed cell migration. This may also be important in host responses to TB [17,246,247]. In my studies, adhesion to collagen matrix decreased MMP-1 secretion but increased cell migration by almost 30% compared to CoMtb-stimulated cells in the absence of ECM. Thus, MMP-1 expression and activity in response to CoMtb

depends on the matrix environment. These findings demonstrate for the first time in TB that MMP-1 secretion is involved in cell migration on mColl-I and may have a role in tissue repair.

Taken together the present data show that, in TB, bronchial epithelial cell adhesion to Coll-I matrix is associated with integrin α2β1 occupancy and clustering which leads to decreased MMP-1 secretion and collagenolytic activity and enhanced cell migration instead of collagen breakdown. In this situation, MMP-1 is co-localized with epithelial α2β1 resulting in localised collagen proteolysis and enhanced cell migration, promoting epithelial monolayer repair with preservation of the ECM. In contrast, soluble Coll-I leads to integrin α2β1 occupancy without clustering, and increases the production of MMP-1 and collagenolytic activity by CoMtb stimulated NHBEs through effects on the actin cytoskeleton and activation of FAK. The *in vitro* effects of soluble Coll-I demonstrated here may reflect the situation *in vivo* when ECM destruction due to Mtb-infected phagocytes results in fragments of Coll-I binding luminal α2β1integrins. Local production of sColl-I by MMP-1 would shift bronchial epithelial cells towards a vicious cycle of matrix degrading phenotype with escalating MMP-1 production and tissue destruction. Here I propose a novel mechanism in which the local ECM environment can determine the tissue MMP response to TB and which may be amenable to targeted drug therapy.

Chapter IV: Integrin regulation of MMP secretion by monocytes in TB

4.1. Introduction

The inflammatory response requires trans-endothelial extravasation and migration of leukocytes within the inflamed tissue environment and localisation of the affected area. During diapedesis, monocytes start to interact with ECM components such as, fibronectin, collagen, laminin-111. It has been suggested that monocytes in the presence of ECM components or fibrinogen show an enhanced phagocytic and oxidative burst function. Cells interact with the ECM via integrin receptors and integrin-mediated activation of monocytes is characterised by a tyrosine-kinase dependent pro-inflammatory signalling response [248].

Table 10- Integrins expressed by monocytes.

Integrin		Ligands
	α1	Collagens (++type IV), laminin
β1	α4	Fibronectin, VCAM-1
	α5	Fibronectin
	α6	Laminin
	αM	ICAM-1, fibrinogen
β2	αL	ICAM-1, -2, -3, collagens
	αX	Fibrinogen, collagen
β3	αV	Collagens, fibronectin, fibrinogen, vitronectin

ICAM- intracellular adhesion molecule; VCAM- vascular cell adhesion molecule

Primary human monocytes express 8 integrin heterodimers (Table 10): α1β1, α3β1, α4β1, α5β1, αVβ3, αXβ2, αMβ2 and αLβ2 [249]. Monocyte recruitment in acute inflammation is mediated, in part, by the β2-integrin receptors, αLβ2 (LFA-1), αMβ2

(MAC-1) and αXβ2 binding to vascular ICAM-1 [250], while integrin α4β1 promotes monocyte arrest and adhesion to VCAM-1[251]. Engagement of β2-integrins leads to inflammatory cell activation and induction of genes encoding for IL-1β and TNF-α [252,253], and has been implicated in modulation of AP-1 and NF-κB activity [254-256]. Integrin αvβ3 is also involved in monocyte recruitment by modulating αLβ2 integrin-dependent monocyte adhesion to ICAM-1. Also, monocytes lacking β3 integrins revealed weak migratory ability [257].

Integrin αvβ3 has also been involved in MMP-2 and 9 activation, interaction with MT1-MMP and cell migration *in vitro* and *in vivo* models of cancer [258-260]. Furthermore, integrin αvβ3 has also been associated with tissue damage in cancer, since overexpression of αvβ3 integrin in breast cancer cells increased formation of osteolytic lesions in mouse models [261].

The tuberculous granuloma is rich in recruited monocytes and monocytes-derived cells which are important sources of MMPs that are strongly implicated in tissue destruction in TB. However, there are no data on how integrin-dependent adhesion to the lung micro-environment might regulate MMP gene expression and secretion from monocytes in TB. Therefore, in this chapter, I will analyse the role of ECM components in regulation of MMP expression in TB, as well as the involvement of specific integrins. This will be compared and contrasted with the effect seen in respiratory epithelial cells in the previous chapter.

4.2. Specific aims

Hypothesis: Integrin-dependent adhesion to the lung ECM micro-environment regulates MMP secretion by monocytes and monocyte-derived cells in TB.

Using primary monocytes infected with Mtb or stimulated with CoMtb, I aimed to:

- Test if cell adhesion to Coll I-IV, Fn and Lam regulates gene expression and secretion of MMPs and their tissue inhibitors (TIMP-1/2);

- Analyse if integrin surface expression changes with Mtb infection and/or adhesion to ECM components;

- Test if integrin activation and signalling by engagement to the ECM regulates the production MMP by infected monocytes;

- Analyse the functional consequences of integrin signalling and MMP production on monocyte migration during infection.

Understanding the roles of the ECM on MMP/TIMP expression is essential for the development of models to investigate new approaches to reducing tissue destruction.

4.3. Results

4.3.1. Effect of adhesion to components of the ECM on MMP-1 expression and secretion by Mtb-infected monocytes

To test the role of the ECM regulation of MMP expression by primary human monocytes in a cellular model of pulmonary TB, plates coated with 100μg/ml Coll-I, 250μg/ml Coll-IV, 20μg/ml Fn and 20μg/ml Lam were used to represent the lung's ECM, as in the previous chapter.

Adhesion to Coll-I, Fn and Lam by Mtb-infected primary human monocytes drove an MMP-1 upregulation of 60% (from 1208.1±186pg/ml to 1934.4±135pg/ml), 63% (1970.3±95pg/ml) and 115% (2606.1±207pg/ml), respectively (Fig. 22 a-d). Adhesion to Coll-IV caused MMP-1 secretion levels equivalent to the ones from cells in the absence of ECM ($p > 0.05$). At the transcriptional level, the presence of matrices in Mtb infection also induced an increased MMP-1 mRNA accumulation, with a 2.6-fold upregulation with Coll-I and a 4.3-fold upregulation with Fn and 3.5-fold with Lam (Fig. 22e-g; $p < 0.001$).
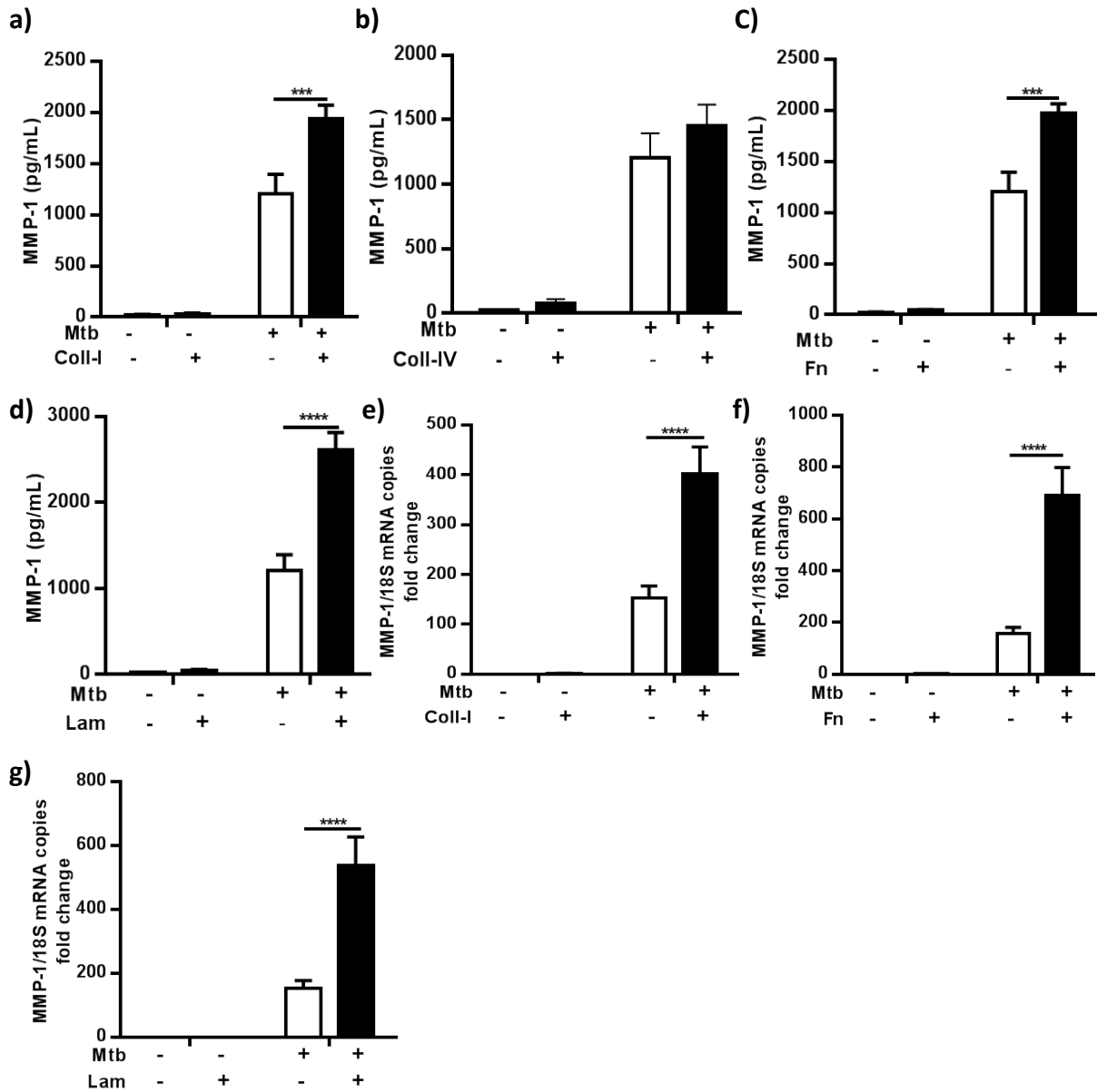
Figure 22. MMP-1 protein secretion and gene expression by Mtb-infected primary monocytes adherent to ECM components.

Plates were seeded with either 100µg/ml Coll-I, 150µg/ml Coll-IV, 20 µg/ml Fn or Lam, or left uncoated. For secretion analysis (a-d), supernatants were collected at 24h post-infection; while for gene expression (e-g) cell lysates were collected at 6h post-infection. Figures show MMP-1 secretion in cells adherent to (a)Coll-I, (b)Coll-IV, (c)Fn, (d)Lam and MMP-1 mRNA accumulation in cells adherent to (e)Coll-I, (f)Fn and (g)Lam. ***p<0.001; ****p<0.001; Coll-I- type I collagen; Fn-

4.3.2. Effect of adhesion to components of the ECM on secretion stromelysins, elastases and gelatinases by Mtb-infected monocytes

Besides MMP-1, primary human monocytes infected with Mtb also express other MMPs, hence I also investigated the effect of the ECM on regulation of other MMPs relevant in TB.

Secretion of MMP-3, -10, -7 and -9 was increased in Mtb infected cells (Fig. 23). However MMP-2 was downregulated in infected cells compared with uninfected controls. The presence of ECM did not affect secretion of MMP-3 and -9 ($p > 0.05$) with Mtb infection, while MMP-7 had an increase of 57% with Coll-I (from 1219.5±79pg/ml to 1918.7±276) and 32% with Fn (1615.0±248pg/ml). No significant increase was seen with Lam. In Mtb infected monocytes, MMP-10 was upregulated by 90% (from 442.5±35pg/ml to 840.3±78pg/ml) with Coll-I, 55% (686±44pg/ml) with Fn and a slight but significant upregulation was seen with Lam (563.4pg/ml; $p < 0.05$).
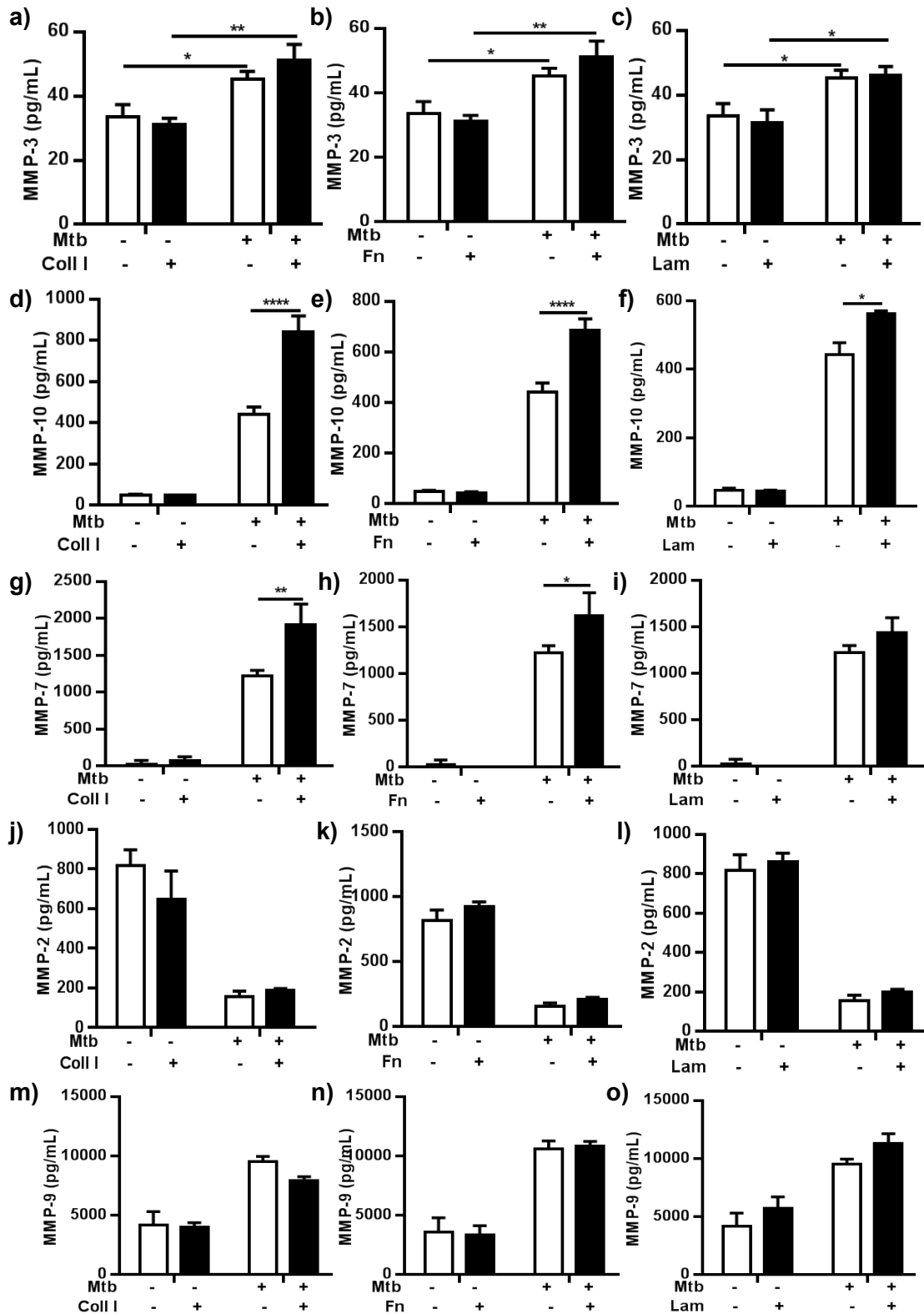
Figure 23. Secretion of MMP-3, -10, -7, -2 and -9 by Mtb-infected primary monocytes adherent to ECM components.

Plates were seeded with either Coll-I, Coll-IV, Fn or Lam, or left uncoated. Supernatants were collected at 24h post-infection and analysed for: (a-c) MMP-3; (d-f) MMP-10; (g-i) MMP-7; (j-l) MMP-2; and (m-o) MMP-9. *p<0.05; **p<0.01; ***p<0.001; ****p<0.001; Coll-I- type I collagen; Fn- fibronectin; Lam- laminin; MMP- matrix metalloproteinase; Mtb- *Mycobacterium tuberculosis.*

4.3.3. Effect of adhesion to components of the ECM on secretion of TIMPs by Mtb-infected monocytes

Next, concentrations of TIMP-1 and -2 were assessed. Mtb infection caused a 2-fold increase in TIMP-1 secretion, while for TIMP-2 a decrease in secretion of approximately 65% was detected (Fig. 24). Adhesion to substrate did not alter concentrations of TIMP-1 or -2, excepting a small increase in TIMP-1 by infected monocytes adherent to Coll-I (from 22.71±8.86ng/ml to 27.69±8.78ng/ml).

Figure 24. TIMP-1 and -2 protein secretion by Mtb-infected primary monocytes adherent to ECM components.

Plates were seeded with either Coll-I, Fn or Lam, or left uncoated. Supernatants were collected at 24h post-infection and analysed for: (a-c) TIMP-1 and (d-f) TIMP-2. ****$p<0.001$; ns- non significant; Coll-I- type I collagen; ECM- extracellular matrix; Fn- fibronectin; Lam- laminin; Mtb- *Mycobacterium tuberculosis.* TIMP- tissue inhibitor of metalloproteinases.

4.3.4. Effect of adhesion to components of the ECM on MMP expression and secretion by CoMtb-stimulated monocytes

In the granuloma, the majority of cells is though to be uninfected and networks between Mtb-infected and uninfected cells upregulate MMP production. Hence, to study the effect of adhesion on monocyte-dependent networks, monocytes were also cultured in the same matrices and stimulated with CoMtb.

Although not as marked as in direct infection, adhesion to Coll-I, Fn and Lam by CoMtb-stimulated primary human monocytes also caused a significant upregulation of MMP-1. Compared with the absence of matrix, Coll-I caused an increase of 22% (from 10450.78±201.7pg/ml to 12770.02±275.6pg/ml), while Fn caused an increase of 47% (15376.78±609.8pg/ml) and Lam an increase of 38% (Fig. 25).
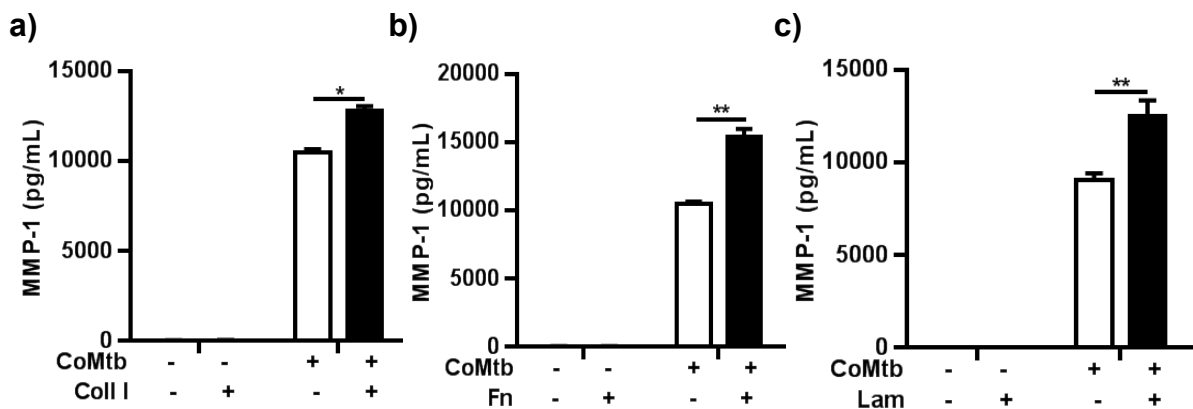
Figure 25. MMP-1 secretion by CoMtb-stimulated monocytes adherent to ECM components.

Plates were seeded with either Coll-I, Fn or Lam, or left uncoated. Supernatants were collected at 24h post-infection. *p<0.05; **p<0.01; CoMtb-conditioned medium of *M. tuberculosis* infected monocytes; Coll I- type I collagen; Fn- fibronectin, Lam- laminin; MMP- matrix metalloproteinase.

Regarding other MMPs, significant differences were only detected for MMP-10 in CoMtb-stimulated cells adherent to ECM (Fig. 26). Adhesion to Coll-I caused an upregulation of 67% (from 2555.33±35.5pg/ml to 4274.32±85.6pg/ml) and Fn drove an upregulation of 62% (4146.21±279.4pg/ml). However, no differences were seen for cells adherent to Lam.
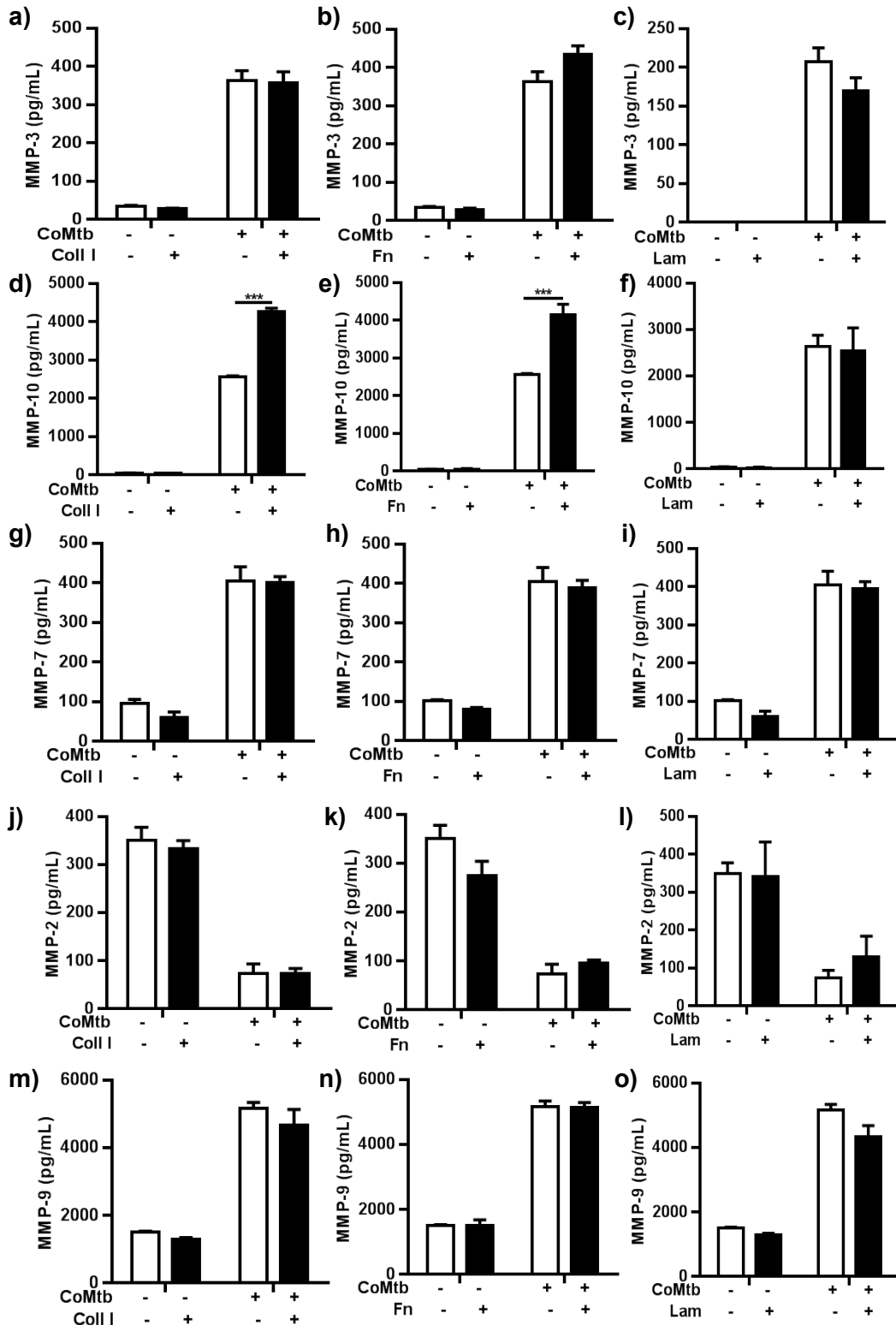
Figure 26. MMP-2, 3, 9 and 10 protein secretion by CoMtb-stimulated monocytes adherent to ECM components.

Plates were seeded with either Coll-I, Coll-IV, Fn or Lam, or left uncoated. Supernatants were collected after 24h and analysed for: (a-c) MMP-3; (d-f) MMP-10; (g-i) MMP-7; (j-l) MMP-2; and (m-o) MMP-9.***p<0.001; Coll-I type I collagen, CoMtb- conditioned medium of *M. tuberculosis* infected monocytes; Fn-fibronectin; Lam-laminin; MMP- matrix metalloproteinase.

4.3.5. Effect of adhesion to components of the ECM on secretion of TIMPs by CoMtb-stimulated monocytes

As already mentioned, analysis of TIMP secretion is also important to understand the net effects of the MMPs analysed. Therefore, the effects of monocyte adhesion to ECM on TIMP-1 and -2 in CoMtb-stimulated cells were also investigated.

CoMtb caused a 2-fold increase in TIMP-1 secretion, while for TIMP-2 a decrease in secretion of approximately 60% was detected (Fig. 27). As previously seen in direct Mtb infection, adhesion to ECM components did not alter concentrations of TIMP-1 or -2 ($p>0.05$).
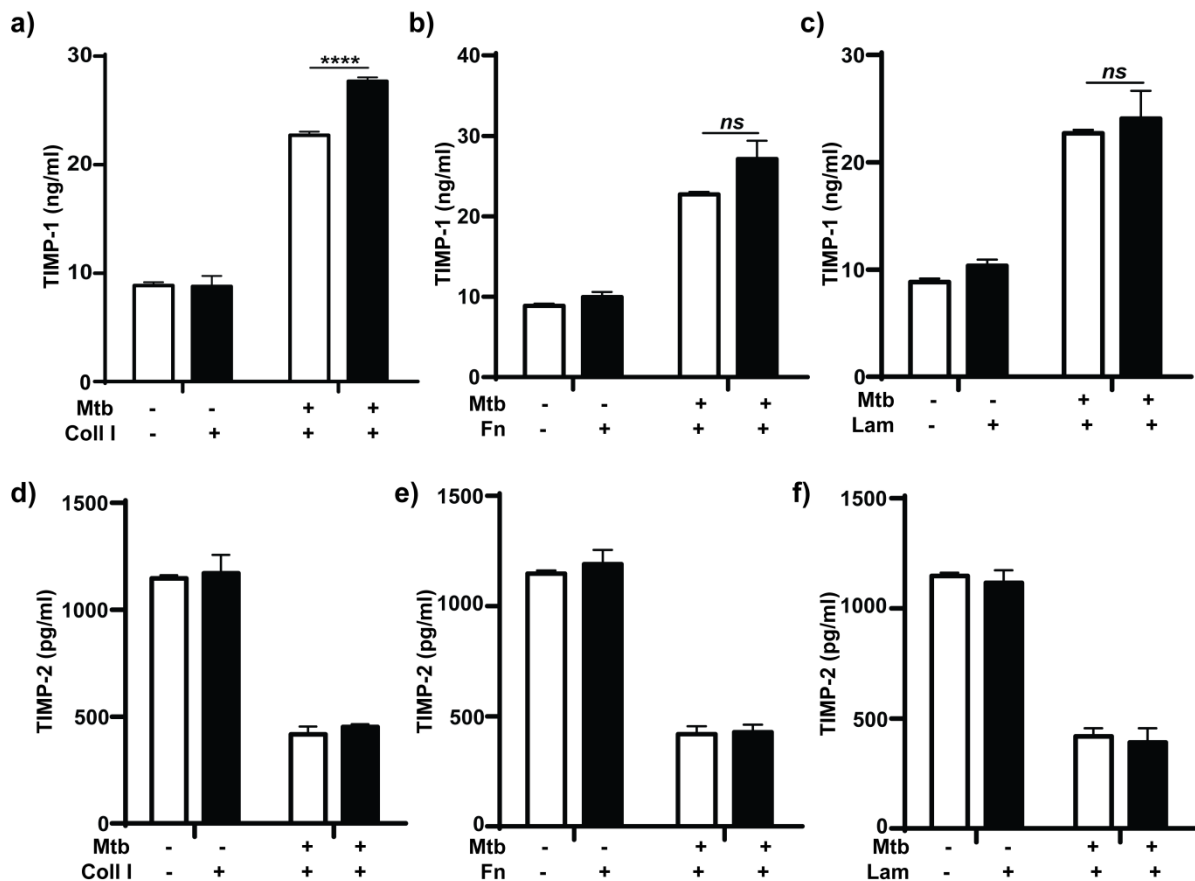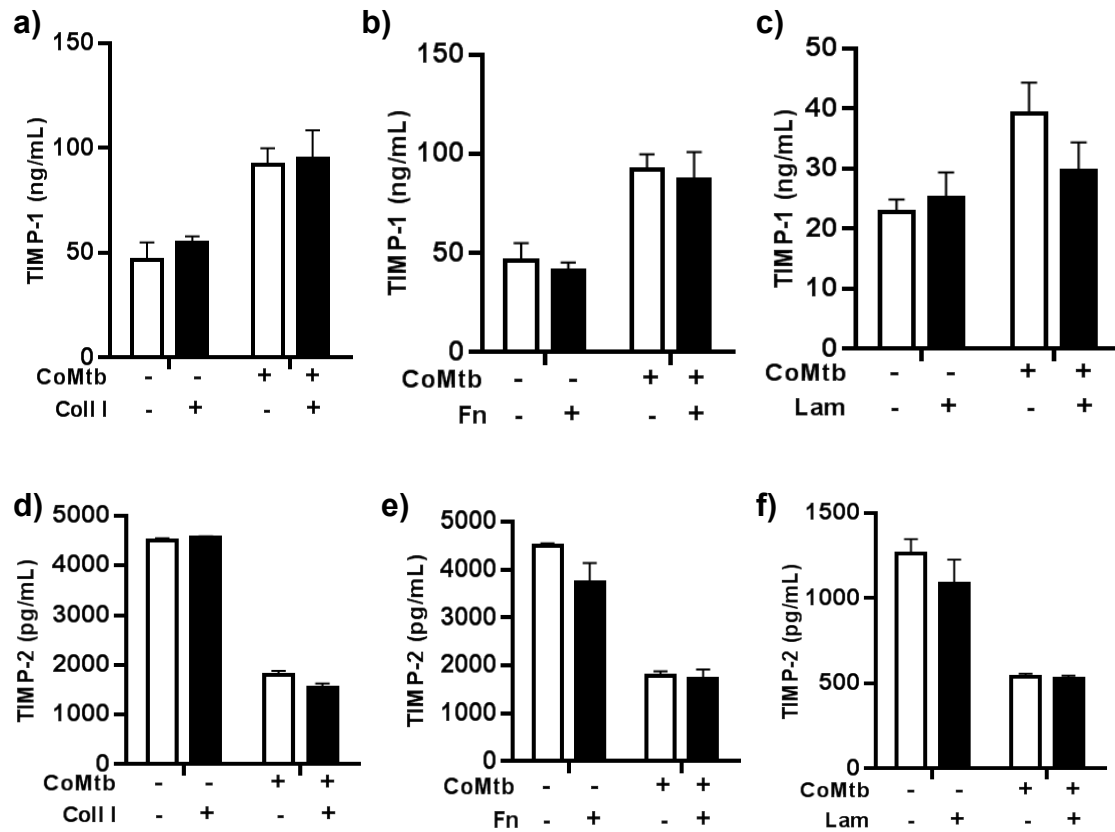
Figure 27. TIMP-1 and 2 protein secretion by CoMtb-stimulated primary monocytes adherent to ECM components.

Plates were seeded with either Coll-I, 20 Fn or Lam, or left uncoated. Supernatants were collected after 24h and analysed for: (a-c) TIMP-1; (d-f) TIMP-2. Coll-I- type I collagen, CoMtb- conditioned medium of *M. tuberculosis* infected monocytes; ECM- extracellular matrix; Fn-fibronectin; Lam-laminin; TIMP- Tissue inhibitor of metalloproteinases.

4.3.6. Integrin regulation of MMP secretion in CoMtb/Mtb stimulated monocytes

Next, analysis of surface expression of beta 1, 2 and 3 integrin subunits was performed by FACS, in order to investigate if the presence of ECM and/or the Mtb/CoMtb inflammatory stimulus altered integrin surface expression (Fig. 28).

MFI for integrin β1 was low in all conditions and close to the negative control (secondary Ab alone). MFIs for β2 integrin were higher, but only a marginal increase in MFI was verified with CoMtb stimulation for cells in the absence of ECM (MFI from 163 to 176), with adhesion to Col I (MFI from 144 to 186) and with adhesion to Fn (MFI from 144 to 169). The presence or absence of ECM by itself also did not caused a significant impact in β3 integrin MFIs. On the other hand, CoMtb stimulation caused an increase in β3 integrin MFIs of 2-fold in the absence of ECM (MFI from 13.7 to 31.3), 3-fold with adhesion to Col I (MFI from 20.4 to 50.4) and 4-fold with adhesion to Fn (MFI from 11.7 to 43.8).
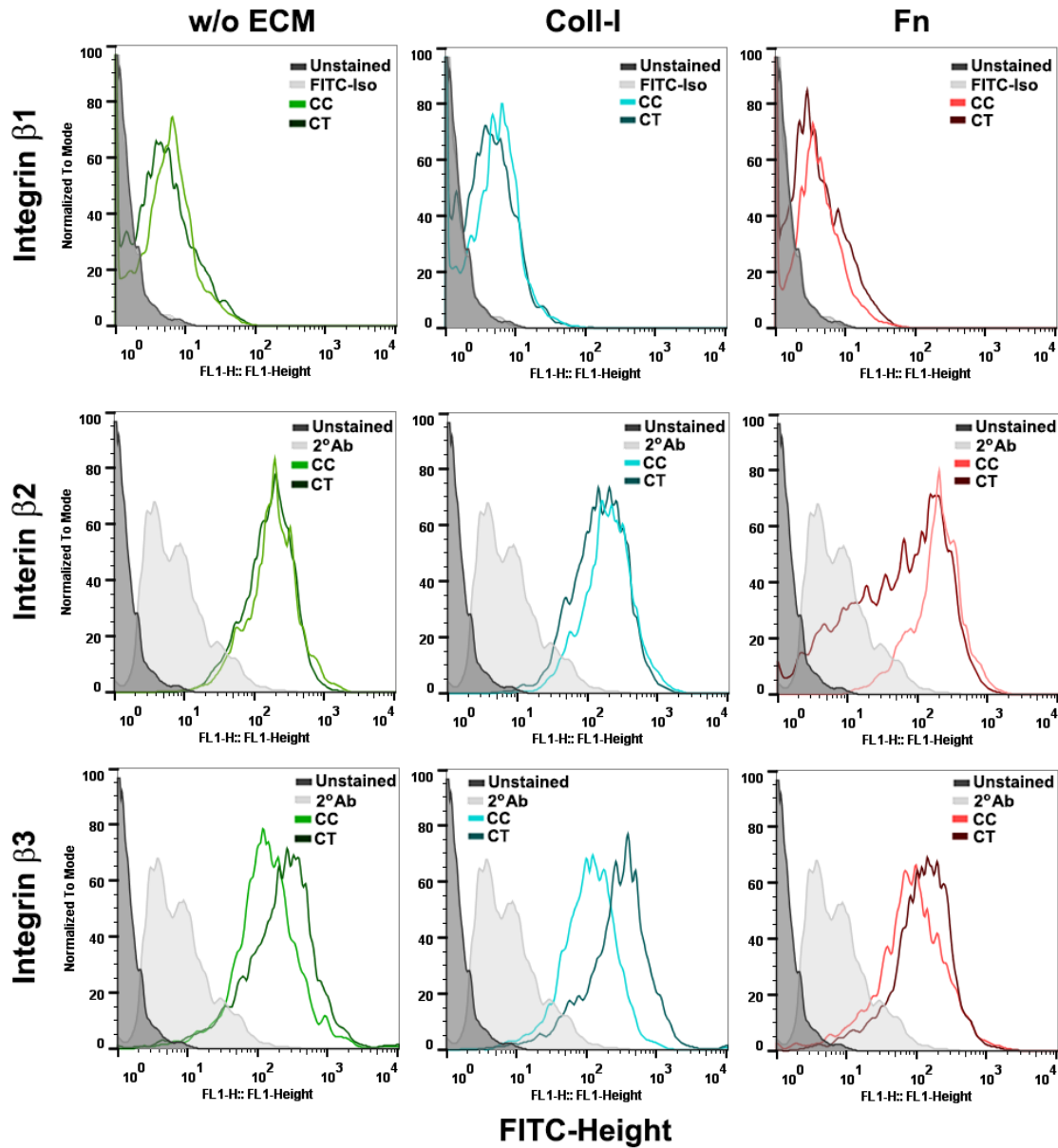
Figure 28. Surface expression of integrin beta subunits in CoMtb-stimulated primary monocytes adherent to ECM components.

Plates were seeded with either 100µg/ml coll-I, 20 µg/ml Fn or Lam, or left uncoated and stimulated for 24h with CoMtb. Cells were fixed, blocked and stained with primary anti-integrin β1, β2 or β3 Abs and secondary FITC-conjugated anti-mouse IgG Ab or just secondary. Purity was accessed using a directly FITC-conjugated anti-CD68 Ab and an IgG1 isotype control. Ab- antibody CC- conditioned medium from uninfected monocytes; Coll-I- type I collagen; CoMtb/CT- conditioned medium from *Mycobacterium tuberculosis* infected monocytes; Fn- fibronectin;w/o ECM- without extracellular matrix.

To confirm the increase seen in surface levels of integrin β3, the MFIs from 4 donors were plotted together to compare surface levels between stimulated and unstimulated monocytes, as well with the absence and presence of ECM components (Fig. 29 a-c).
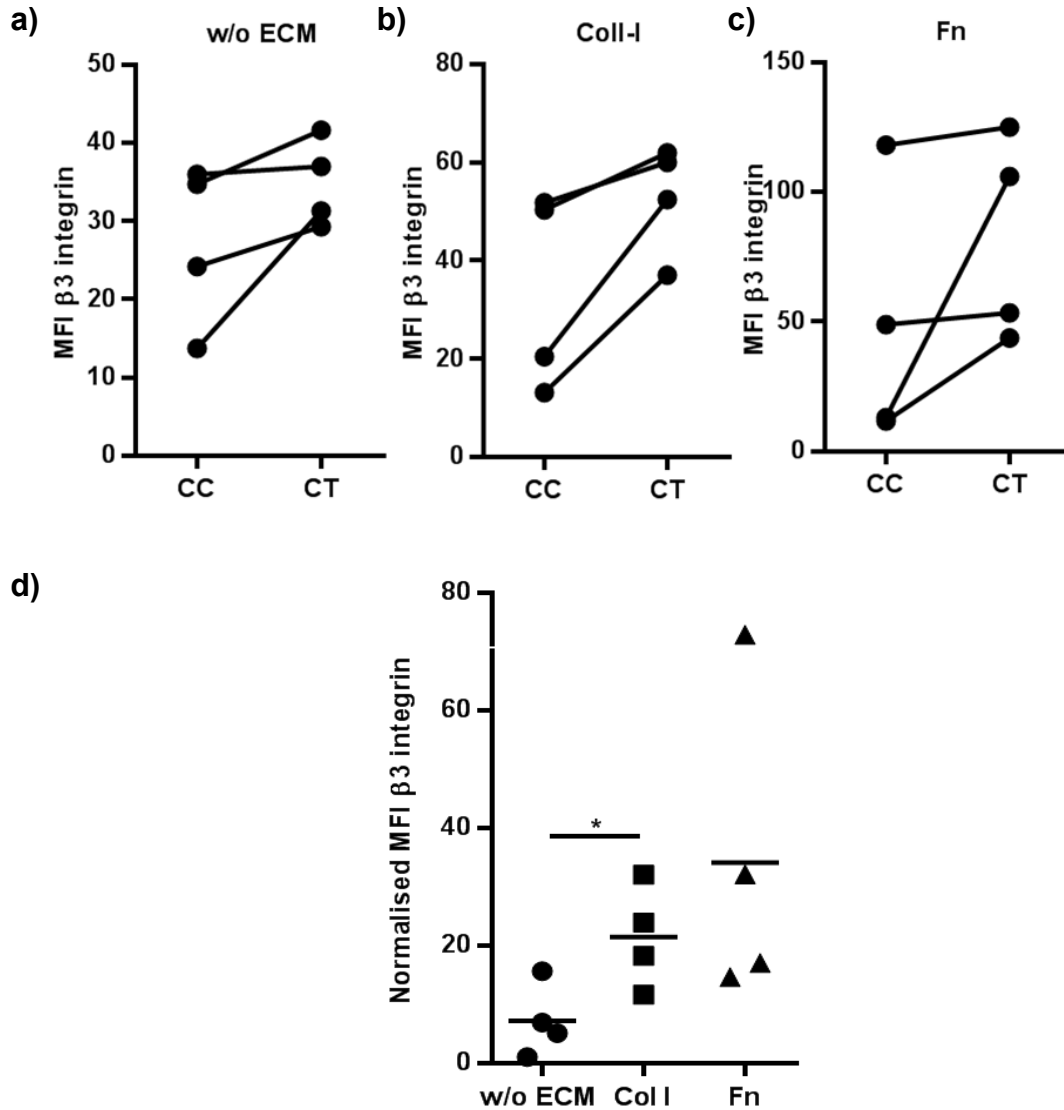
Figure 29. Surface expression of integrin β3 subunit in CoMtb-stimulated primary monocytes adherent to ECM components.

Plates were seeded with either 100μg/ml coll-I, 20 μg/ml Fn, or left uncoated and stimulated for 24h with CoMtb. Cells were fixed, blocked and stained with primary anti-integrin β3 Abs and secondary FITC-conjugated anti-mouse IgG Ab or just secondary. Purity was accessed using a directly FITC-conjugated anti-CD68 Ab and an IgG1 isotype control. Figures show MFI for integrin β3 in monocytes (a)w/o ECM; (b)adherent to Coll-I; (c)adherent to Fn, (d) MFIs normalised to correspondent controls.*p<0.05.Coll-I type I collagen; Fn- fibronectin; MFI- mean fluorescence intensity; w/o ECM- without extracellular matrix,

Although means did not reach statistical significance, a trend of higher surface levels of integrin β3 in CoMtb-stimulated cells compared with controls is evident. Also, in normalised samples to corresponding controls, the presence of Fn and Coll-I also appears to increase integrin β3 (Fig. 29d). Since the only integrin heterodimer expressed by primary human monocytes that contained the subunit β3 is the receptor αVβ3, MFIs from 4 donors were pooled to compare surface levels of the integrin αV subunit (Fig. 30).

Similarly to what was seen for cell surface levels of integrin β3 subunit, CoMtb stimulation appeared to increase integrin αV MFIs, although they did not reach statistical significance ($p > 0.05$) (Fig. 30a-c). By normalising MFI levels from stimulated monocytes with their respective controls, it was verified that monocytes adherent to Coll-I had significantly higher MFIs for integrin αV ($p < 0.05$) than in the absence of ECM. Cells adherent to Fn also appeared to have higher MFIs for integrin αV; however, due to the low number of donors, they did not reach statistical significance (Fig. 30d).
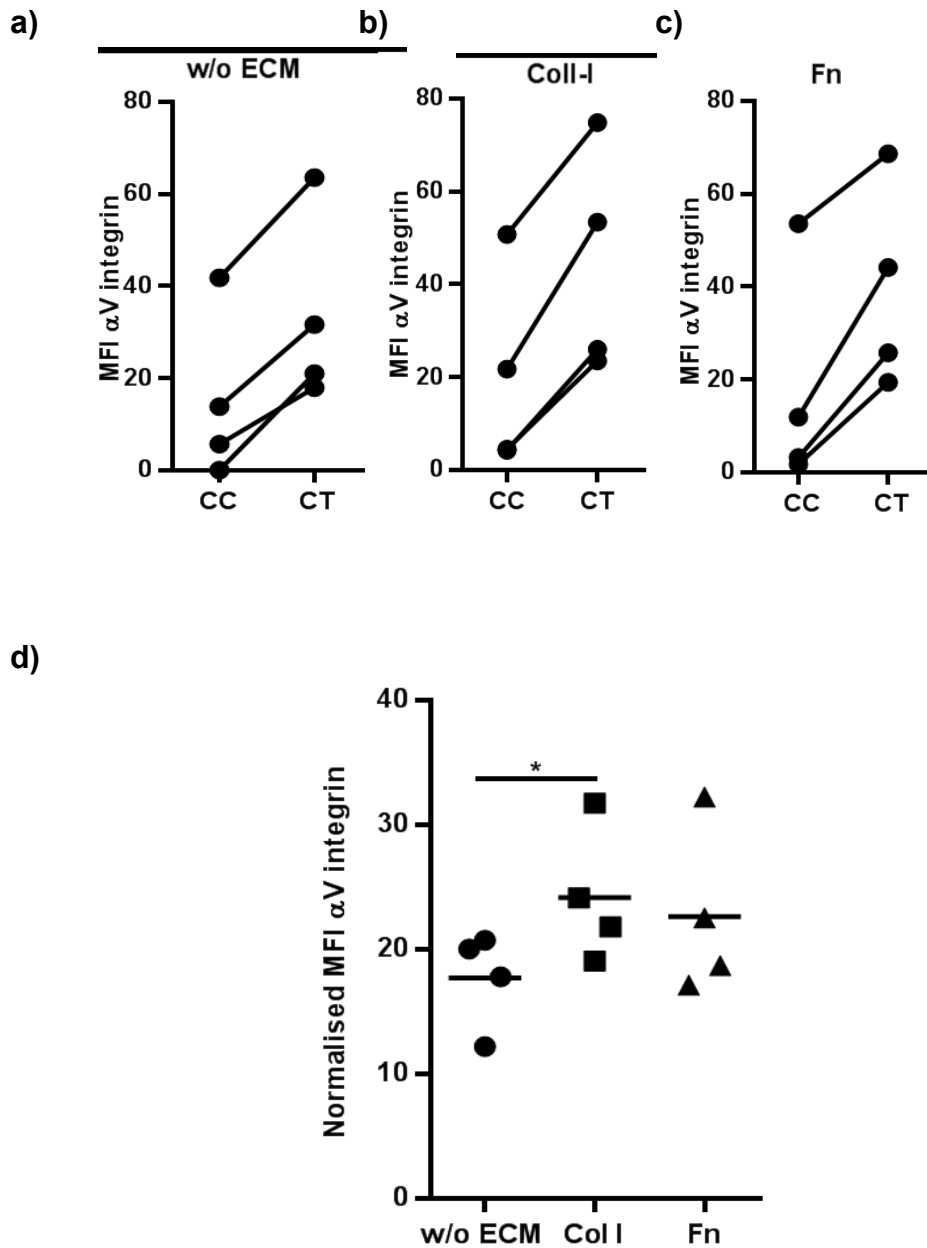
Figure 30. Surface expression of integrin αV subunit in CoMtb-stimulated primary monocytes adherent to ECM components.

Plates were seeded with either 100µg/ml coll-I, 20 µg/ml Fn, or left uncoated and stimulated for 24h with CoMtb. Cells were fixed, blocked and stained with primary anti-integrin αV Ab and secondary FITC-conjugated anti-mouse IgG Ab or just secondary. Purity was accessed using a directly FITC-conjugated anti-CD68 Ab and an IgG1 isotype control. Figures show MFIs for integrin αV for monocytes (a) w/o ECM; (b)adherent to Coll-I; (c)adherent to Fn; (d)MFIs normalised to respective controls. *p<0.05. Ab- antibodies; Coll-I type I collagen; Fn- fibronectin; MFI- mean fluorescence intensity; w/o ECM- without extracellular matrix.

To investigate if the increased seen in integrin αVβ3 with CoMtb-stimulation was involved in regulation of MMP expression in TB, monocytes were seeded in plates coated with immobilised anti-beta integrin antibodies, functioning as integrin agonists [234,235,262].

Concentrations of MMP-1 and MMP-10 secreted by Mtb-infected and CoMtb-stimulated monocytes were analysed, since these were shown to be the most highly upregulated by cell adhesion to ECM. Activation of integrin β1 did not significantly alter MMP-1 by activated cells (Fig. 31), while integrin β2 activation led to a small decrease in MMP-1 (from 1138.3±132.7pg/ml to 793.5±89.6pg/ml). However, engagement of integrin β3 caused an increase of 84% (from 1206.8± 40.8pg/ml to 2218.06±252.97pg/ml) on MMP-1 by infected monocytes and 50% (1712.8±78.5 pg/ml) with CoMtb stimulation (Fig. 31a, c). For MMP-10, the highest increase was also seen in integrin β3 activated cells, with an increase of 57% (from 712.8±28.9pg/ml to 1115.9±86pg/ml) in Mtb-infected cells and an almost 3-fold increase (from 679.62±93.1pg/ml to 1895.12±363.7pg/ml) with CoMtb-stimulation (Fig. 31b, d). In direct infection, a smaller increase in MMP-10 was also detected with integrin β1 activation (1002.44± 79.4pg/ml).
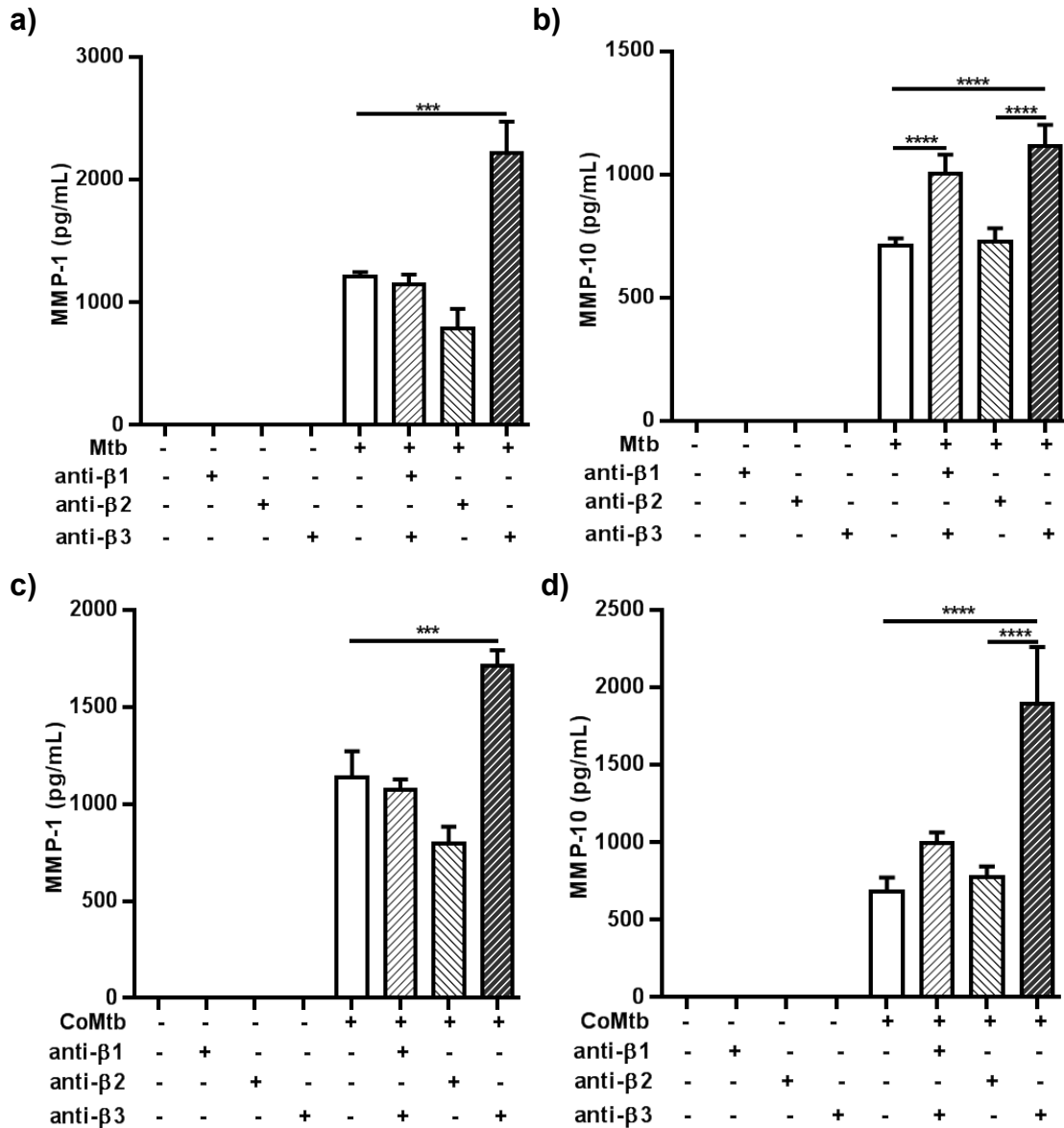
Figure 31. Integrin beta subunits regulation of Mtb-infected or CoMtb-stimulated primary monocytes.

Plates were coated with goat anti-mouse Fc region, blocked and coated with 20µg/ml either mouse anti-integrin β1, β2 or β3 Abs or left uncoated and stimulated for 24h with CoMtb or directly infected with Mtb (MOI=1). Supernatants were collected and assayed for MMP-1 and MMP-10. Figures show in Mtb infected cells (a)MMP-1 and (b)MMP-10 secretion and (c)MMP-1, (d)MMP-10 secretion in CoMtb stimulated cells adherent to bound anti-integrin Abs. * $p<0.05$; ***$p<0.001$; ****$p<0.0001$; CoMtb- conditioned medium from *Mycobacterium tuberculosis* infected monocytes; MMP- matrix metalloproteinase.

To confirm that it was integrin αVβ3 driving the increase in MMP-1 by Mtb-infected monocytes, the above experiments were repeated, this time using coated anti-αV antibodies. Activation of αV in Mtb-infected monocytes led to an increase of 13-fold for MMP-1. Activation of αV also led to an increase in controls, which suggests that this subunit may be the effector driving MMP-1 upregulation (Fig. 32).
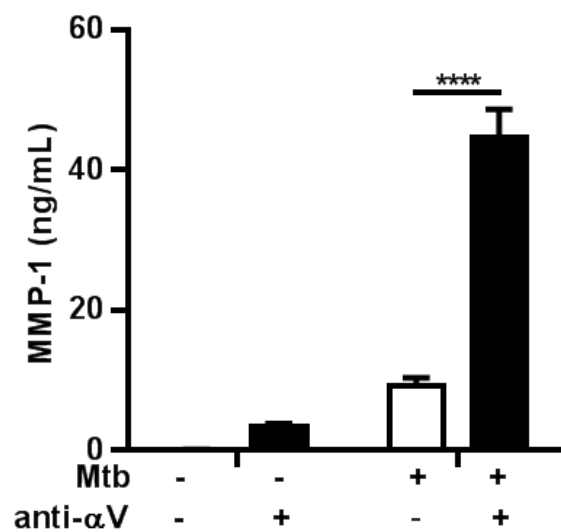
Figure 32. Integrin αV subunit regulates secretion of MMP-1 by Mtb-infected primary monocytes.

Plates were coated with goat anti-mouse Fc region, blocked and coated with 20µg/ml mouse anti-integrin αV Abs or left uncoated and stimulated for 24h with CoMtb or directly infected with Mtb (MOI=1). Supernatants were collected and assayed for MMP-1 and MMP-10. ****p<0.0001; MMP-1- matrix metalloproteinase 1; Mtb- *Mycobacterium tuberculosis.*

4.3.7. Integrin αVβ3 interacts with MMP-1 and is necessary for monocyte migration in tuberculosis.

I next investigated the functional effect of the increase seen in integrin αVβ3 expression following Mtb-infection and CoMtb-stimulation. For this, transwell assays were performed, where CoMtb was added in a 1:2 dilution to the basolateral compartment, transwells were coated with Coll-I and $5x10^5$ monocytes were added to the apical compartment. Cells were either pre-incubated with anti-β3 or anti-αV blocking antibodies or left in RPMI. Monocytes were left to transmigrate for 2h and migrating cells were collected from the basal side and counted by FACS. With CoMtb, the number of transmigrated monocytes was over 2-fold higher than in controls (Fig. 33a), confirming that CoMtb is a chemotactic stimulus for monocyte migration. However, blockade of either the β3 or the αV integrin subunits led to a dramatic decrease in monocyte transmigration, with 96% fewer transmigrated monocytes with integrin β3 inhibition and 92% fewer monocytes with αV subunit inhibition. Since αVβ3 integrin is required for monocyte migration in TB, thus slides from Mtb-infected monocytes were stained for αVβ3 integrin and MMP-1 and 10. By confocal microscopy with phase contrast we verified that with Mtb infection αVβ3 integrin tended to co-localise with MMP-1 and MMP-10 (Fig. 33b).

a)

b)
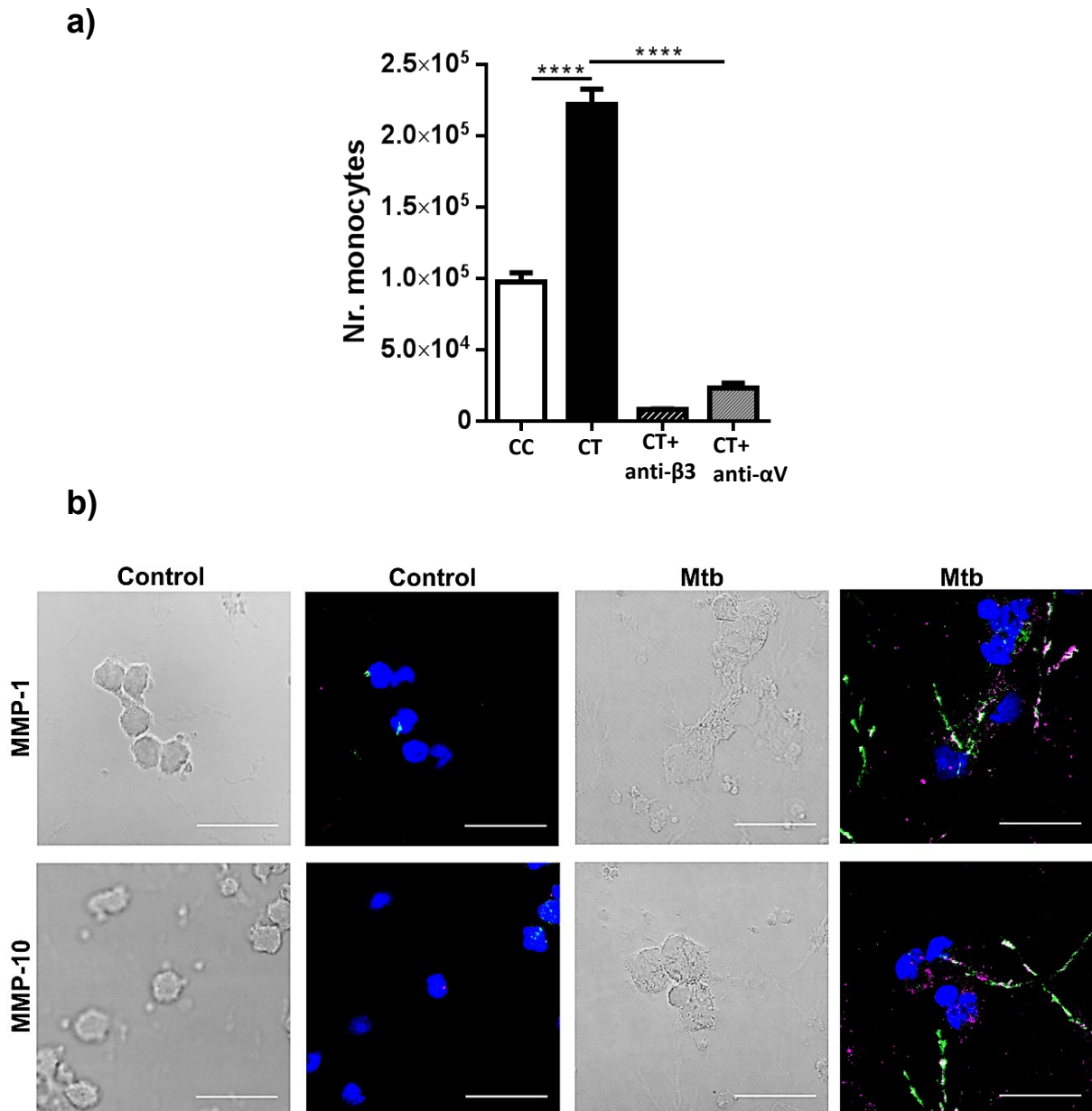
Figure 33. Integrin αVβ3 is required for monocyte transmigration and co-localizes with MMP-1/10 in Mtb infection.

Transwells were coated with Coll-I and CoMtb or CoMCont was added to the basal side in an 1:2 dilution. Cells were incubated with or without anti-integrin, added to the apical side and let to migrate for 1h. Cells were collected from the basal side and counted by FACS. For confocal microscopy (b) 8-well chamber slides were coated with collagen and monocytes were infected with Mtb (MOI=1). Cells were fixed, blocked and stained with DAPI for nucleic acids (blue), integrin αVβ3 (green) and MMP-1 or 10 (magenta). Scale bar: 25μm. ****p<0.0001; Mtb- Mycobacterium tuberculosis; CoMtb/CT- Conditioned medium from Mtb-infected monocytes; CoMCont/CC- Conditioned medium from uninfected monocytes; MMP- matrix metalloproteinase.

4.4. Discussion

In TB, monocytes are major drivers of MMP expression leading to tissue destruction and are also involved in migration to foci of Mtb infection and granuloma formation. The ECM is an important regulator of local immune response and it is likely to have important implications in TB. However, *in vitro* studies tend to disregard the role of the ECM in TB. In the present study I have dissected the role of the ECM in regulation of MMP production during infection. I found that Mtb-infected monocytes in the presence of ECM components, significantly increased MMP-1 and MMP-10. MMP-1, as already mentioned, is the main collagenase involved in Coll-I breakdown leading to tissue destruction and cavitation in TB [84]. MMP-10 is a stromelysin which can degrade many components of the ECM, including collagen types III–V and fibronectin. It can also activate other MMPs, including MMP-1, MMP-7, MMP-8, and MMP-9. This study showed that MMP-10 secretion levels were significantly increased in the presence of both Coll-I and fibronectin. As MMP-10 does not directly degrade Coll-I, it is likely the up-regulation observed was a regulatory mechanism whereby MMP-10 secretion is increased, favouring activation of pro-MMP-1 to produce a matrix degrading phenotype. MMP-10 has been shown to have a 10-fold weaker affinity to TIMP-1 and TIMP-2 when compared to MMP-3, another stormelysin [263]. This study has shown that the upregulation of MMP-10 in the presence of the ECM is accompanied by little or no change to overall TIMP secretion. This, coupled with a lower affinity of inhibition by TIMP-1 and TIMP-2, leads to a net effect of increased MMP-10 activity. In TB, MMP-10 could be an important factor in the activation of other MMPs, such as MMP-1, in human

monocytes and could play a more important role in the activation of pro-MMPs when compared to other stromelysins such as MMP-3.

A recent study from our group demonstrated that in pulmonary TB, Coll-I destruction is an early event in TB pathogenesis and reduces survival of Mtb-infected cells, leading to development of caseous necrosis, which favours survival of the pathogen [264]. In the previous chapter, I have demonstrated that in bronchial epithelial cells, the presence of an intact ECM caused integrin α2β1-dependent activation and signalling, leading to increased cell migration and promoting epithelial repair, while degraded Coll-I shifted the epithelium towards a matrix degrading phenotype. In monocytes, adhesion to the ECM has been shown to modulate gene expression profiles via integrins [265]. In the present study I have shown that Mtb-infection is associated with an increased surface expression of integrin αVβ3, which is known to bind to different components of the ECM, such as collagens, fibronectin, laminins-10/11 and fibrinogen [266]. FACS analysis showed that CoMtb stimulation leads to an increase in αVβ3 surface levels, which appear to be further increased when the ECM is present. This indicates that the CoMtb inflammatory stimulus leads to an increase in the receptor which is activated in presence of specific ECM components and leads to an up-regulated expression of MMP-1 and -10.

Although traditionally viewed as a host strategy to control infection, excessive monocyte migration may also have deleterious effects, leading to deregulated inflammation and favouring tissue damage. In the zebrafish model of TB,

macrophages were shown to migrate into granulomas after becoming infected, allowing mycobacterial expansion. Also, they may egress the granuloma, disseminating infection to new sites [267]. In the present study I have shown that CoMtb acts as a chemoattractant for monocytes and that integrin αVβ3 was required for monocyte migration. Also I found that with Mtb-infection integrin αVβ3 colocalised with MMP-1 and MMP-10.

One caveat of this study was the lack of monocyte phenotypic analysis at the end of experiments. It is likely that during isolation of CD16+ monocytes, culture and stimulation with Mtb or CoMtb monocytes differentiate into an intermideate phenotype more akin of macrophages. The tuberculous granuloma, is rich in recruited monocytes and monocytes-derived macrophages which are important sources of MMPs. Therefore it is possible that different phenotypes of monocyte correspondent to different stages of differentiation/polarization will be present in the infected tissue. Also, a study in zebrafish demonstrated that infected microphages egress the granuloma, and infected macrophages are required for hematogenous dissemination [267]. However, in this study they have not analysed phenotypic changes in monocytes/macrophages, therefore more studies are needed to address these events in TB.

Tissue destruction is a determinant event in TB immunopathology and can affect disease outcome. I have demonstrated that, in pulmonary TB, the ECM regulates both epithelial and monocyte expression of MMP-1 and that integrins are important

regulators of these responses. Therapies directed towards the host immune response are emerging as novel strategies in the treatment of TB [268]. Therapies directed to reducing ECM degradation may have an important impact in reducing morbidity and mortality in TB, by reducing excessive inflammation and promoting tissue regeneration and an efficient immune response.

Chapter V: Blood-brain barrier disruption in central nervous system tuberculosis

5.1. Introduction

CNS TB is associated with high mortality and disease pathology is characterised by a marked inflammatory response with widespread destruction of CNS tissues.

The BBB separates the circulating blood from the brain extracellular fluid and maintains the homeostasis of the microenvironment. It comprises capillary endothelial cells surrounded by basement membranes (composed mainly of Coll-IV and Lam) and the astrocytic perivascular end-feet. The barrier functions of the brain endothelium are dependent on TJ, which are composed of TJPs, such as occludins, claudin-5 and -3, JAMs and cytoplasmic adaptor proteins (e.g. ZO-1 and -2), which connect them to the actin cytoskeleton, allowing TJs to form a seal [201].

Astrocyte and pericyte-derived Hh proteins have been shown to control BBB formation during development but, recently, they were also found to have a crucial role in maintenance of TJ integrity in adult tissues as well as tissue repair [206,269].

Models of CNS neuroinflammation have provided evidence linking the CNS inflammatory response to enhanced BBB permeability and disturbance of brain function, often accompanied by a large influx of leukocytes. The role of MMPs in BBB disruption in bacterial meningitis is becoming increasingly clear. MMPs are produced by multiple cell types, including the endothelium, astrocytes, microglia and neurons as well as infiltrating leukocytes.

The mechanism by which Mtb reaches the CNS is still not well characterised. Some have postulated that free bacilli may traverse across the endothelial barrier [222],

while others suggested that bacilli enter via the passage of infected monocytes [270,271]. Using an *in vitro* monolayer of human brain microvascular endothelial cells, Jain *et al.* shown that the virulent strains of Mtb H37Rv and CDC1551 were able to traverse the endothelial monolayer [222] and later, Be *et al*. found that the virulence factor pknD was required for CNS invasion [272]. However, in their *in vitro* model they have not included other cells that comprise the BBB (e.g. astrocytes), hence it is unclear what role these cells play in defence against entry into the brain parenchyma. Also, they have never accessed BBB integrity during infection.

5.2. Specific aims

Hypothesis: Mtb-driven MMP production by astrocytes and phagocytes leads to BBB disruption, which contributes to CNS TB immunopathology.

Using primary human astrocytes and a brain microvascular endothelial cell line, this study aimed to:

- Develop a BBB cellular model to study BBB function during CNS infection;

- Test if TB-driven MMP activity disrupts affects BBB function *in vitro;*

- Investigate the signalling pathways involved in BBB disruption by Mtb infection.

5.3. Results

5.3.1. Cellular model of the blood-brain barrier

Studies have reported the role of astrocytes in blood-brain barrier regulation [172], however most studies still use a single culture of human endothelial cells in their BBB models. Therefore, I have started by comparing TEER and TJP expression between single hCMEC/D3 cultures and co-cultures with human primary astrocytes (Fig. 34). Co-cultures increased TEER of approximately 10% (from $142.2\pm2.7\Omega.cm^2$ to $157.3\pm2.2\Omega.cm^2$) and cell lysates showed a higher content of claudin-5 and claudin-3. Also, EM images (Fig. 34d, e) revealed that in the co-culture model, endothelial cells establish tight junctions. This indicates that co-cultures may lead to stronger barrier functions thean the single brain endothelial cell culture. Furthermore, this model allows the study of astrocyte response during Mtb infection.
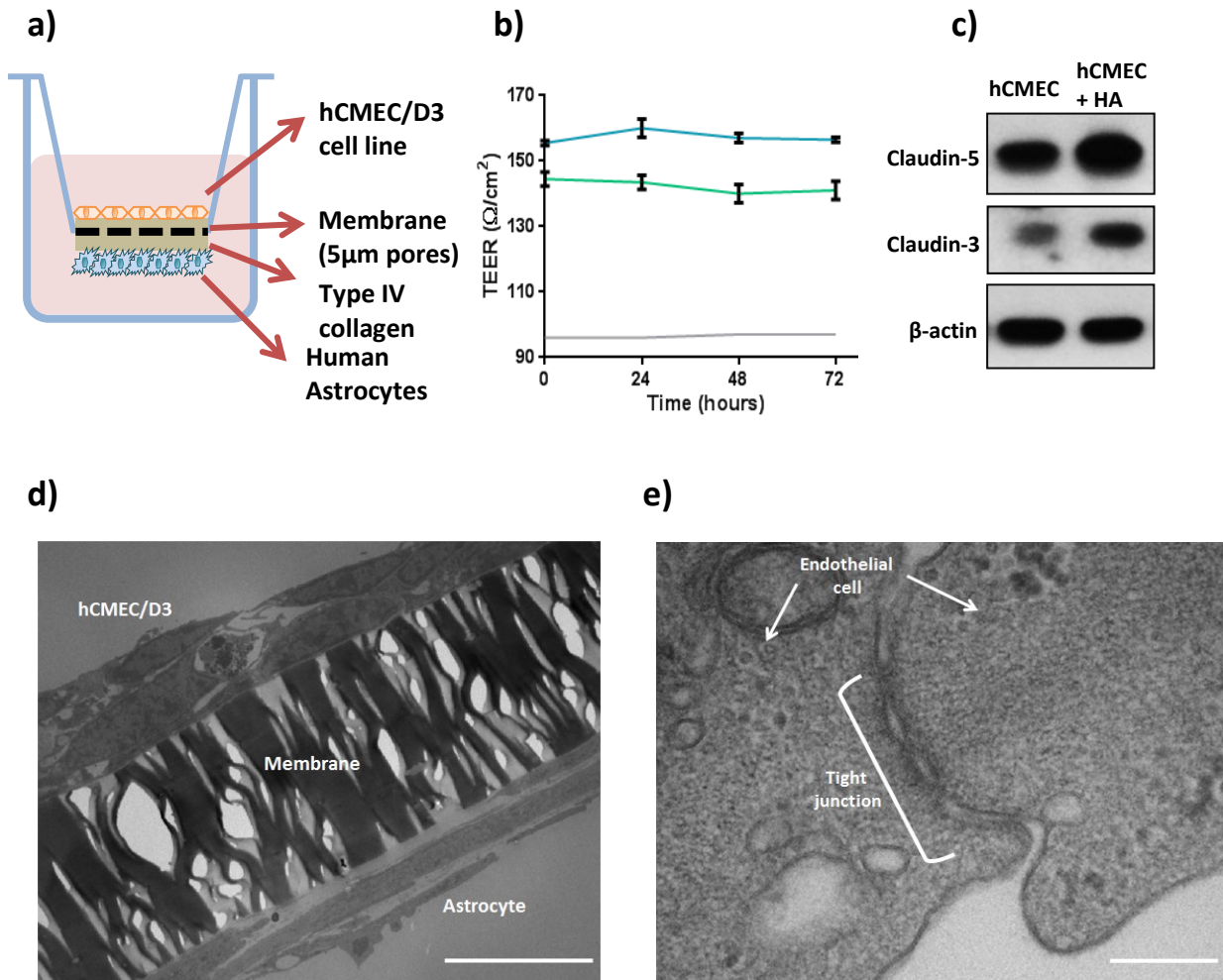
Figure 34. Blood-brain barrier model.

a) schematic representation of the cellular BBB co-culture model. b) TEER measured during 72h after BBB maturation. Green line- single culture hCMEC/D3; blue line- co-culture model. Figure represents two independent experiments performed in triplicate. c) Western blot for claudin-5 and β-actin as loading control. Figure represents three independent experiments. d, e) Electron microscopy images of d) the co-culture model (scale bar- 10μm); and (e) hCMEC/D3 tight junction in the co-culture model (scale bar- 200nm). BBB- blood brain barrier; HA-human astrocytes; hCMEC/D3-Immortalized human brain microvascular cell line; TEER- trans-endothelial electrical resistance

5.3.2. CoMtb stimulation causes disruption of the Blood-brain barrier

To mimic the signalling networks during Mtb infection that could lead to BBB opening, CoMtb or CoMCont was added to the basolateral side of the BBB, to stimulate astrocytes and brain endothelial cells (Fig. 35a). CoMtb stimulation, of the BBB decreased TEER from 154 ± 1.2ohm.cm^2 to 111.6 ± 4.7ohm.cm^2, while Papp increased approximately 2.4-fold with sodium-fluorescein and 2.5-fold with 3KDa dextran-fluorescein after 72h (Fig. 35b, c).

Degradation of Coll-IV, which is one of the main components of basement membranes, was detected by an increase in green fluorescence by confocal microscopy (Fig. 35d) and protein content of the TJPs ZO-1, claudin-3, claudin-5 and occludin were also decreased with infection (Fig. 35e).
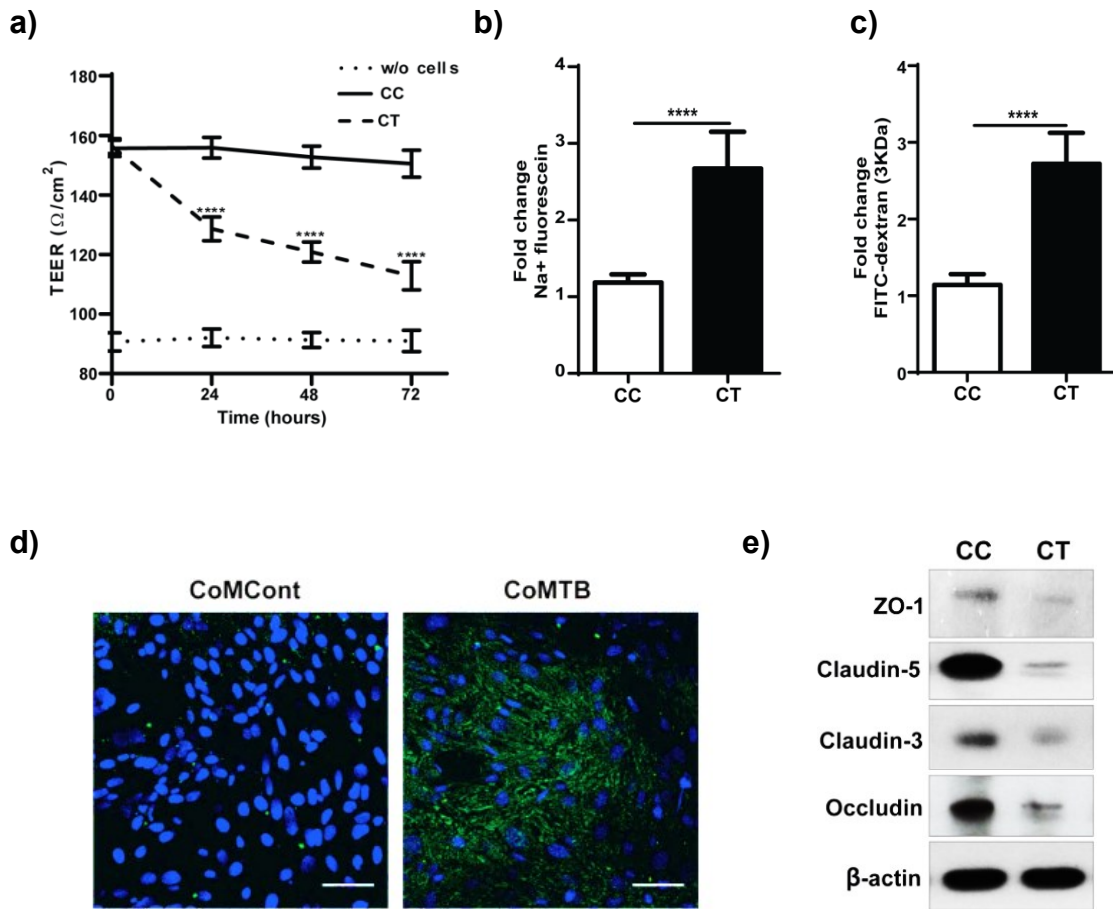
Figure 35. CoMtb causes BBB disruption.

HA and hCMEC/D3 were co-cultured in transwells coated with type IV collagen. BBB was matured for 6-10 days and wells stimulated for 72h with CoMtb or CoMCont. For confocal microscopy, wells were coated with DQ type IV collagen and cells fixed and stained with DAPI. For western blot, samples were loaded together with a ladder in a gel and blotted. Membrane was cut according to expected protein size and each segment incubated with respective antibodies. For claudin-3, membrane was stripped from anti-claudin-5 Abs and reprobed with anti-claudin-3 Ab. Figures show (a) TEER; permeability to (b)Na$^+$ fluorescein and (c) 3KDa FITC-dextran; (d) confocal images of endothelial layer where blue is the nucleus and green are areas of degraded collagen. (e) western blot for the TJP ZO-1, claudin-5, claudin-3 and occludin, using β-actin as loading control.

**** $p < 0.0001$; ns- non significant; Scale bar: 50µm. BBB-Blood-brain barrier; CoMCont/CC-conditioned medium from uninfected monocytes; CoMtb/CT-Conditioned medium of *Mycobacterium tuberculosis* infected macrophages; HA-human astrocytes.

MMP concentrations increased 125-fold for MMP-1(from 0.35±2 to 43.8±5.1ng/mL; Fig. 36a), 37-fold for MMP-3 (0.057±0.013 to 2.11±0.35ng/ml; Fig. 36c), 9-fold for MMP-7 (0.24±0.067 to 2.11±0.3ng/ml; Fig. 36d), 20-fold for MMP-8 (0.057±0.029 to 1.14±0.15ng/ml; Fig. 36e) and 619-fold for MMP-9 (0.072±0.014 to 44.6±8.9ng/ml; Fig. 36f). No significant differences were seen for MMP-2 (Fig. 36b) or TIMP-1(Fig. 36g). However TIMP-2 was found to be significantly decreased (Fig. 36h).
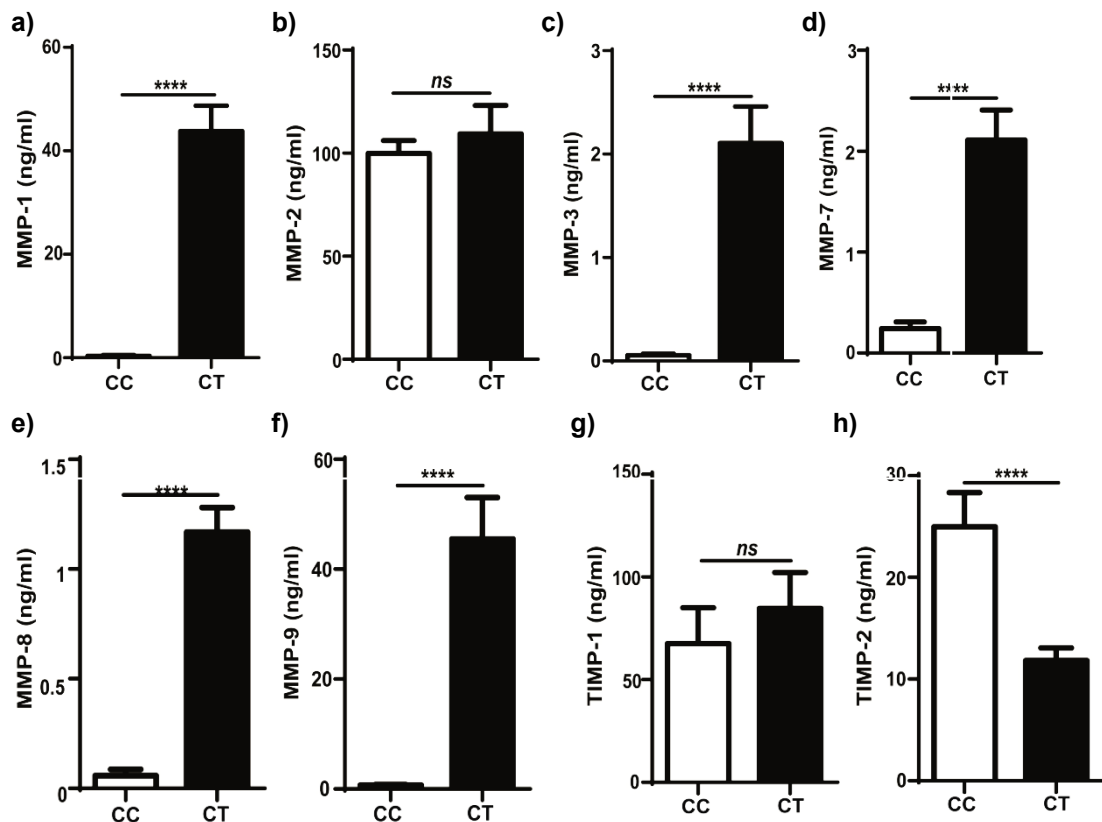
Figure 36. CoMtb causes MMP upregulation by the BBB.

HA and hCMEC/D3 were co-cultured in transwells coated with type IV collagen. BBB was matured for 6-10 days and wells stimulated for 72h with CoMtb or CoMCont. Supernatants were analysed for secreted (a) MMP-1; (b)MMP-2; (c)MMP-3: (d)MMP-7; (e)MMP-8; (f)MMP-9; (g)TIMP-1 and (h)TIMP-2.

**** p<0.0001; ns- non significant; BBB-Blood-brain barrier; CC- conditioned medium from uninfected monocytes; CT-Conditioned medium of *Mycobacterium tuberculosis* infected macrophages; MMP- matrix metalloproteinase; TIMP- tissue inhibitor of metalloproteinases.

To identify the role of astrocytes in BBB disruption, 1.25×10^7 mycobacteria (MOI=10) were added to the apical side of each transwell and incubated for 72h. After 24h post-infection, approximately 3.75×10^3 mycobacteria (0.03%) were detected in the basal side of the BBB. Although not as marked as when using CoMtb, Papp to sodium-fluorescein increased by 50% (Fig. 37a, b) and a small increase was detected for MMP-1, -9 and -7 (Fig. 37b).

No differences in BBB integrity and MMP secretion were detected when monolayers of endothelial cells were cultured with Mtb (Fig. 38). Also, only MMP-1, -2 and -9 were detectable, which means that the other MMPs are produced by the activated astrocytes. This data suggests that mycobacterial invasion and traversing of the BBB by itself does not disrupt the BBB and indicates that microglial/macrophage and astrocyte activation and signalling are required for opening of the BBB.
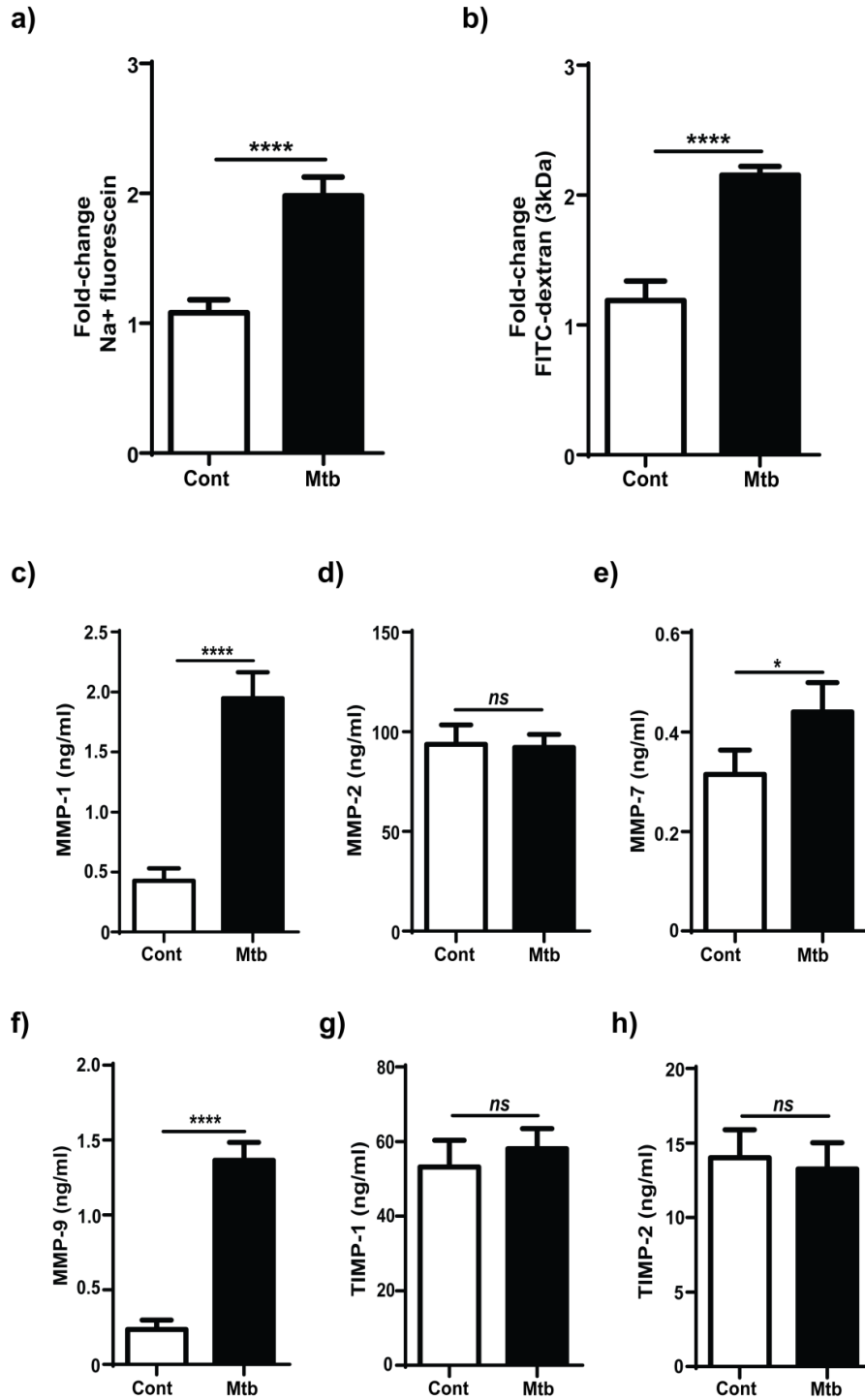
Figure 37. Mtb infection disrupts the blood-brain barrier.

BBB was infected with Mtb at an MOI of 10 and incubated for 72h. Supernatants were collected, filtered and used for MMP and TIMP quantification. (a) Fold-change in permeability to sodium-fluorescein; (b) fold-change in permeability to 3kDa FITC-dextran; secreted concentrations of (c) MMP-1; (d) MMP-2; (e)MMP-7; (f) MMP-9; (g)TIMP-1 and (h) TIMP-2. **** p<0.0001; *p<0.05; ns- non significant; Cont- control; Mtb- *Mycobacterium tuberculosis;* MMP- matrix metalloproteinase; TIMP- tissue inhibitor of metalloproteinases.
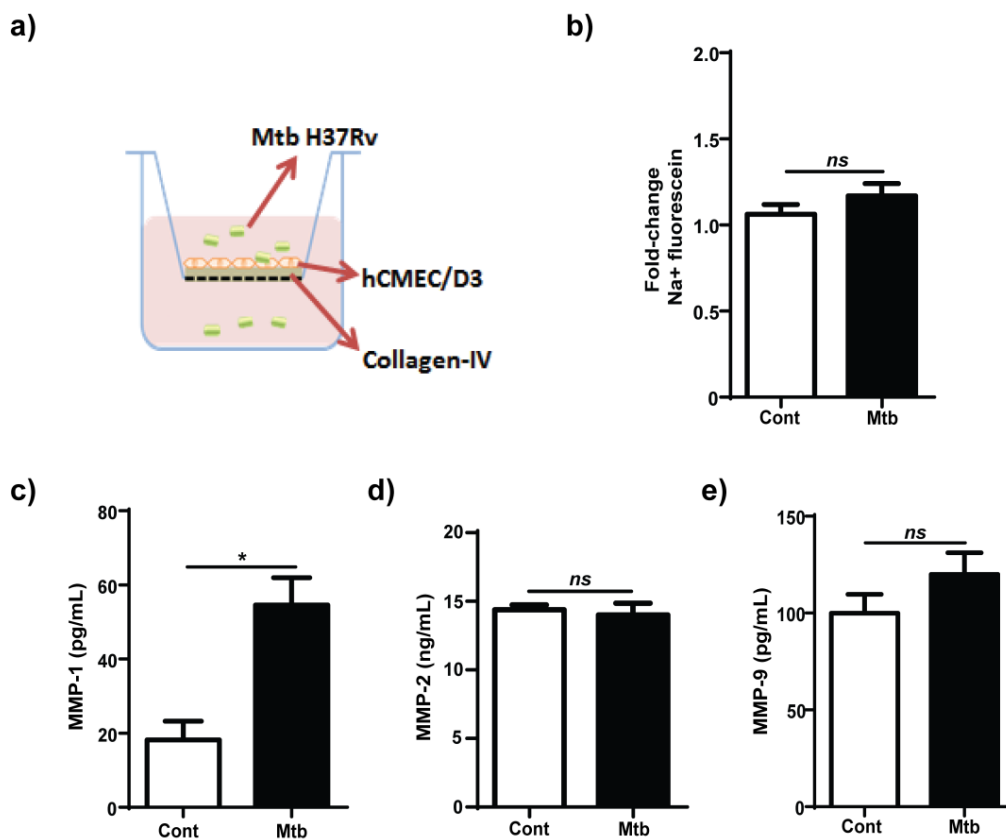
Figure 38. Astrocytes are necessary for blood-brain barrier disruption in tuberculosis.

Endothelial cells were infected with Mtb at an MOI of 10 and incubated for 72h. Supernatants were collected, filtered and used for MMP and TIMP quantification. (a) Diagram of endothelial monolayer; (b) Fold-change in permeability to sodium-fluorescein; secreted concentrations of (c) MMP-1; (d) MMP-2; (e)MMP-9.*p<0.05; ns- non significant; Cont- control; Mtb- *Mycobacterium tuberculosis;* MMP- matrix metalloproteinase; TIMP- tissue inhibitor of metalloproteinases.

5.3.3. *Inhibition of MMP activity revert BBB disruption*

To confirm that the increased MMP concentration was driving BBB disruption, stimulated cells were co-incubated with Ro32-3555, a chemical inhibitor that blocks activity of collagenases and gelatinases.

Treatment with 10µM Ro32-3555 prevented CoMtb-dependent BBB disruption, with TEER and Papp remaining similar to controls (Fig. 39a, b). Coll-IV degradation was decreased by MMP blockade, while levels of the TJP ZO-1, claudin-3, claudin-5 and occludin were increased (Fig. 39c-e).
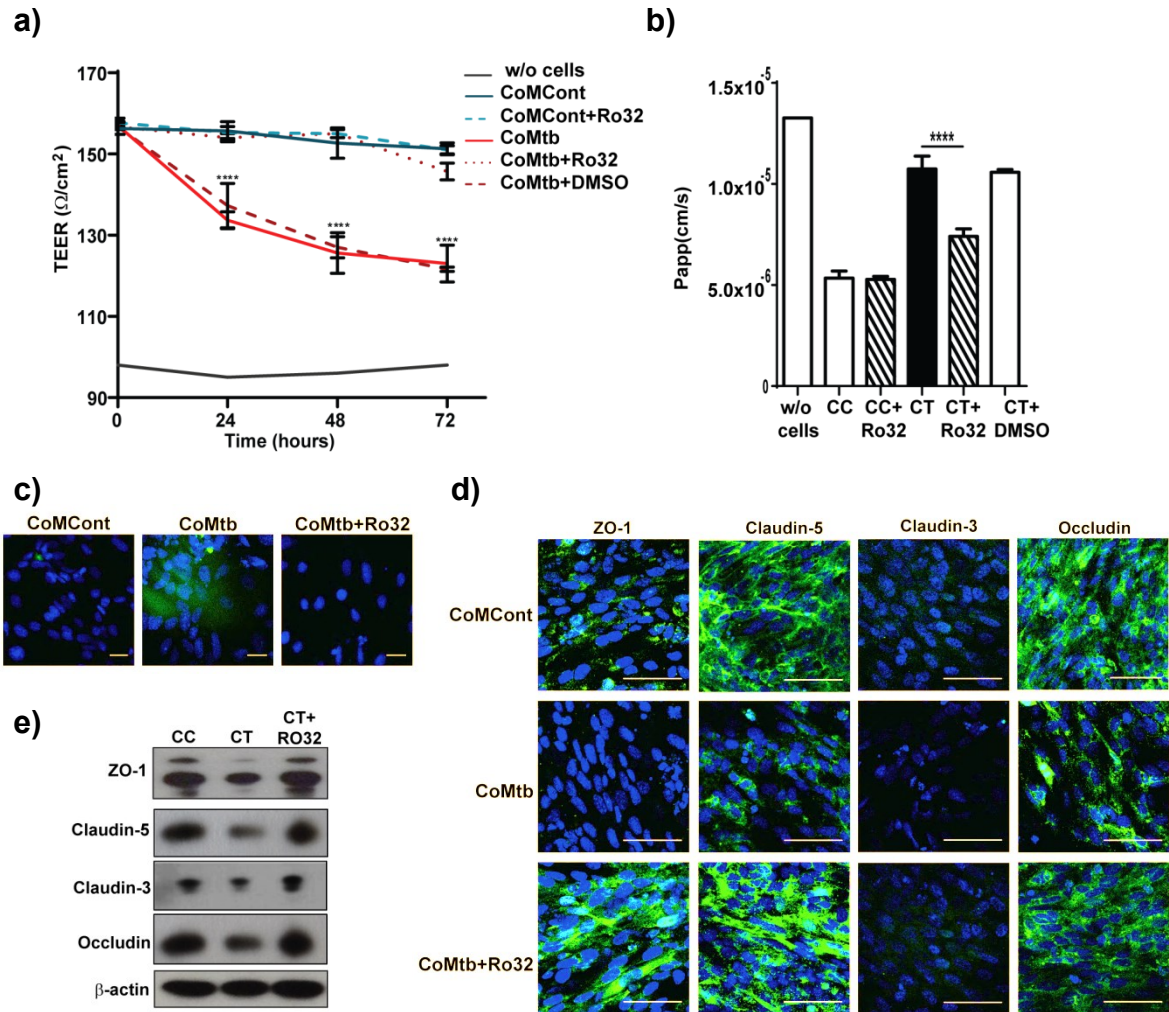
Figure 39. Blood-brain barrier disruption with CoMtb stimulation.

BBB stimulated for 72h with CoMtb or CoMCont. For confocal microscopy transwells were coated with (c) DQ collagen-IV and/or fixed and stained with DAPI (blue), (d) rabbit anti-human ZO-1, claudin-5, -3, occludin Ab and FITC-conjugated goat anti-rabbit IgG Ab (green). (e) For western blots, membranes were incubated with same TJP primary Ab and HRP conjugated goat anti-rabbit IgG Ab. **** $p < 0.0001$; ns-non significant; scale bar: 50µm. Ab- antibody; BBB- blood-brain barrier; CoMtb/CT-Conditioned medium of *Mycobacterium tuberculosis* infected monocytes; CoMCont/CC- control medium from uninfected monocytes; Ro-32- Ro-32-3555 chemical inhibitor.

5.3.4. *CoMtb stimulation increases expression of adhesion molecules by the endothelium leading to increased leukocyte transmigration*

Another consequence of CNS TB and a disrupted BBB is a deregulated influx of neutrophils and monocytes, which amplifies and perpetuates inflammation. In the present *in vitro* model, CoMtb stimulation led to increased levels of the adhesion molecules ICAM-1 (from 0.8±0.19 to 20.5±1.8ng/ml), VCAM-1 (0.5±0.13 to 27.5±3.8ng/ml), P-Selectin (0.03±0.012 to 1.35±0.34ng/ml) and E-Selectin (0.01±0.002 to 0.53±0.05ng/ml) (Fig. 40).

Transmigration of primary neutrophils and monocytes was preferentially paracellular (Fig. 40e) and increased 64% and 5-fold (from 2.49×10^4 monocytes/2h to 1.24×10^5/2h) respectively in pre-stimulated barriers. Addition of Ro32-3555 reverted transmigration to control levels (Fig. 40f, g).
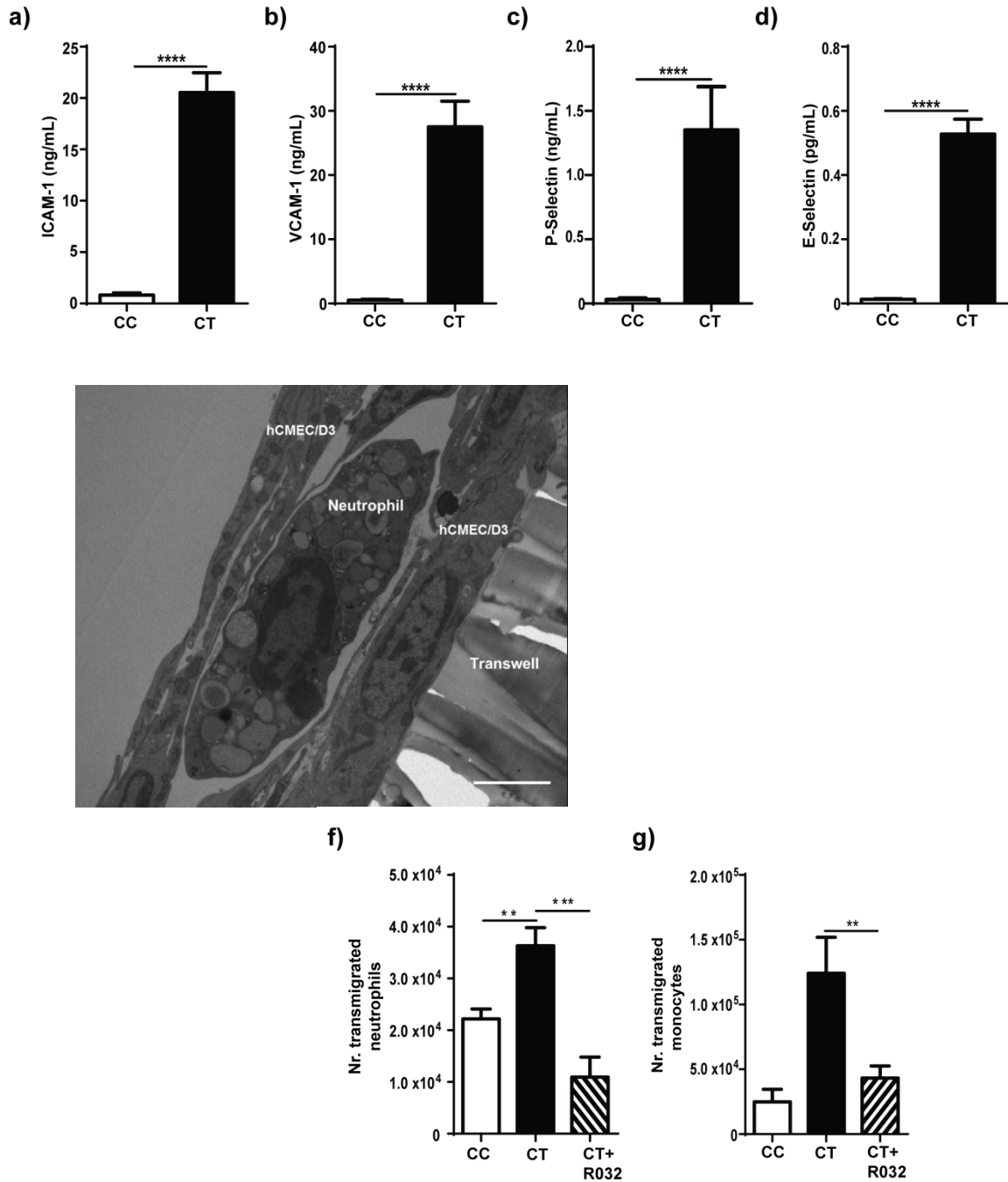
Figure 40. CoMtb stimulation increases expression of adhesion molecules and leukocyte transmigration across the barrier.

BBB stimulated for 72h with CoMtb or CoMCont. Supernatants were collected for Luminex of: a)ICAM-1, b)VCAM-1, c)P-Selectin and d)E-Selectin. For transmigration neutrophils (f) or monocytes (g) were labelled with a green cell tracker and 5.5×10^6 cells added to the apical side of pre-stimulated BBB and let to migrate for 2h. Transmigrated cells were collected and analysed by FACS. Figure e) is an electron microscopy image of a neutrophil during transmigration. Scale bar: 2μm. **p<0.01; ***p<0.001; **** p<0.0001; CC- conditioned medium from uninfected monocytes; CT- conditioned medium of *Mycobacterium tuberculosis* infected monocytes; Ro32- chemical inhibitor Ro32-3555.

Besides preventing BBB disruption, blocking MMP activity also led to reduced ICAM-1 shedding which may also contribute to a decrease in leukocyte transmigration (Fig. 41a, b).
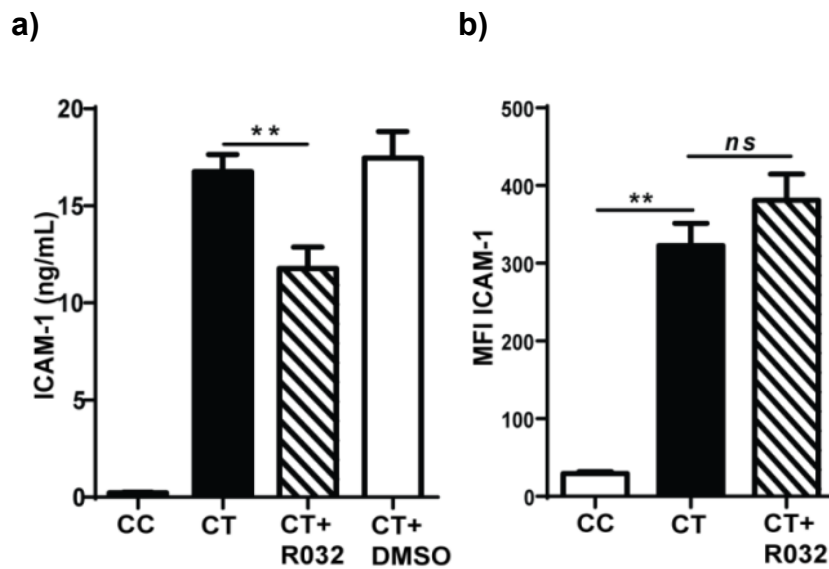
Figure 41. MMP blockade decreased ICAM-1 shedding in CoMtb-stimulated BBB.

BBB stimulated for 72h with CoMtb or CoMCont. Supernatants were collected for Luminex of: a) ICAM-1, and (b) endothelial cells detached, fixed, labelled for ICAM-1 and analysed by FACS. **p<0.01; ns-non significant. BBB- blood-brain barrier; CC- conditioned medium from uninfected monocytes; CT-conditioned medium of *Mycobacterium tuberculosis* infected monocytes; MMP-matrix metalloproteinase; MFI- mean fluorescence intensity; Ro32- chemical inhibitor Ro32-3555.

5.3.5. Mtb-driven MMP-9 upregulation causes opening of the BBB

MMP-9 activity has been involved in TJP degradation in neuroinflammation. Therefore it was investigated whether MMP-9 is the main effector driving BBB disruption. For this, 20ng of activated rhMMP-9 was used to compare BBB integrity with control and CoMtb-stimulated wells. Active rhMMP-9 caused a decrease in TEER and Papp, which was blocked when the MMP chemical inhibitor was added (Fig. 42a, b). MMP-9 activity was also specifically blocked in CoMtb-stimulated BBB using 25µg/ml anti-human MMP-9 blocking antibodies (Fig. 42d). In stimulated wells where MMP-9 was blocked, Papp significantly decreased by 40%. In CoMtb-stimulated BBB stained for MMP-9, it was observed a marked increase in MMP-9 (Fig. 42c). No significant differences were seen between CoMtb-stimulated BBB when MMP-1 was blocked by antibodies, nor by addition of active rhMMP-1 (Fig. 43a, b).
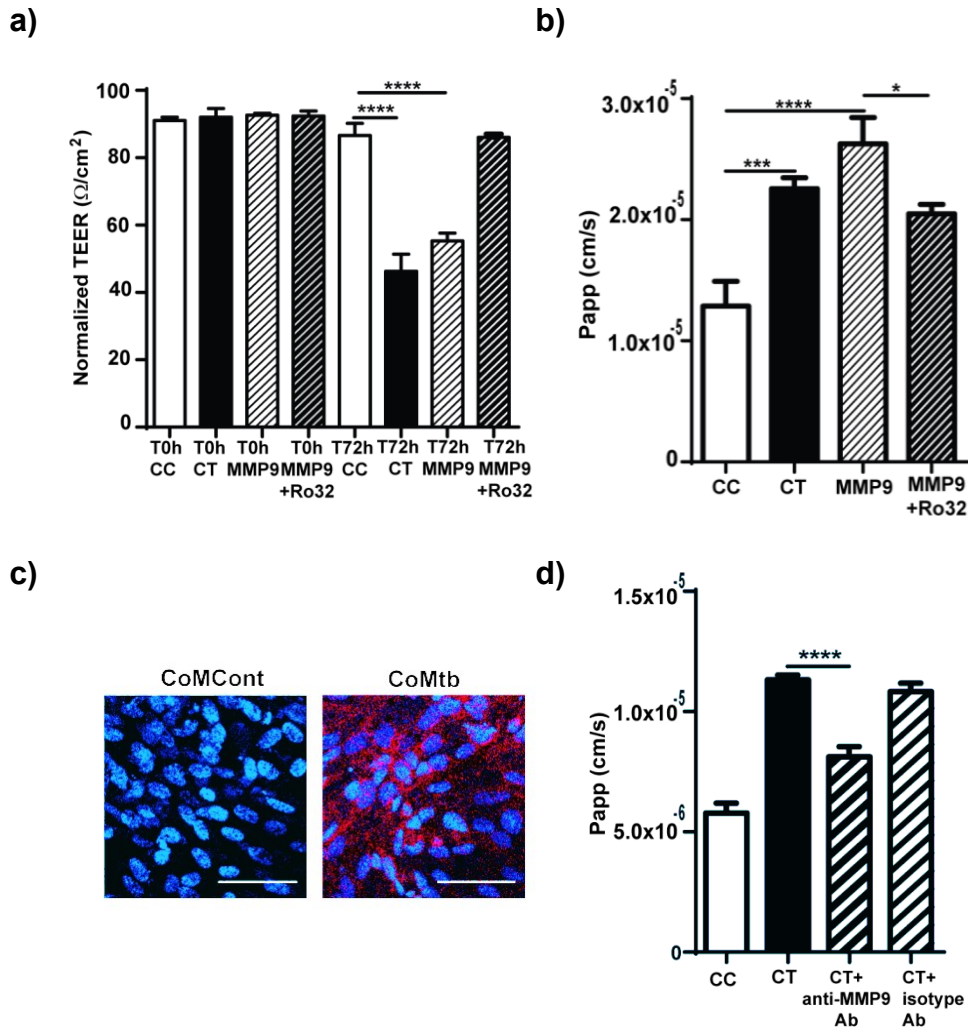
Figure 42. Blood-brain barrier disruption is caused by MMP-9.

BBB stimulated for 72h with CoMtb, CoMCont or 20ng rhMMP-9. (a)TEER; (b) Papp tosodium-fluorescein; (c) For confocal microscopy, cells fixed and stained with DAPI (blue), mouse anti-human MMP-9 primary Ab and cy5 conjugated goat anti-mouse Ab (red). (d) For MMP-9 blocking, cells were incubated with 20μg/ml of mouse anti-human MMP-9 antibody (clone) or a mouse IgG isotype control Ab. *p<0.05; ***p<0.001; ****p<0.0001; ns-non significant; scale bar: 50μm. Ab- antibody; BBB- blood-brain barrier; CoMCont/CC- conditioned medium from uninfected monocytes; CoMtb/CT-conditioned medium of *Mycobacterium tuberculosis* infected monocytes; MMP- matrix metalloproteinase; Ro32- Ro32-3555 chemical inhibitor.
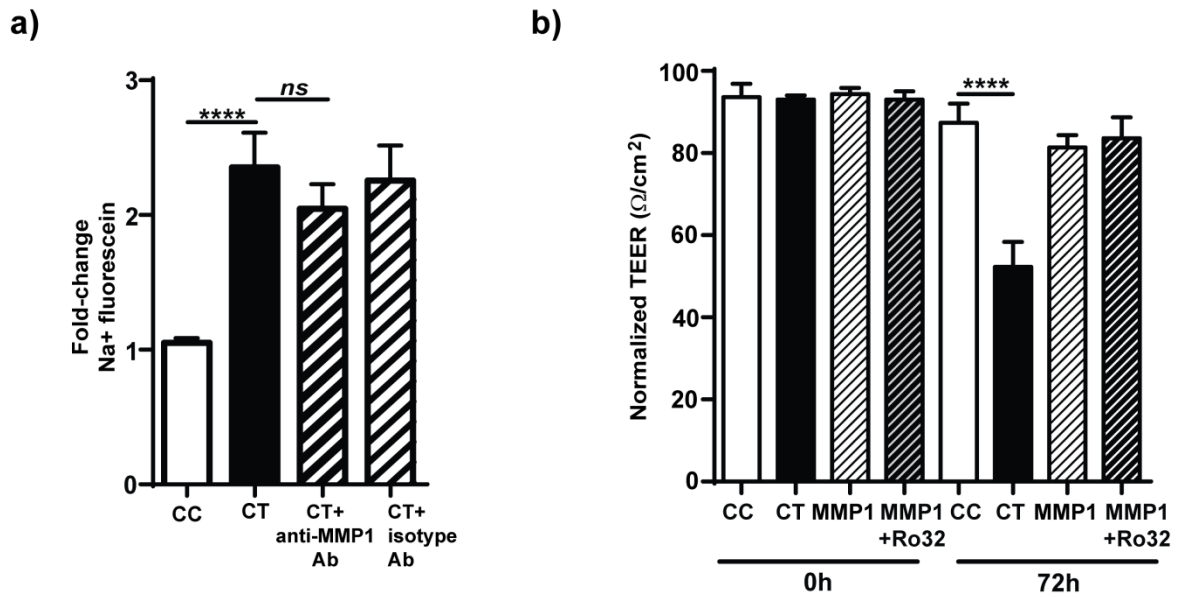
Figure 43. MMP-1 does not disrupt the BBB.

BBB stimulated for 72h with CoMtb, CoMCont or 20ng rhMMP-1. (a) Fold-change in permeability to sodium-fluorescein with addition of 25µg/ml of anti-MMP-1 blocking antibodies; (b) TEER with addition of active rhMMP-1. ****$p<0.0001$; ns-non significant. Ab- antibody; BBB- blood-brain barrier; CC- conditioned medium from uninfected monocytes; CT- conditioned medium of *Mycobacterium tuberculosis* infected monocytes; MMP- matrix metalloproteinase; Ro32- Ro32-3555 chemical inhibitor.

5.3.5. TJP gene expression is decreased by Mtb infection

I have observed that during Mtb invasion of the CNS, MMP-9 is upregulated leading to degradation of TJs and disruption of the BBB. Therefore, TJP gene expression was next analysed in infection. With Mtb infection, occludin mRNA was decreased by 90% and claudin-5 by 43% in hCMEC/D3 (Fig. 44a, b).
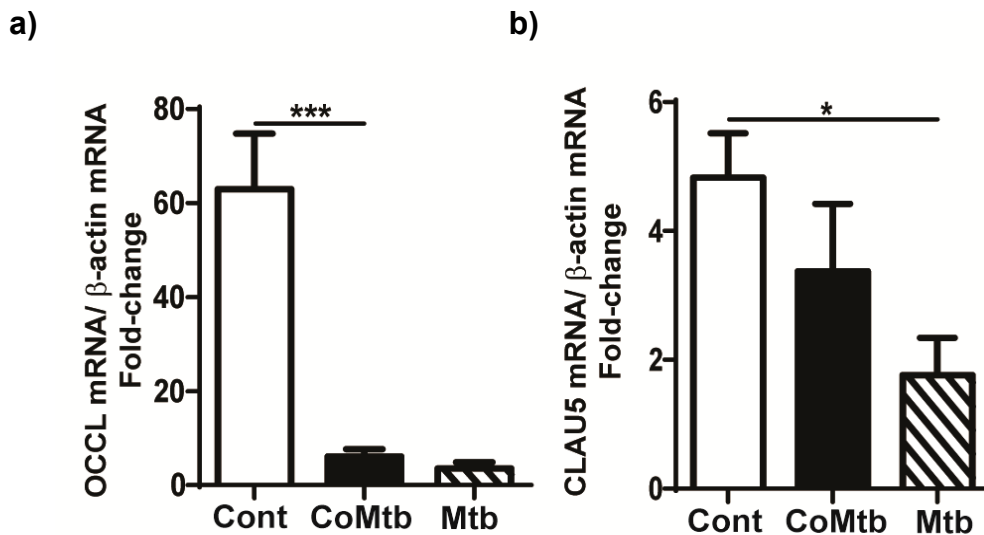
Figure 44. TJP gene expression is decreased in Mtb infection.

BBB stimulated for 72h with CoMtb or infected by Mtb (MOI=10). (a) Fold-change in occludin mRNA; (b) Fold-change in claudin-5 mRNA. β-actin mRNA was used as control.

***p<0.001; *p<0.05. BBB- blood-brain barrier; Cont- control medium; CoMtb- conditioned medium of *Mycobacterium tuberculosis* infected monocytes; CLAU5- claudin-5; Mtb- *Mycobacterium tuberculosis*; OCCL-occludin; TJP- tight junction protein.

The transcription factors Gli-1/2 regulate TJP gene expression, therefore their involvement was investigated. Staining Gli-1 revealed a decrease in nuclear translocation of the transcription factor in CoMtb-stimulated transwells (Fig. 45a). Blockade of the transcription factors Gli-1/2 with 10µM GANT-61 caused a 50% increase in Papp to sodium-fluorescein in controls but no further increase in CoMtb stimulated BBB (Fig. 45b).
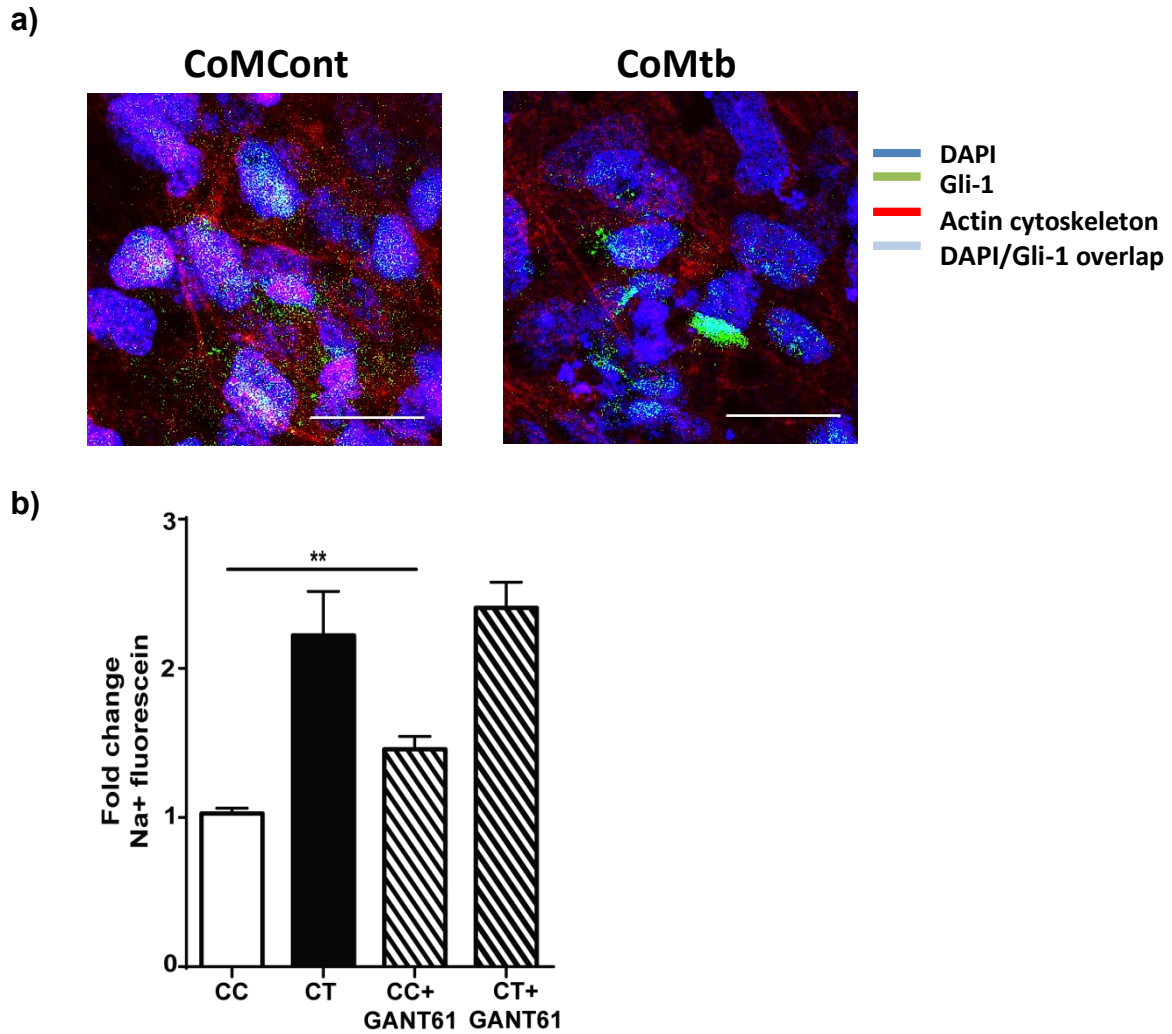
Figure 45. Endothelial Gli-1/2 activity is decreased with CoMtb-stimulation.

BBB stimulated for 72h with CoMtb. (a)Confocal microscopy of transwells stained for nucleic acids with DAPI (blue), cytoskeleton (red) and Gli-1 (green). Light blue correspond to areas of nucleus/Gli-1 overlap. Scale bar- 50μm. (b) Fold-change in permeability to sodium-fluorescein with addition of 10μM GANT61. **p<0.01. CoMCont/CC- conditioned medium from uninfected monocytes; CoMtb/CT-conditioned medium of *Mycobacterium tuberculosis* infected monocytes.

The Hh signalling pathway is known to regulate Gli-1/2 and has recently been implicated in maintenance of TJ integrity in the adult BBB. Therefore, the involvement of the Hh pathway in the decreased TJ gene expression was investigated. To analyse if during Mtb infection the production of Shh was decreased, BBB were stained for Shh. In CoMtb stimulated BBB, Shh at the surface of hCMEC/D3 was significantly decreased (Fig. 46a). This decrease was also apparent in endothelial cell lysates and reversed by MMP blockade with 10µM Ro32-3555 (Fig. 46b).
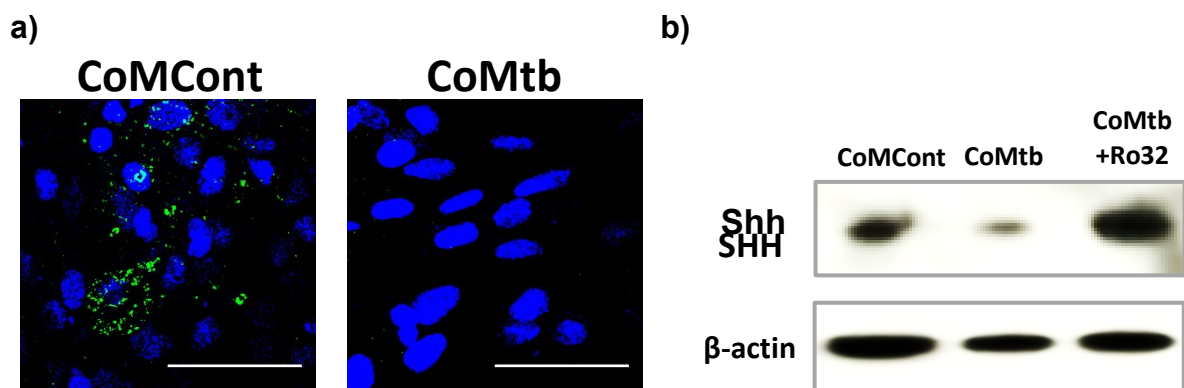
Figure 46. Endothelial Gli-1/2 activity is decreased with CoMtb-stimulation.

BBB stimulated for 72h with CoMtb. (a)Confocal microscopy of endothelial layer stained for nucleic acids with DAPI (blue), Shh (green). Scale bar- 50µm; (b) Western blot for hCMEC/D3 cell lysates labelled for Shh and β-actin as loading control. CoMCont- conditioned medium from uninfected monocytes; CoMtb- conditioned medium from *Mycobacterium tuberculosis* infected monocytes; Ro32-Ro32-3555 chemical inhibitor; Shh- Sonic hedgehog homolog.

To further confirm that decreased TJP expression during Mtb infection is due to a decrease in the Hh signalling, 100ng/ml rhShh was added to CoMtb-stimulated BBB. Addition of rhShh improved barrier functions, with a decrease in Papp to 3KDa FITC-dextran and increase in TJs proteins ZO-1, claudin-3, claudin -5 and occludin (Fig. 47).
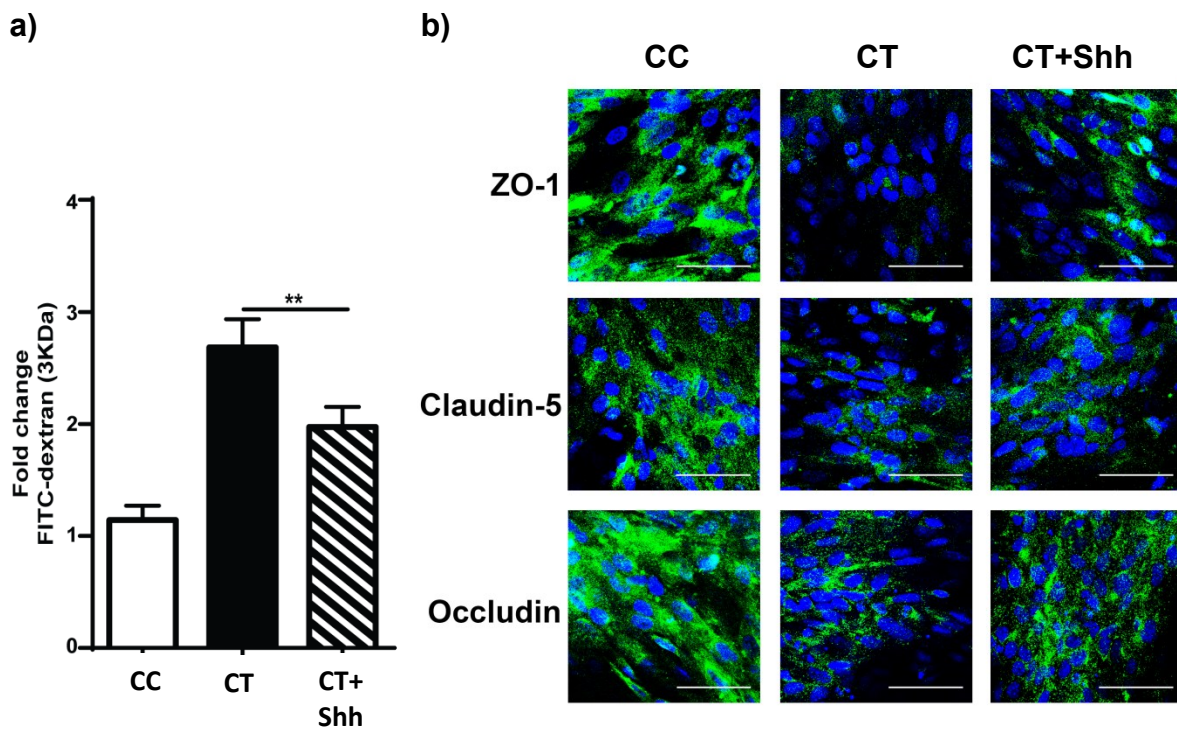
Figure 47. Addition of rhShh partially revert BBB disruption.

BBB stimulated for 72h with CoMtb or CoMcont and/or 100ng/ml rhShh. (a)Fold-change in permeability to 3KDa FITC-dextran; (b) Confocal microscopy of transwells stained for nucleic acids with DAPI (blue), and TJP (green). Scale bar- 50µm. **$p<0.01$. CoMCont/CC- conditioned medium from uninfected monocytes; CoMtb/CT- conditioned medium from *Mycobacterium tuberculosis* infected monocytes; rhShh- recombinant human sonic hedgehog homolog.

Since Hh pathway is downregulated in brain endothelial cells during Mtb infection, Shh production by astrocytes was analysed. Shh gene expression was significantly downregulated by CoMtb stimulation. However, no significant differences were found at the Shh protein levels in astrocytes (Fig. 48a, b). Recently the secreted glycoprotein SCUBE2 (signal peptide, cubulin domain, epidermal growth factor-like protein 2) was implicated in efficient Shh proteolytic processing and secretion from producing cells [273]. Therefore, I analysed the levels of SCUBE2 in astrocytes. In CoMtb-stimulated BBB, astrocytes had significantly lower levels of SCUBE2 than controls (Fig. 48c), which indicates that this decrease may be affecting Shh delivery to hCMEC/D3 during infection.
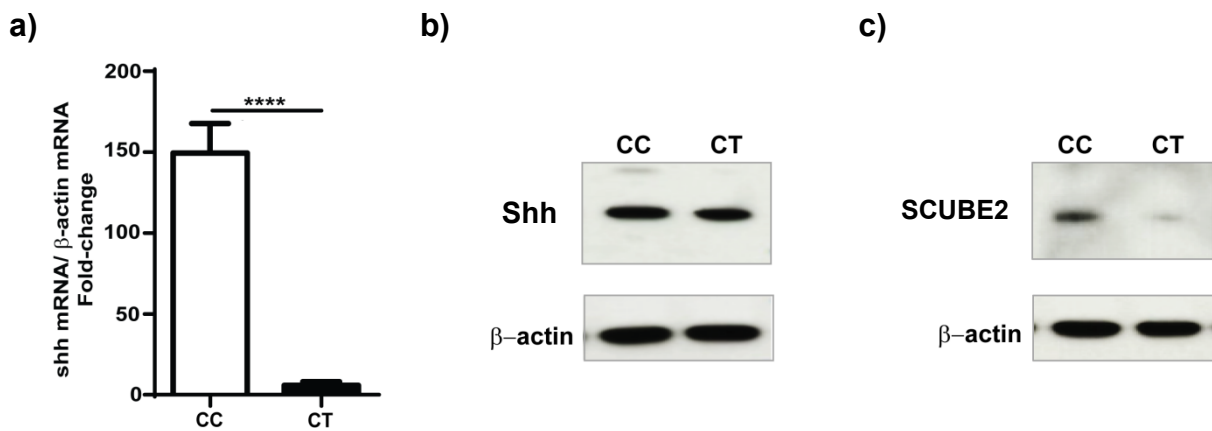
Figure 48. Astrocyte Shh gene expression and SCUBE2 protein levels are decreased by CoMtb.

Human astrocytes were stimulated with CoMtb or CoMcont for 6h for gene expression and for 72h for proteinlysates. (a)Fold-change in shh mRNA. β-actin mRNA was used as control. Western blots from total astrocyte lysates for (b) Shh and (c) SCUBE2. β-actin was used as loading control. ****$p < 0.0001$. CC- conditioned medium from uninfected monocytes; CT- conditioned medium from *Mycobacterium tuberculosis* infected monocytes; Shh- sonic hedgehog homolog; SCUBE2- signal peptide, cubulin domain, epidermal growth factor-like protein 2.

5.4. Discussion

CNS TB and particularly TB meningitis is associated with cerebral oedema and increased intracranial pressure derived from BBB disruption. However no studies have been performed to understand the mechanisms leading to BBB opening in TB.

In the present study I developed an *in vitro* co-culture model of CNS TB and verified that Mtb and monocyte dependent networks lead to astrocyte activation and upregulation of MMP production. MMP-9 was found to be the main MMP responsible for ECM and TJPs degradation, since an upregulation of over 600-fold was detected and MMP-9 inhibition by specific blocking antibodies partially reversed BBB disruption. This data is consistent with studies in multiple sclerosis, Alzheimer's disease and other bacterial meningitis, where MMP-9 has been reported as the main MMP driving BBB dysfunction and neuronal injury [274-276]. One study in children with TB meningitis reported that increased VEGF levels correlated with CSF-serum albumin ratios and mononuclear cell counts [277]. Although VEGF levels were not analysed in the present and my group was not able to find significant correlations in previous studies, it is known that this growth factor increases MMP-9 gene expression which is consistent with my data.

Although I was not able associate other MMPs with the phenotype I have detected a significant increase of over 20-fold for MMP-1, MMP-3 and MMP-8. MMP-1 is able to degrade fibrillar Coll-I and is the main collagenase driving cavitation in pulmonary

TB. However, the extracellular matrix in the CNS is poor in Coll-I and is mainly composed by HA, aggrecan and tenascins and basement membranes by Coll-IV and Lam [278], all substrates for gelatinases such as MMP-9. Nevertheless, MMP-1 has other non-matrix substrates such as IL-1β and proTNF-α which may also contribute to increase inflammation. MMP-3, a stromelysin, is a known activator of proMMP-9 and proTNF-α, which may contribute to the final net effect of total active MMP-9, especially because no increase was detected for the corresponding MMP inhibitors. MMP-8 has been involved in the cleavage of the TJP occludin in *Neisseria meningitidis* infection [179], which may contribute to the phenotype seen in my model.

I found that, in response to Mtb infection, MMP-9 was mainly astrocyte derived since no significant increases in MMP-9 secretion and BBB disruption were detected in the absence of astrocytes. Although I have detected a pathological effect from astrocytes, these are crucial to maintain BBB integrity. Recently the Hh pathway has been implicated in BBB integrity in the adult CNS [206,279] and human astrocytes are the main cells expressing Shh. In my study I found that gene expression of the TJPs claudin-5 and occludin was decreased during Mtb-infection and this was associated with a decreased activity of the transcription factors Gli-1/2, the final mediators of the Hh pathway. Using Smo knockout mice, Alvarez *et al*. found that silencing Hh lead to low levels of claudin-3/-5, occludin and ZO-1 and a fragmented basement membrane. Moreover, they found that the Hh pathway is key in controlling the pro-inflammatory response during experimental autoimmune encephalitis [206].

In the present study I found that the Hh pathway was decreased during Mtb infection and upregulation of the Hh pathway by addition of a smo agonist or rhSHH decreased permeability, increased TEER and TJP expression. One study using mouse primary cells also found that condition medium of astrocytes and recombinant rhShh increased TJP expression and reported that IL-1β was associated with decreased Shh gene expression by astrocytes[269]. Although I also found a decrease in Shh gene expression I was not able to detect a significant decrease at the protein level. The secreted glycoprotein SCUBE2 has been implicated in efficient Shh proteolytic processing and secretion [273,280] and in my model, I found that during Mtb infection astrocytes had significantly lower levels of SCUBE2 than controls. This might cause an accumulation of Shh protein in the astrocytes without delivery to the target endothelial cells leading to downregulation of the Hh pathway. There is not an extensive knowledge about the Shh pathway and SCUBE2. SCUBE3 is a homolog of SCUBE2 and has a protein sequence similarity of 90% for the CUB domain and 77% homology for the EGF repeats. The spacer regions are the most divergent with only 50% homology [281]. SCUBE 3 was found to be proteolytically cleaved by the gelatinases MMP-2 and MMP-9 [282], while one study in cancer, showed that SCUBE2 can be cleaved by recombinant MMP-2 with generation of an NH2 terminal 72kDa fragment and a COOH terminal 55kDa fragment [283]. Therefore, the increased activity seen for MMP-9 might be responsible for the degradation detected for SCUBE2 in my model leading to decreased Shh delivery to the brain endothelial cells.

Taken together my data demonstrates that, in CNS tuberculosis, astrocyte-derived MMP-9 causes breakdown of tissue and tight junctions leading to BBB disruption, facilitating increased leukocyte migration which, in turn, sustains inflammation. Shh is a potential new target to restore BBB function and decrease inflammation and could be used as adjuvant therapy in CNS TB.

Conclusions

The ECM gives tissues specificity and is a key element in the control of local immune function. In TB, tissue destruction is a determinant event in immunopathology and can affect disease outcome. I have demonstrated that in pulmonary TB, the ECM regulates both epithelial and monocyte expression of MMP-1 and that integrins are important regulators of these responses. During infection, integrins integrate important cues from the ECM environment providing cells a local context to other inflammatory stimuli. I have demonstrated that during infection, intact matrix Coll-I decreased MMP-1 secretion and collagenolytic activity in bronchial epithelial cells and enhanced cell migration instead of collagen breakdown. In this situation, MMP-1 was co-localised with epithelial α2β1 resulting in localised collagen proteolysis and enhanced cell migration, promoting epithelial monolayer repair with preservation of the ECM. However, sColl-I led to integrin α2β1 occupancy without clustering and increased the production of MMP-1 and collagenolytic activity. In Mtb-infected or CoMtb-stimulated monocytes, surface expression of integrin αVβ3 was upregulated and this was shown to be responsible for MMP-1/10 upregulation in the presence of Coll-I and Fn.

In vivo, soluble Coll-I results from fragments released from the ECM as a result of increased proteolysis, like the one resulting from MMP-1 secreted by recruited monocytes during Mtb infection. The present work has shown that local production of sColl-I by MMP-1 appears to shift bronchial epithelial cells towards a matrix degrading phenotype, with escalating MMP-1 production and tissue destruction.

Hence, the local ECM environment can determine the tissue MMP response to TB, which may be amenable to targeted drug therapy.

In the CNS, the ECM is mainly composed by HA, aggrecan and tenascins, while the basement membrane is composed by Coll-IV and Lam, which are natural substrates for gelatinases. During Mtb-infection a significant upregulation of MMP-1 was detected; however, tissue destruction and TJP breakdown was caused by gelatinolytic activity of astrocyte-derived MMP-9. Nevertheless, MMP-1 has other non-matrix substrates such as IL1-β and proTNF-α which may also contribute to increased inflammation. BBB disruption due to MMP-9 activity also facilitates leukocyte transmigration, which in turn sustains CNS inflammation. In CNS TB, BBB disruption may be a key and targetable event in immunopathology.

Future prespectives

The results from the present work have provided important evidence that the ECM is a key element in regulation of the tissue immune response to TB. In this chapter I shall discuss possible directions of research looking at further expanding the knowledge of TB immunopathology.

Most studies in the field of TB have been focused on therapies to eliminate the microorganism and less effort has been directed to the immunopathological response of the host and the way the pathogen exploits this response in its favour. Previous work from my group has hypothesised that ECM breakdown, namely Coll-I, was required for the development of caseous necrosis [85,264]. My work using an *in vitro* model of pulmonary TB supported this hypothesis. It was demonstrated that through integrins engagement and signalling the respiratory epithelium can integrate signals from the ECM. Activated monocytes increase their expression of integrin αVβ3, which becomes activated when monocytes reach the lung driving cell migration and collagenase expression. The resulting presence of degraded Coll-I in the environment blocks epithelial ability to migrate and repair the tissue, skewing the immune response in favor of the pathogen. Hence, tissue pathology occurs primarily due to the host response, which highlights the role for immunomodulatory therapy in TB.

The evidences from this study support the emergent concept that collagen destruction is an early event in TB pathology, preceding caseation. This opposes the previous paradigm that ECM destruction is a consequence of caseous necrosis [284,285]. To prove this concept, future MMP inhibition studies in an animal model that recapitulates the key pathological features of human TB should ideally be performed, in order to demonstrate that collagenase inhibition reduces Mtb–driven immunopathology. Animal models used in research such as zebrafish, mice, guinea pigs, rabbits do not completely replicate the immunopathology seen in humans. For example, mouse models demonstrate minimal delayed-type hypersensitivity response and do not form true caseous necrosis or cavities in response to Mtb, while the guinea pig although showing a delayed-type hypersensitivity response, they also demonstrate a very high mortality compared with humans. The spectrum of TB disease is better replicated in the rabbit model demonstrates pulmonary cavities in established disease [286]. Cavitation is, however, more pronounced in rabbits exposed to Mycobacterium bovis than to Mtb.

Regarding the work using the CNS TB *in vitro* model, it has demonstrated for the first time that BBB dysfunction is a key element in development of immunopathology. Future research will require *in vivo* work would to better understand the mechanisms that contribute to Mtb dissemination from the lung to the brain and the mechanisms leading to opening of the BBB. However, to study interventions based on observations from the BBB cellular model, it is vital to first develop better *in vivo* models.

Currently existing models of CNS TB do not satisfactorily fulfil the required features, which were also limited to the use of the laboratory strain of Mtb H37Rv, and experiments using both aerosol and intra-venous routes of infection demonstrated minimal H37Rv infection in the CNS [287]. This limitation has been well recognised and been overcomed using murine intracerebral injections in studies involving H37Rv. However, this method is extremely invasive although it may be associated with BBB disruption since in this model, Mtb was detected relatively early in the lungs of CNS-infected mice [288]. Some studies in guinea pigs were successful in detecting Mtb in the brain following aerosol infection[272]. However, guinea pigs are highly susceptible and quickly succumb to infection making data collection difficult. This clearly illustrates the need to develop new *in vivo* models to study BBB disruption during CNS TB.

Paradoxical worsening of symptoms and lesion in CNS TB may occur days to months after starting anti-tuberculous therapy. We thus need anti-tuberculous agents with good CNS tissue penetration and that have immunomodulatory activity to prevent BBB disruption which I believe leads to the paradoxical reaction seen following initiation of therapy. There are several new drugs in the pipeline. Among them bedaquiline (TMC207), delamanid (OPC67683), pretomanid (PA-824) which have the potential of shorten pulmonary TB therapy. Bedaquiline has already been approved by the US Food and Drug Administration for treatment of drug-resistant TB[289]. However, there are still no data on the efficacy and safety of these drugs on treatment of extra-pulmonary TB. Corticosteroids are often administered as adjunctive therapy in CNS TB paradoxical reactions but some cases may prove refractory.It is therefore necessary to evaluate other potential immunomodulatory agents.

In both pulmonary and CNS TB, we found a key role for MMP activity in immunopathology, therefore MMPs are a likely candidate as a drug-target. A range of MMP inhibitors, (e.g. batimastat, marimastat, Ro32-3555) have been developed for use in cancer and trialed for rheumatoid arthritis. However, they failed to produce positive outcomes in the clinical trials due to pronounced adverse effects on the musculoskeletal system, which lead to non-adherence to the drugs. New anti-MMP drugs should therefore be developed and MMP has a drug target deserve further testing, especially in the field of infection, where the duration of drug treatment is considerably shorter.

In summary, future research should be directed towards understanding host response to Mtb and focused in developing therapeutic approaches to reduce tissue destruction. Strategies to preserve the ECM in patients with TB may reduce morbidity and mortality and restore an efficient immune response to Mtb infection.

References

1   WHO: Global tuberculosis report 2013. 2013

2   Schluger NW: Drug-resistant tuberculosis: What is to be done? Chest 2009;136:333-335.

3   Gandhi NR, Nunn P, Dheda K, Schaaf HS, Zignol M, van Soolingen D, Jensen P, Bayona J: Multidrug-resistant and extensively drug-resistant tuberculosis: A threat to global control of tuberculosis. Lancet 2010;375:1830-1843.

4   Rock RB, Olin M, Baker CA, Molitor TW, Peterson PK: Central nervous system tuberculosis: Pathogenesis and clinical aspects. Clin Microbiol Rev 2008;21:243-261, table of contents.

5   Kwan CK, Ernst JD: HIV and tuberculosis: A deadly human syndemic. Clin Microbiol Rev 2011;24:351-376.

6   Nelson CA, Zunt JR: Tuberculosis of the central nervous system in immunocompromised patients: HIV infection and solid organ transplant recipients. Clin Infect Dis 2011;53:915-926.

7   van Crevel R, Ottenhoff TH, van der Meer JW: Innate immunity to *Mycobacterium tuberculosis*. Clin Microbiol Rev 2002;15:294-309.

8   Lowe DM, Redford PS, Wilkinson RJ, O'Garra A, Martineau AR: Neutrophils in tuberculosis: Friend or foe? Trends Immunol 2011

9   Huynh KK, Joshi SA, Brown EJ: A delicate dance: Host response to mycobacteria. Curr Opin Immunol 2011;23:464-472.

10   Friedland JS: Tackling tissue destruction in tuberculosis. Trans R Soc Trop Med Hyg 2008;102:953-954.

11   Nagase H, Visse R, Murphy G: Structure and function of matrix metalloproteinases and TIMPs. Cardiovasc Res 2006;69:562-573.

12   Bode W, Gomis-Ruth FX, Stockler W: Astacins, serralysins, snake venom and matrix metalloproteinases exhibit identical zinc-binding environments (hexxhxxgxxh

and met-turn) and topologies and should be grouped into a common family, the 'metzincins'. FEBS Lett 1993;331:134-140.

13   Greenlee KJ, Werb Z, Kheradmand F: Matrix metalloproteinases in lung: Multiple, multifarious, and multifaceted. Physiol Rev 2007;87:69-98.

14   Bove PF, Wesley UV, Greul AK, Hristova M, Dostmann WR, van der Vliet A: Nitric oxide promotes airway epithelial wound repair through enhanced activation of MMP-9. Am J Respir Cell Mol Biol 2007;36:138-146.

15   Wesley UV, Bove PF, Hristova M, McCarthy S, van der Vliet A: Airway epithelial cell migration and wound repair by ATP-mediated activation of dual oxidase 1. J Biol Chem 2007;282:3213-3220.

16   Visse R, Nagase H: Matrix metalloproteinases and tissue inhibitors of metalloproteinases: Structure, function, and biochemistry. Circ Res 2003;92:827-839.

17   Dumin JA, Dickeson SK, Stricker TP, Bhattacharyya-Pakrasi M, Roby JD, Santoro SA, Parks WC: Pro-collagenase-1 (matrix metalloproteinase-1) binds the alpha(2)beta(1) integrin upon release from keratinocytes migrating on type i collagen. J Biol Chem 2001;276:29368-29374.

18   Yan C, Boyd DD: Regulation of matrix metalloproteinase gene expression. J Cell Physiol 2007;211:19-26.

19   Green JA, Elkington PT, Pennington CJ, Roncaroli F, Dholakia S, Moores RC, Bullen A, Porter JC, Agranoff D, Edwards DR, Friedland JS: *Mycobacterium tuberculosis* upregulates microglial matrix metalloproteinase-1 and -3 expression and secretion via NF-kappaB- and activator protein-1-dependent monocyte networks. J Immunol 2010;184:6492-6503.

20   O'Kane CM, Elkington PT, Jones MD, Caviedes L, Tovar M, Gilman RH, Stamp G, Friedland JS: STAT3, p38 MAPK, and NF-kappaB drive unopposed monocyte-dependent fibroblast MMP-1 secretion in tuberculosis. Am J Respir Cell Mol Biol 2010;43:465-474.

21   Gum R, Wang H, Lengyel E, Juarez J, Boyd D: Regulation of 92 KDa type IV collagenase expression by the jun aminoterminal kinase- and the extracellular signal-regulated kinase-dependent signaling cascades. Oncogene 1997;14:1481-1493.

22   Simon C, Goepfert H, Boyd D: Inhibition of the p38 mitogen-activated protein kinase by SB203580 blocks PMA-induced MR92,000 type IV collagenase secretion and *in vitro* invasion. Cancer Res 1998;58:1135-1139.

23   McCawley LJ, Li S, Wattenberg EV, Hudson LG: Sustained activation of the mitogen-activated protein kinase pathway. A mechanism underlying receptor tyrosine kinase specificity for matrix metalloproteinase-9 induction and cell migration. J Biol Chem 1999;274:4347-4353.

24   Reddy KB, Krueger JS, Kondapaka SB, Diglio CA: Mitogen-activated protein kinase (MAPK) regulates the expression of progelatinase B (MMP-9) in breast epithelial cells. Int J Cancer 1999;82:268-273.

25   Cohen M, Meisser A, Haenggeli L, Bischof P: Involvement of mapk pathway in TNF-alpha-induced MMP-9 expression in human trophoblastic cells. Mol Hum Reprod 2006;12:225-232.

26   Chou YC, Sheu JR, Chung CL, Chen CY, Lin FL, Hsu MJ, Kuo YH, Hsiao G: Nuclear-targeted inhibition of NF-kappaB on MMP-9 production by n-2-(4-bromophenyl) ethyl caffeamide in human monocytic cells. Chem Biol Interact 2010;184:403-412.

27   Vincenti MP, Coon CI, Brinckerhoff CE: Nuclear factor kappab/p50 activates an element in the distal matrix metalloproteinase 1 promoter in interleukin-1beta-stimulated synovial fibroblasts. Arthritis Rheum 1998;41:1987-1994.

28   Bond M, Chase AJ, Baker AH, Newby AC: Inhibition of transcription factor NF-kappaB reduces matrix metalloproteinase-1, -3 and -9 production by vascular smooth muscle cells. Cardiovasc Res 2001;50:556-565.

29   Rice JC, Allis CD: Histone methylation versus histone acetylation: New insights into epigenetic regulation. Curr Opin Cell Biol 2001;13:263-273.

30   Mayo MW, Denlinger CE, Broad RM, Yeung F, Reilly ET, Shi Y, Jones DR: Ineffectiveness of histone deacetylase inhibitors to induce apoptosis involves the transcriptional activation of NF-kappa B through the AKT pathway. J Biol Chem 2003;278:18980-18989.

31   Song C, Zhu S, Wu C, Kang J: Histone deacetylase (HDAC) 10 suppresses cervical cancer metastasis through inhibition of matrix metalloproteinase (MMP) 2 and 9 expression. J Biol Chem 2013;288:28021-28033.

32   Young DA, Lakey RL, Pennington CJ, Jones D, Kevorkian L, Edwards DR, Cawston TE, Clark IM: Histone deacetylase inhibitors modulate metalloproteinase gene expression in chondrocytes and block cartilage resorption. Arthritis Res Ther 2005;7:R503-512.

33   Kaneko F, Saito H, Saito Y, Wakabayashi K, Nakamoto N, Tada S, Suzuki H, Tsunematsu S, Kumagai N, Ishii H: Down-regulation of matrix-invasive potential of human liver cancer cells by type I interferon and a histone deacetylase inhibitor sodium butyrate. Int J Oncol 2004;24:837-845.

34   Kuljaca S, Liu T, Tee AE, Haber M, Norris MD, Dwarte T, Marshall GM: Enhancing the anti-angiogenic action of histone deacetylase inhibitors. Mol Cancer 2007;6:68.

35   Lee KH, Choi EY, Kim MK, Kim KO, Jang BI, Kim SW, Kim SW, Song SK, Kim JR: Inhibition of histone deacetylase activity down-regulates urokinase plasminogen activator and matrix metalloproteinase-9 expression in gastric cancer. Mol Cell Biochem 2010;343:163-171.

36   Vinodhkumar R, Song YS, Ravikumar V, Ramakrishnan G, Devaki T: Depsipeptide a histone deacetlyase inhibitor down regulates levels of matrix metalloproteinases 2 and 9 mRNA and protein expressions in lung cancer cells (A549). Chem Biol Interact 2007;165:220-229.

37   Brooks PC, Stromblad S, Sanders LC, von Schalscha TL, Aimes RT, Stetler-Stevenson WG, Quigley JP, Cheresh DA: Localization of matrix metalloproteinase MMP-2 to the surface of invasive cells by interaction with integrin alpha v beta 3. Cell 1996;85:683-693.

38   Yu Q, Stamenkovic I: Localization of matrix metalloproteinase 9 to the cell surface provides a mechanism for CD44-mediated tumor invasion. Genes Dev 1999;13:35-48.

39   Redondo-Munoz J, Ugarte-Berzal E, Garcia-Marco JA, del Cerro MH, Van den Steen PE, Opdenakker G, Terol MJ, Garcia-Pardo A: Alpha4beta1 integrin and 190-

kda CD44v constitute a cell surface docking complex for gelatinase B/MMP-9 in chronic leukemic but not in normal B cells. Blood 2008;112:169-178.

40   Bjorklund M, Heikkila P, Koivunen E: Peptide inhibition of catalytic and noncatalytic activities of matrix metalloproteinase-9 blocks tumor cell migration and invasion. J Biol Chem 2004;279:29589-29597.

41   Adair-Kirk TL, Senior RM: Fragments of extracellular matrix as mediators of inflammation. Int J Biochem Cell Biol 2008;40:1101-1110.

42   Herrera I, Cisneros J, Maldonado M, Ramirez R, Ortiz-Quintero B, Anso E, Chandel NS, Selman M, Pardo A: Matrix metalloproteinase (MMP)-1 induces lung alveolar epithelial cell migration and proliferation, protects from apoptosis, and represses mitochondrial oxygen consumption. J Biol Chem 2013;288:25964-25975.

43   Hautamaki RD, Kobayashi DK, Senior RM, Shapiro SD: Requirement for macrophage elastase for cigarette smoke-induced emphysema in mice. Science 1997;277:2002-2004.

44   Matias-Roman S, Galvez BG, Genis L, Yanez-Mo M, de la Rosa G, Sanchez-Mateos P, Sanchez-Madrid F, Arroyo AG: Membrane type 1-matrix metalloproteinase is involved in migration of human monocytes and is regulated through their interaction with fibronectin or endothelium. Blood 2005;105:3956-3964.

45   Warner RL, Beltran L, Younkin EM, Lewis CS, Weiss SJ, Varani J, Johnson KJ: Role of stromelysin 1 and gelatinase b in experimental acute lung injury. Am J Respir Cell Mol Biol 2001;24:537-544.

46   Gearing AJ, Beckett P, Christodoulou M, Churchill M, Clements J, Davidson AH, Drummond AH, Galloway WA, Gilbert R, Gordon JL, et al.: Processing of tumour necrosis factor-alpha precursor by metalloproteinases. Nature 1994;370:555-557.

47   Schonbeck U, Mach F, Libby P: Generation of biologically active IL-1 beta by matrix metalloproteinases: A novel caspase-1-independent pathway of IL-1 beta processing. J Immunol 1998;161:3340-3346.

48   Ito A, Mukaiyama A, Itoh Y, Nagase H, Thogersen IB, Enghild JJ, Sasaguri Y, Mori Y: Degradation of interleukin 1beta by matrix metalloproteinases. J Biol Chem 1996;271:14657-14660.

49   Van Lint P, Libert C: Chemokine and cytokine processing by matrix metalloproteinases and its effect on leukocyte migration and inflammation. J Leukoc Biol 2007;82:1375-1381.

50   McQuibban GA, Gong JH, Tam EM, McCulloch CA, Clark-Lewis I, Overall CM: Inflammation dampened by gelatinase a cleavage of monocyte chemoattractant protein-3. Science 2000;289:1202-1206.

51   Rodriguez D, Morrison CJ, Overall CM: Matrix metalloproteinases: What do they not do? New substrates and biological roles identified by murine models and proteomics. Biochim Biophys Acta 2010;1803:39-54.

52   Boire A, Covic L, Agarwal A, Jacques S, Sherifi S, Kuliopulos A: Par1 is a matrix metalloprotease-1 receptor that promotes invasion and tumorigenesis of breast cancer cells. Cell 2005;120:303-313.

53   Hadler-Olsen E, Fadnes B, Sylte I, Uhlin-Hansen L, Winberg JO: Regulation of matrix metalloproteinase activity in health and disease. The FEBS journal 2011;278:28-45.

54   Kwan JA, Schulze CJ, Wang W, Leon H, Sariahmetoglu M, Sung M, Sawicka J, Sims DE, Sawicki G, Schulz R: Matrix metalloproteinase-2 (MMP-2) is present in the nucleus of cardiac myocytes and is capable of cleaving poly (ADP-ribose) polymerase (PARP) in vitro. FASEB J 2004;18:690-692.

55   Si-Tayeb K, Monvoisin A, Mazzocco C, Lepreux S, Decossas M, Cubel G, Taras D, Blanc JF, Robinson DR, Rosenbaum J: Matrix metalloproteinase 3 is present in the cell nucleus and is involved in apoptosis. Am J Pathol 2006;169:1390-1401.

56   Aldonyte R, Brantly M, Block E, Patel J, Zhang J: Nuclear localization of active matrix metalloproteinase-2 in cigarette smoke-exposed apoptotic endothelial cells. Exp Lung Res 2009;35:59-75.

57   Limb GA, Matter K, Murphy G, Cambrey AD, Bishop PN, Morris GE, Khaw PT: Matrix metalloproteinase-1 associates with intracellular organelles and confers resistance to lamin a/c degradation during apoptosis. Am J Pathol 2005;166:1555-1563.

58   Yang E, Boire A, Agarwal A, Nguyen N, O'Callaghan K, Tu P, Kuliopulos A, Covic L: Blockade of PAR1 signaling with cell-penetrating pepducins inhibits akt survival pathways in breast cancer cells and suppresses tumor survival and metastasis. Cancer Res 2009;69:6223-6231.

59   Eguchi T, Kubota S, Kawata K, Mukudai Y, Uehara J, Ohgawara T, Ibaragi S, Sasaki A, Kuboki T, Takigawa M: Novel transcription-factor-like function of human matrix metalloproteinase 3 regulating the CTGF/CCN2 gene. Mol Cell Biol 2008;28:2391-2413.

60   Marchant DJ, Bellac CL, Moraes TJ, Wadsworth SJ, Dufour A, Butler GS, Bilawchuk LM, Hendry RG, Robertson AG, Cheung CT, Ng J, Ang L, Luo Z, Heilbron K, Norris MJ, Duan W, Bucyk T, Karpov A, Devel L, Georgiadis D, Hegele RG, Luo H, Granville DJ, Dive V, McManus BM, Overall CM: A new transcriptional role for matrix metalloproteinase-12 in antiviral immunity. Nat Med 2014;20:493-502.

61   Wilson CL, Ouellette AJ, Satchell DP, Ayabe T, Lopez-Boado YS, Stratman JL, Hultgren SJ, Matrisian LM, Parks WC: Regulation of intestinal alpha-defensin activation by the metalloproteinase matrilysin in innate host defense. Science 1999;286:113-117.

62   Dunsmore SE, Saarialho-Kere UK, Roby JD, Wilson CL, Matrisian LM, Welgus HG, Parks WC: Matrilysin expression and function in airway epithelium. J Clin Invest 1998;102:1321-1331.

63   Lopez-Boado YS, Wilson CL, Parks WC: Regulation of matrilysin expression in airway epithelial cells by *Pseudomonas aeruginosa* flagellin. J Biol Chem 2001;276:41417-41423.

64   Dobaczewski M, Gonzalez-Quesada C, Frangogiannis NG: The extracellular matrix as a modulator of the inflammatory and reparative response following myocardial infarction. J Mol Cell Cardiol 2010;48:504-511.

65   Chen Y, Nixon NB, Dawes PT, Mattey DL: Influence of variations across the MMP-1 and -3 genes on the serum levels of MMP-1 and -3 and disease activity in rheumatoid arthritis. Genes Immun 2012;13:29-37.

66   Egeblad M, Werb Z: New functions for the matrix metalloproteinases in cancer progression. Nat Rev Cancer 2002;2:161-174.

67   Yoon SO, Park SJ, Yun CH, Chung AS: Roles of matrix metalloproteinases in tumor metastasis and angiogenesis. J Biochem Mol Biol 2003;36:128-137.

68   Shuman Moss LA, Jensen-Taubman S, Stetler-Stevenson WG: Matrix metalloproteinases: Changing roles in tumor progression and metastasis. Am J Pathol 2012;181:1895-1899.

69   Hong JS, Greenlee KJ, Pitchumani R, Lee SH, Song LZ, Shan M, Chang SH, Park PW, Dong C, Werb Z, Bidani A, Corry DB, Kheradmand F: Dual protective mechanisms of matrix metalloproteinases 2 and 9 in immune defense against *Streptococcus pneumoniae*. J Immunol 2011;186:6427-6436.

70   Renckens R, Roelofs JJ, Florquin S, de Vos AF, Lijnen HR, van't Veer C, van der Poll T: Matrix metalloproteinase-9 deficiency impairs host defense against abdominal sepsis. J Immunol 2006;176:3735-3741.

71   Polimeni M, Valente E, Ulliers D, Opdenakker G, Van den Steen PE, Giribaldi G, Prato M: Natural haemozoin induces expression and release of human monocyte tissue inhibitor of metalloproteinase-1. PLoS One 2013;8:e71468.

72   Prato M, Gallo V, Giribaldi G, Aldieri E, Arese P: Role of the nf-kappab transcription pathway in the haemozoin- and 15-hete-mediated activation of matrix metalloproteinase-9 in human adherent monocytes. Cell Microbiol 2010;12:1780-1791.

73   Prato M, D'Alessandro S, Van den Steen PE, Opdenakker G, Arese P, Taramelli D, Basilico N: Natural haemozoin modulates matrix metalloproteinases and induces morphological changes in human microvascular endothelium. Cell Microbiol 2011;13:1275-1285.

74   Szklarczyk A, Stins M, Milward EA, Ryu H, Fitzsimmons C, Sullivan D, Conant K: Glial activation and matrix metalloproteinase release in cerebral malaria. J Neurovirol 2007;13:2-10.

75   Dietmann A, Helbok R, Lackner P, Issifou S, Lell B, Matsiegui PB, Reindl M, Schmutzhard E, Kremsner PG: Matrix metalloproteinases and their tissue inhibitors (timps) in *Plasmodium falciparum* malaria: Serum levels of TIMP-1 are associated with disease severity. J Infect Dis 2008;197:1614-1620.

76   Straat K, de Klark R, Gredmark-Russ S, Eriksson P, Soderberg-Naucler C: Infection with human cytomegalovirus alters the MMP-9/TIMP-1 balance in human macrophages. J Virol 2009;83:830-835.

77   North RJ, Jung YJ: Immunity to tuberculosis. Annu Rev Immunol 2004;22:599-623.

78   Elkington PT, D'Armiento JM, Friedland JS: Tuberculosis immunopathology: The neglected role of extracellular matrix destruction. Sci Transl Med 2011;3:71ps76.

79   Elkington PT, Nuttall RK, Boyle JJ, O'Kane CM, Horncastle DE, Edwards DR, Friedland JS: *Mycobacterium tuberculosis*, but not vaccine BCG, specifically upregulates matrix metalloproteinase-1. Am J Respir Crit Care Med 2005;172:1596-1604.

80   Elkington PT, Green JA, Emerson JE, Lopez-Pascua LD, Boyle JJ, O'Kane CM, Friedland JS: Synergistic up-regulation of epithelial cell matrix metalloproteinase-9 secretion in tuberculosis. Am J Respir Cell Mol Biol 2007;37:431-437.

81   Ugarte-Gil CA, Elkington P, Gilman RH, Coronel J, Tezera LB, Bernabe-Ortiz A, Gotuzzo E, Friedland JS, Moore DA: Induced sputum MMP-1, -3 & -8 concentrations during treatment of tuberculosis. PLoS One 2013;8:e61333.

82   Quiding-Jarbrink M, Smith DA, Bancroft GJ: Production of matrix metalloproteinases in response to mycobacterial infection. Infect Immun 2001;69:5661-5670.

83   Rivera-Marrero CA, Schuyler W, Roser S, Roman J: Induction of mmp-9 mediated gelatinolytic activity in human monocytic cells by cell wall components of mycobacterium tuberculosis. Microb Pathog 2000;29:231-244.

84   Elkington P, Shiomi T, Breen R, Nuttall RK, Ugarte-Gil CA, Walker NF, Saraiva L, Pedersen B, Mauri F, Lipman M, Edwards DR, Robertson BD, D'Armiento J, Friedland JS: MMP-1 drives immunopathology in human tuberculosis and transgenic mice. J Clin Invest 2011;121:1827-1833.

85   Seddon J, Kasprowicz V, Walker NF, Yuen HM, Sunpath H, Tezera L, Meintjes G, Wilkinson RJ, Bishai WR, Friedland JS, Elkington PT: Procollagen iii n-

terminal propeptide and desmosine are released by matrix destruction in pulmonary tuberculosis. J Infect Dis 2013

86   Price NM, Gilman RH, Uddin J, Recavarren S, Friedland JS: Unopposed matrix metalloproteinase-9 expression in human tuberculous granuloma and the role of tnf-alpha-dependent monocyte networks. J Immunol 2003;171:5579-5586.

87   Stomrud E, Bjorkqvist M, Janciauskiene S, Minthon L, Hansson O: Alterations of matrix metalloproteinases in the healthy elderly with increased risk of prodromal alzheimer's disease. Alzheimers Res Ther 2010;2:20.

88   Rosenberg GA: Matrix metalloproteinases and their multiple roles in neurodegenerative diseases. Lancet Neurol 2009;8:205-216.

89   Miners JS, Baig S, Palmer J, Palmer LE, Kehoe PG, Love S: Abeta-degrading enzymes in alzheimer's disease. Brain Pathol 2008;18:240-252.

90   Yong VW, Power C, Forsyth P, Edwards DR: Metalloproteinases in biology and pathology of the nervous system. Nat Rev Neurosci 2001;2:502-511.

91   Harris JE, Fernandez-Vilaseca M, Elkington PT, Horncastle DE, Graeber MB, Friedland JS: IFNgamma synergizes with il-1beta to up-regulate mmp-9 secretion in a cellular model of central nervous system tuberculosis. FASEB J 2007;21:356-365.

92   Harris JE, Nuttall RK, Elkington PT, Green JA, Horncastle DE, Graeber MB, Edwards DR, Friedland JS: Monocyte-astrocyte networks regulate matrix metalloproteinase gene expression and secretion in central nervous system tuberculosis *in vitro* and *in vivo*. J Immunol 2007;178:1199-1207.

93   Vincenti MP, Brinckerhoff CE: Signal transduction and cell-type specific regulation of matrix metalloproteinase gene expression: Can MMPs be good for you? J Cell Physiol 2007;213:355-364.

94   Agrawal S, Anderson P, Durbeej M, van Rooijen N, Ivars F, Opdenakker G, Sorokin LM: Dystroglycan is selectively cleaved at the parenchymal basement membrane at sites of leukocyte extravasation in experimental autoimmune encephalomyelitis. J Exp Med 2006;203:1007-1019.

95   Li YJ, Wang ZH, Zhang B, Zhe X, Wang MJ, Shi ST, Bai J, Lin T, Guo CJ, Zhang SJ, Kong XL, Zuo X, Zhao H: Disruption of the blood-brain barrier after

generalized tonic-clonic seizures correlates with cerebrospinal fluid MMP-9 levels. J Neuroinflammation 2013;10:80.

96   Green JA, Dholakia S, Janczar K, Ong CW, Moores R, Fry J, Elkington PT, Roncaroli F, Friedland JS: *Mycobacterium tuberculosis*-infected human monocytes down-regulate microglial MMP-2 secretion in CNS tuberculosis via TNFalpha, NFkappaB, p38 and caspase 8 dependent pathways. J Neuroinflammation 2011;8:46.

97   Rozario T, DeSimone DW: The extracellular matrix in development and morphogenesis: A dynamic view. Dev Biol 2010;341:126-140.

98   Dunsmore SE, Rannels DE: Extracellular matrix biology in the lung. Am J Physiol 1996;270:L3-27.

99   Foronjy RF, Okada Y, Cole R, D'Armiento J: Progressive adult-onset emphysema in transgenic mice expressing human MMP-1 in the lung. Am J Physiol Lung Cell Mol Physiol 2003;284:L727-737.

100   Shapiro SD, Endicott SK, Province MA, Pierce JA, Campbell EJ: Marked longevity of human lung parenchymal elastic fibers deduced from prevalence of d-aspartate and nuclear weapons-related radiocarbon. J Clin Invest 1991;87:1828-1834.

101   Ruoslahti E: Fibronectin and its receptors. Annu Rev Biochem 1988;57:375-413.

102   Hattori A, Hozumi K, Ko JA, Chikama T, Oomikawa K, Kato J, Ishida K, Hoshi N, Katagiri F, Kikkawa Y, Nomizu M, Nishida T: Sequence specificity of the phsrn peptide from fibronectin on corneal epithelial migration. Biochem Biophys Res Commun 2009;379:346-350.

103   Timpl R, Rohde H, Robey PG, Rennard SI, Foidart JM, Martin GR: Laminin--a glycoprotein from basement membranes. J Biol Chem 1979;254:9933-9937.

104   Nguyen NM, Senior RM: Laminin isoforms and lung development: All isoforms are not equal. Dev Biol 2006;294:271-279.

105   Alberts B., Johnson A., Lewis J., Raff M., Roberts K., P. W: The extracellular matrix of animals; Molecular biology of the cell, 4th edition. New york, Garland Science, 2002

106   Elkington PT, Ugarte-Gil CA, Friedland JS: Matrix metalloproteinases in tuberculosis. Eur Respir J;38:456-464.

107   Ruoslahti E: Brain extracellular matrix. Glycobiology 1996;6:489-492.

108   Lau LW, Cua R, Keough MB, Haylock-Jacobs S, Yong VW: Pathophysiology of the brain extracellular matrix: A new target for remyelination. Nat Rev Neurosci 2013;14:722-729.

109   Kirmse R, Otto H, Ludwig T: Interdependency of cell adhesion, force generation and extracellular proteolysis in matrix remodeling. J Cell Sci 2011;124:1857-1866.

110   Syedain ZH, Weinberg JS, Tranquillo RT: Cyclic distension of fibrin-based tissue constructs: Evidence of adaptation during growth of engineered connective tissue. Proc Natl Acad Sci U S A 2008;105:6537-6542.

111   Langford-Smith A, Keenan TD, Clark SJ, Bishop PN, Day AJ: The role of complement in age-related macular degeneration: Heparan sulphate, a zip code for complement factor H? J Innate Immun 2014;6:407-416.

112   Clark SJ, Bishop PN, Day AJ: The proteoglycan glycomatrix: A sugar microenvironment essential for complement regulation. Front Immunol 2013;4:412.

113   Clark SJ, Keenan TD, Fielder HL, Collinson LJ, Holley RJ, Merry CL, van Kuppevelt TH, Day AJ, Bishop PN: Mapping the differential distribution of glycosaminoglycans in the adult human retina, choroid, and sclera. Invest Ophthalmol Vis Sci 2011;52:6511-6521.

114   Stamenkovic I: Extracellular matrix remodelling: The role of matrix metalloproteinases. J Pathol 2003;200:448-464.

115   Sheppard D: Functions of pulmonary epithelial integrins: From development to disease. Physiol Rev 2003;83:673-686.

116   Clark EA, Brugge JS: Integrins and signal transduction pathways: The road taken. Science 1995;268:233-239.

117   Giancotti FG: Complexity and specificity of integrin signalling. Nat Cell Biol 2000;2:E13-14.

118   Hynes RO: Integrins: Versatility, modulation, and signaling in cell adhesion. Cell 1992;69:11-25.

119   Campbell ID, Humphries MJ: Integrin structure, activation, and interactions. Cold Spring Harb Perspect Biol 2011;3

120   Xiong JP, Stehle T, Zhang R, Joachimiak A, Frech M, Goodman SL, Arnaout MA: Crystal structure of the extracellular segment of integrin alpha vbeta3 in complex with an arg-gly-asp ligand. Science 2002;296:151-155.

121   Adair BD, Xiong JP, Maddock C, Goodman SL, Arnaout MA, Yeager M: Three-dimensional em structure of the ectodomain of integrin {alpha}v{beta}3 in a complex with fibronectin. J Cell Biol 2005;168:1109-1118.

122   Askari JA, Tynan CJ, Webb SE, Martin-Fernandez ML, Ballestrem C, Humphries MJ: Focal adhesions are sites of integrin extension. J Cell Biol 2010;188:891-903.

123   Harburger DS, Calderwood DA: Integrin signalling at a glance. J Cell Sci 2009;122:159-163.

124   Cambier S, Mu DZ, O'Connell D, Boylen K, Travis W, Liu WH, Broaddus VC, Nishimura SL: A role for the integrin alphavbeta8 in the negative regulation of epithelial cell growth. Cancer Res 2000;60:7084-7093.

125   Damjanovich L, Albelda SM, Mette SA, Buck CA: Distribution of integrin cell adhesion receptors in normal and malignant lung tissue. Am J Respir Cell Mol Biol 1992;6:197-206.

126   Weinacker A, Ferrando R, Elliott M, Hogg J, Balmes J, Sheppard D: Distribution of integrins alpha v beta 6 and alpha 9 beta 1 and their known ligands, fibronectin and tenascin, in human airways. Am J Respir Cell Mol Biol 1995;12:547-556.

127   Carter WG, Ryan MC, Gahr PJ: Epiligrin, a new cell adhesion ligand for integrin alpha 3 beta 1 in epithelial basement membranes. Cell 1991;65:599-610.

128   Eble JA, Wucherpfennig KW, Gauthier L, Dersch P, Krukonis E, Isberg RR, Hemler ME: Recombinant soluble human alpha 3 beta 1 integrin: Purification, processing, regulation, and specific binding to laminin-5 and invasin in a mutually exclusive manner. Biochemistry 1998;37:10945-10955.

129   Pilewski JM, Latoche JD, Arcasoy SM, Albelda SM: Expression of integrin cell adhesion receptors during human airway epithelial repair *in vivo*. Am J Physiol 1997;273:L256-263.

130   Krissansen GW, Elliott MJ, Lucas CM, Stomski FC, Berndt MC, Cheresh DA, Lopez AF, Burns GF: Identification of a novel integrin beta subunit expressed on cultured monocytes (macrophages). Evidence that one alpha subunit can associate with multiple beta subunits. J Biol Chem 1990;265:823-830.

131   DiPersio CM, Shah S, Hynes RO: Alpha 3a beta 1 integrin localizes to focal contacts in response to diverse extracellular matrix proteins. J Cell Sci 1995;108 (Pt 6):2321-2336.

132   Lee JE, Kang CS, Guan XY, Kim BT, Kim SH, Lee YM, Moon WS, Kim DK: Discoidin domain receptor 2 is involved in the activation of bone marrow-derived dendritic cells caused by type I collagen. Biochem Biophys Res Commun 2007;352:244-250.

133   Poudel B, Yoon DS, Lee JH, Lee YM, Kim DK: Collagen i enhances functional activities of human monocyte-derived dendritic cells via discoidin domain receptor 2. Cell Immunol 2012;278:95-102.

134   Midwood K, Sacre S, Piccinini AM, Inglis J, Trebaul A, Chan E, Drexler S, Sofat N, Kashiwagi M, Orend G, Brennan F, Foxwell B: Tenascin-C is an endogenous activator of toll-like receptor 4 that is essential for maintaining inflammation in arthritic joint disease. Nat Med 2009;15:774-780.

135   Schaefer L: Extracellular matrix molecules: Endogenous danger signals as new drug targets in kidney diseases. Curr Opin Pharmacol 2010;10:185-190.

136   Weathington NM, van Houwelingen AH, Noerager BD, Jackson PL, Kraneveld AD, Galin FS, Folkerts G, Nijkamp FP, Blalock JE: A novel peptide cxcr ligand derived from extracellular matrix degradation during airway inflammation. Nat Med 2006;12:317-323.

137   Gaggar A, Jackson PL, Noerager BD, O'Reilly PJ, McQuaid DB, Rowe SM, Clancy JP, Blalock JE: A novel proteolytic cascade generates an extracellular matrix-derived chemoattractant in chronic neutrophilic inflammation. J Immunol 2008;180:5662-5669.

138   Malik M, Bakshi CS, McCabe K, Catlett SV, Shah A, Singh R, Jackson PL, Gaggar A, Metzger DW, Melendez JA, Blalock JE, Sellati TJ: Matrix metalloproteinase 9 activity enhances host susceptibility to pulmonary infection with type a and b strains of *Francisella tularensis*. J Immunol 2007;178:1013-1020.

139   Baranek T, Debret R, Antonicelli F, Lamkhioued B, Belaaouaj A, Hornebeck W, Bernard P, Guenounou M, Le Naour R: Elastin receptor (spliced galactosidase) occupancy by elastin peptides counteracts proinflammatory cytokine expression in lipopolysaccharide-stimulated human monocytes through NF-kappaB down-regulation. J Immunol 2007;179:6184-6192.

140   Moreth K, Frey H, Hubo M, Zeng-Brouwers J, Nastase MV, Hsieh LT, Haceni R, Pfeilschifter J, Iozzo RV, Schaefer L: Biglycan-triggered TLR-2- and TLR-4-signaling exacerbates the pathophysiology of ischemic acute kidney injury. Matrix Biol 2014;35:143-151.

141   Hudson MC, Ramp WK, Frankenburg KP: *Staphylococcus aureus* adhesion to bone matrix and bone-associated biomaterials. FEMS Microbiol Lett 1999;173:279-284.

142   Arciola CR, Campoccia D, Gamberini S, Donati ME, Montanaro L: Presence of fibrinogen-binding adhesin gene in *Staphylococcus epidermidis* isolates from central venous catheters-associated and orthopaedic implant-associated infections. Biomaterials 2004;25:4825-4829.

143   Harris LG, Richards RG: *Staphylococci* and implant surfaces: A review. Injury 2006;37 Suppl 2:S3-14.

144   Kreikemeyer B, Klenk M, Podbielski A: The intracellular status of *Streptococcus pyogenes*: Role of extracellular matrix-binding proteins and their regulation. Int J Med Microbiol 2004;294:177-188.

145   Farfan MJ, Cantero L, Vidal R, Botkin DJ, Torres AG: Long polar fimbriae of enterohemorrhagic *Escherichia coli* O157:H7 bind to extracellular matrix proteins. Infect Immun 2011;79:3744-3750.

146   Ottonello L, Dapino P, Amelotti M, Barbera P, Arduino N, Bertolotto M, Dallegri F: Activation of neutrophil respiratory burst by cytokines and

chemoattractants. Regulatory role of extracellular matrix glycoproteins. Inflamm Res 1998;47:345-350.

147   Davies LC, Jenkins SJ, Allen JE, Taylor PR: Tissue-resident macrophages. Nat Immunol 2013;14:986-995.

148   Sokolowska M, Chen LY, Eberlein M, Martinez-Anton A, Liu Y, Alsaaty S, Qi HY, Logun C, Horton M, Shelhamer JH: Low molecular weight hyaluronan activates cytosolic phospholipase a2alpha and eicosanoid production in monocytes and macrophages. J Biol Chem 2014;289:4470-4488.

149   Mantovani A, Biswas SK, Galdiero MR, Sica A, Locati M: Macrophage plasticity and polarization in tissue repair and remodelling. J Pathol 2013;229:176-185.

150   Hinz B, Phan SH, Thannickal VJ, Prunotto M, Desmouliere A, Varga J, De Wever O, Mareel M, Gabbiani G: Recent developments in myofibroblast biology: Paradigms for connective tissue remodeling. Am J Pathol 2012;180:1340-1355.

151   Wilson MS, Wynn TA: Pulmonary fibrosis: Pathogenesis, etiology and regulation. Mucosal Immunol 2009;2:103-121.

152   Karsdal MA, Nielsen MJ, Sand JM, Henriksen K, Genovese F, Bay-Jensen AC, Smith V, Adamkewicz JI, Christiansen C, Leeming DJ: Extracellular matrix remodeling: The common denominator in connective tissue diseases. Possibilities for evaluation and current understanding of the matrix as more than a passive architecture, but a key player in tissue failure. Assay and drug development technologies 2013;11:70-92.

153   Parker MW, Rossi D, Peterson M, Smith K, Sikstrom K, White ES, Connett JE, Henke CA, Larsson O, Bitterman PB: Fibrotic extracellular matrix activates a profibrotic positive feedback loop. J Clin Invest 2014;124:1622-1635.

154   Kropski JA, Lawson WE, Young LR, Blackwell TS: Genetic studies provide clues on the pathogenesis of idiopathic pulmonary fibrosis. Dis Model Mech 2013;6:9-17.

155   Stahl M, Schupp J, Jager B, Schmid M, Zissel G, Muller-Quernheim J, Prasse A: Lung collagens perpetuate pulmonary fibrosis via CD204 and M2 macrophage activation. PLoS One 2013;8:e81382.

156   Li R, Maminishkis A, Zahn G, Vossmeyer D, Miller SS: Integrin alpha5beta1 mediates attachment, migration, and proliferation in human retinal pigment epithelium: Relevance for proliferative retinal disease. Invest Ophthalmol Vis Sci 2009;50:5988-5996.

157   Sharma M, Tiwari A, Sharma S, Bhoria P, Gupta V, Gupta A, Luthra-Guptasarma M: Fibrotic remodeling of the extracellular matrix through a novel (engineered, dual-function) antibody reactive to a cryptic epitope on the n-terminal 30 kda fragment of fibronectin. PLoS One 2013;8:e69343.

158   Kenne E, Soehnlein O, Genove G, Rotzius P, Eriksson EE, Lindbom L: Immune cell recruitment to inflammatory loci is impaired in mice deficient in basement membrane protein laminin alpha4. J Leukoc Biol 2010;88:523-528.

159   Wu C, Ivars F, Anderson P, Hallmann R, Vestweber D, Nilsson P, Robenek H, Tryggvason K, Song J, Korpos E, Loser K, Beissert S, Georges-Labouesse E, Sorokin LM: Endothelial basement membrane laminin alpha5 selectively inhibits T lymphocyte extravasation into the brain. Nat Med 2009;15:519-527.

160   Lammermann T, Bader BL, Monkley SJ, Worbs T, Wedlich-Soldner R, Hirsch K, Keller M, Forster R, Critchley DR, Fassler R, Sixt M: Rapid leukocyte migration by integrin-independent flowing and squeezing. Nature 2008;453:51-55.

161   Jacobelli J, Friedman RS, Conti MA, Lennon-Dumenil AM, Piel M, Sorensen CM, Adelstein RS, Krummel MF: Confinement-optimized three-dimensional t cell amoeboid motility is modulated via myosin IIa-regulated adhesions. Nat Immunol 2010;11:953-961.

162   Overstreet MG, Gaylo A, Angermann BR, Hughson A, Hyun YM, Lambert K, Acharya M, Billroth-Maclurg AC, Rosenberg AF, Topham DJ, Yagita H, Kim M, Lacy-Hulbert A, Meier-Schellersheim M, Fowell DJ: Inflammation-induced interstitial migration of effector CD4(+) T cells is dependent on integrin alphaV. Nat Immunol 2013;14:949-958.

163   Salmon H, Franciszkiewicz K, Damotte D, Dieu-Nosjean MC, Validire P, Trautmann A, Mami-Chouaib F, Donnadieu E: Matrix architecture defines the preferential localization and migration of T cells into the stroma of human lung tumors. J Clin Invest 2012;122:899-910.

164   Bollyky PL, Wu RP, Falk BA, Lord JD, Long SA, Preisinger A, Teng B, Holt GE, Standifer NE, Braun KR, Xie CF, Samuels PL, Vernon RB, Gebe JA, Wight TN, Nepom GT: Ecm components guide IL-10 producing regulatory T-cell (TR1) induction from effector memory T-cell precursors. Proc Natl Acad Sci U S A 2011;108:7938-7943.

165   Wilson CL, Hine DW, Pradipta A, Pearson JP, van Eden W, Robinson JH, Knight AM: Presentation of the candidate rheumatoid arthritis autoantigen aggrecan by antigen-specific B cells induces enhanced CD4(+) T helper type 1 subset differentiation. Immunology 2012;135:344-354.

166   Ciechomska M, Wilson CL, Floudas A, Hui W, Rowan AD, van Eden W, Robinson JH, Knight AM: Antigen-specific B lymphocytes acquire proteoglycan aggrecan from cartilage extracellular matrix resulting in antigen presentation and CD4+ T-cell activation. Immunology 2014;141:70-78.

167   Debret R, Antonicelli F, Theill A, Hornebeck W, Bernard P, Guenounou M, Le Naour R: Elastin-derived peptides induce a T-helper type 1 polarization of human blood lymphocytes. Arterioscler Thromb Vasc Biol 2005;25:1353-1358.

168   Lee SH, Goswami S, Grudo A, Song LZ, Bandi V, Goodnight-White S, Green L, Hacken-Bitar J, Huh J, Bakaeen F, Coxson HO, Cogswell S, Storness-Bliss C, Corry DB, Kheradmand F: Antielastin autoimmunity in tobacco smoking-induced emphysema. Nat Med 2007;13:567-569.

169   Alamein MA, Stephens S, Liu Q, Skabo S, Warnke PH: Mass production of nanofibrous extracellular matrix with controlled 3D morphology for large-scale soft tissue regeneration. Tissue engineering Part C, Methods 2013;19:458-472.

170   Kim DH, Lipke EA, Kim P, Cheong R, Thompson S, Delannoy M, Suh KY, Tung L, Levchenko A: Nanoscale cues regulate the structure and function of macroscopic cardiac tissue constructs. Proc Natl Acad Sci U S A 2010;107:565-570.

171   Kim J, Kim HN, Lim KT, Kim Y, Seonwoo H, Park SH, Lim HJ, Kim DH, Suh KY, Choung PH, Choung YH, Chung JH: Designing nanotopographical density of extracellular matrix for controlled morphology and function of human mesenchymal stem cells. Sci Rep 2013;3:3552.

172	Abbott NJ, Ronnback L, Hansson E: Astrocyte-endothelial interactions at the blood-brain barrier. Nat Rev Neurosci 2006;7:41-53.

173	Yaffe Y, Shepshelovitch J, Nevo-Yassaf I, Yeheskel A, Shmerling H, Kwiatek JM, Gaus K, Pasmanik-Chor M, Hirschberg K: The marvel transmembrane motif of occludin mediates oligomerization and targeting to the basolateral surface in epithelia. J Cell Sci 2012;125:3545-3556.

174	Walter JK, Castro V, Voss M, Gast K, Rueckert C, Piontek J, Blasig IE: Redox-sensitivity of the dimerization of occludin. Cell Mol Life Sci 2009;66:3655-3662.

175	Lochhead JJ, McCaffrey G, Quigley CE, Finch J, DeMarco KM, Nametz N, Davis TP: Oxidative stress increases blood-brain barrier permeability and induces alterations in occludin during hypoxia-reoxygenation. J Cereb Blood Flow Metab 2010;30:1625-1636.

176	Lochhead JJ, McCaffrey G, Sanchez-Covarrubias L, Finch JD, Demarco KM, Quigley CE, Davis TP, Ronaldson PT: Tempol modulates changes in xenobiotic permeability and occludin oligomeric assemblies at the blood-brain barrier during inflammatory pain. Am J Physiol Heart Circ Physiol 2012;302:H582-593.

177	McCaffrey G, Seelbach MJ, Staatz WD, Nametz N, Quigley C, Campos CR, Brooks TA, Davis TP: Occludin oligomeric assembly at tight junctions of the blood-brain barrier is disrupted by peripheral inflammatory hyperalgesia. J Neurochem 2008;106:2395-2409.

178	Medina R, Rahner C, Mitic LL, Anderson JM, Van Itallie CM: Occludin localization at the tight junction requires the second extracellular loop. J Membr Biol 2000;178:235-247.

179	Schubert-Unkmeir A, Konrad C, Slanina H, Czapek F, Hebling S, Frosch M: *Neisseria meningitidis* induces brain microvascular endothelial cell detachment from the matrix and cleavage of occludin: A role for MMP-8. PLoS Pathog 2010;6:e1000874.

180	Xu R, Feng X, Xie X, Zhang J, Wu D, Xu L: Hiv-1 tat protein increases the permeability of brain endothelial cells by both inhibiting occludin expression and cleaving occludin via matrix metalloproteinase-9. Brain Res 2012;1436:13-19.

181   Moroi S, Saitou M, Fujimoto K, Sakakibara A, Furuse M, Yoshida O, Tsukita S: Occludin is concentrated at tight junctions of mouse/rat but not human/guinea pig sertoli cells in testes. Am J Physiol 1998;274:C1708-1717.

182   Saitou M, Furuse M, Sasaki H, Schulzke JD, Fromm M, Takano H, Noda T, Tsukita S: Complex phenotype of mice lacking occludin, a component of tight junction strands. Mol Biol Cell 2000;11:4131-4142.

183   Schulzke JD, Gitter AH, Mankertz J, Spiegel S, Seidler U, Amasheh S, Saitou M, Tsukita S, Fromm M: Epithelial transport and barrier function in occludin-deficient mice. Biochim Biophys Acta 2005;1669:34-42.

184   Wolburg H, Wolburg-Buchholz K, Kraus J, Rascher-Eggstein G, Liebner S, Hamm S, Duffner F, Grote EH, Risau W, Engelhardt B: Localization of claudin-3 in tight junctions of the blood-brain barrier is selectively lost during experimental autoimmune encephalomyelitis and human glioblastoma multiforme. Acta Neuropathol 2003;105:586-592.

185   Morita K, Sasaki H, Furuse M, Tsukita S: Endothelial claudin: Claudin-5/tmvcf constitutes tight junction strands in endothelial cells. J Cell Biol 1999;147:185-194.

186   Ohtsuki S, Sato S, Yamaguchi H, Kamoi M, Asashima T, Terasaki T: Exogenous expression of claudin-5 induces barrier properties in cultured rat brain capillary endothelial cells. J Cell Physiol 2007;210:81-86.

187   Piehl C, Piontek J, Cording J, Wolburg H, Blasig IE: Participation of the second extracellular loop of claudin-5 in paracellular tightening against ions, small and large molecules. Cell Mol Life Sci 2010;67:2131-2140.

188   Piontek J, Winkler L, Wolburg H, Muller SL, Zuleger N, Piehl C, Wiesner B, Krause G, Blasig IE: Formation of tight junction: Determinants of homophilic interaction between classic claudins. FASEB J 2008;22:146-158.

189   Zhang J, Piontek J, Wolburg H, Piehl C, Liss M, Otten C, Christ A, Willnow TE, Blasig IE, Abdelilah-Seyfried S: Establishment of a neuroepithelial barrier by claudin5a is essential for zebrafish brain ventricular lumen expansion. Proc Natl Acad Sci U S A 2010;107:1425-1430.

190   Nitta T, Hata M, Gotoh S, Seo Y, Sasaki H, Hashimoto N, Furuse M, Tsukita S: Size-selective loosening of the blood-brain barrier in claudin-5-deficient mice. J Cell Biol 2003;161:653-660.

191   Liu Y, Nusrat A, Schnell FJ, Reaves TA, Walsh S, Pochet M, Parkos CA: Human junction adhesion molecule regulates tight junction resealing in epithelia. J Cell Sci 2000;113 (Pt 13):2363-2374.

192   Naik UP, Naik MU, Eckfeld K, Martin-DeLeon P, Spychala J: Characterization and chromosomal localization of JAM-1, a platelet receptor for a stimulatory monoclonal antibody. J Cell Sci 2001;114:539-547.

193   Ebnet K, Suzuki A, Ohno S, Vestweber D: Junctional adhesion molecules (JAMs): More molecules with dual functions? J Cell Sci 2004;117:19-29.

194   Gumbiner B, Lowenkopf T, Apatira D: Identification of a 160-kda polypeptide that binds to the tight junction protein ZO-1. Proc Natl Acad Sci U S A 1991;88:3460-3464.

195   Haskins J, Gu L, Wittchen ES, Hibbard J, Stevenson BR: Zo-3, a novel member of the maguk protein family found at the tight junction, interacts with ZO-1 and occludin. J Cell Biol 1998;141:199-208.

196   Bazzoni G, Martinez-Estrada OM, Orsenigo F, Cordenonsi M, Citi S, Dejana E: Interaction of junctional adhesion molecule with the tight junction components ZO-1, cingulin, and occludin. J Biol Chem 2000;275:20520-20526.

197   Furuse M, Itoh M, Hirase T, Nagafuchi A, Yonemura S, Tsukita S, Tsukita S: Direct association of occludin with ZO-1 and its possible involvement in the localization of occludin at tight junctions. J Cell Biol 1994;127:1617-1626.

198   Umeda K, Ikenouchi J, Katahira-Tayama S, Furuse K, Sasaki H, Nakayama M, Matsui T, Tsukita S, Furuse M, Tsukita S: ZO-1 and ZO-2 independently determine where claudins are polymerized in tight-junction strand formation. Cell 2006;126:741-754.

199   Saitou M, Fujimoto K, Doi Y, Itoh M, Fujimoto T, Furuse M, Takano H, Noda T, Tsukita S: Occludin-deficient embryonic stem cells can differentiate into polarized epithelial cells bearing tight junctions. J Cell Biol 1998;141:397-408.

200   Nusrat A, Brown GT, Tom J, Drake A, Bui TT, Quan C, Mrsny RJ: Multiple protein interactions involving proposed extracellular loop domains of the tight junction protein occludin. Mol Biol Cell 2005;16:1725-1734.

201   Fanning AS, Ma TY, Anderson JM: Isolation and functional characterization of the actin binding region in the tight junction protein ZO-1. FASEB J 2002;16:1835-1837.

202   Luissint AC, Artus C, Glacial F, Ganeshamoorthy K, Couraud PO: Tight junctions at the blood brain barrier: Physiological architecture and disease-associated dysregulation. Fluids and barriers of the CNS 2012;9:23.

203   Fuccillo M, Joyner AL, Fishell G: Morphogen to mitogen: The multiple roles of hedgehog signalling in vertebrate neural development. Nat Rev Neurosci 2006;7:772-783.

204   Nagase T, Nagase M, Machida M, Fujita T: Hedgehog signalling in vascular development. Angiogenesis 2008;11:71-77.

205   Hochman E, Castiel A, Jacob-Hirsch J, Amariglio N, Izraeli S: Molecular pathways regulating pro-migratory effects of hedgehog signaling. J Biol Chem 2006;281:33860-33870.

206   Alvarez JI, Dodelet-Devillers A, Kebir H, Ifergan I, Fabre PJ, Terouz S, Sabbagh M, Wosik K, Bourbonniere L, Bernard M, van Horssen J, de Vries HE, Charron F, Prat A: The hedgehog pathway promotes blood-brain barrier integrity and CNS immune quiescence. Science 2011;334:1727-1731.

207   Briscoe J, Ericson J: Specification of neuronal fates in the ventral neural tube. Curr Opin Neurobiol 2001;11:43-49.

208   Minagar A, Alexander JS: Blood-brain barrier disruption in multiple sclerosis. Mult Scler 2003;9:540-549.

209   Andersen IH, Marker O, Thomsen AR: Breakdown of blood-brain barrier function in the murine lymphocytic choriomeningitis virus infection mediated by virus-specific CD8+ T cells. J Neuroimmunol 1991;31:155-163.

210   Chai Q, He WQ, Zhou M, Lu H, Fu ZF: Enhancement of blood-brain barrier permeability and reduction of tight junction protein expression are modulated by chemokines/cytokines induced by rabies virus infection. J Virol 2014;88:4698-4710.

211   Wang T, Town T, Alexopoulou L, Anderson JF, Fikrig E, Flavell RA: Toll-like receptor 3 mediates west nile virus entry into the brain causing lethal encephalitis. Nat Med 2004;10:1366-1373.

212   Banks WA, Ercal N, Price TO: The blood-brain barrier in neuroaids. Current HIV research 2006;4:259-266.

213   Pfister HW, Feiden W, Einhaupl KM: Spectrum of complications during bacterial meningitis in adults. Results of a prospective clinical study. Arch Neurol 1993;50:575-581.

214   Chodobski A, Zink BJ, Szmydynger-Chodobska J: Blood-brain barrier pathophysiology in traumatic brain injury. Translational stroke research 2011;2:492-516.

215   Koedel U, Scheld WM, Pfister HW: Pathogenesis and pathophysiology of pneumococcal meningitis. Lancet Infect Dis 2002;2:721-736.

216   Nau R, Bruck W: Neuronal injury in bacterial meningitis: Mechanisms and implications for therapy. Trends Neurosci 2002;25:38-45.

217   Quagliarello V, Scheld WM: Bacterial meningitis: Pathogenesis, pathophysiology, and progress. N Engl J Med 1992;327:864-872.

218   Rosenberg GA, Cunningham LA, Wallace J, Alexander S, Estrada EY, Grossetete M, Razhagi A, Miller K, Gearing A: Immunohistochemistry of matrix metalloproteinases in reperfusion injury to rat brain: Activation of MMP-9 linked to stromelysin-1 and microglia in cell cultures. Brain Res 2001;893:104-112.

219   Faurschou M, Borregaard N: Neutrophil granules and secretory vesicles in inflammation. Microbes and infection / Institut Pasteur 2003;5:1317-1327.

220   Newby AC: Metalloproteinase expression in monocytes and macrophages and its relationship to atherosclerotic plaque instability. Arterioscler Thromb Vasc Biol 2008;28:2108-2114.

221   Kolb SA, Lahrtz F, Paul R, Leppert D, Nadal D, Pfister HW, Fontana A: Matrix metalloproteinases and tissue inhibitors of metalloproteinases in viral meningitis: Upregulation of MMP-9 and TIMP-1 in cerebrospinal fluid. J Neuroimmunol 1998;84:143-150.

222   Jain SK, Paul-Satyaseela M, Lamichhane G, Kim KS, Bishai WR: *Mycobacterium tuberculosis* invasion and traversal across an in vitro human blood-brain barrier as a pathogenic mechanism for central nervous system tuberculosis. J Infect Dis 2006;193:1287-1295.

223   Elkington PT, Green JA, Friedland JS: Filter sterilization of highly infectious samples to prevent false negative analysis of matrix metalloproteinase activity. J Immunol Methods 2006;309:115-119.

224   Crosby LM, Waters CM: Epithelial repair mechanisms in the lung. Am J Physiol Lung Cell Mol Physiol 2010;298:L715-731.

225   Hynes RO: Integrins: Bidirectional, allosteric signaling machines. Cell 2002;110:673-687.

226   Matlin KSH, B.; Zuk, A.: Integrins in epithelial cell polarity: Using antibodies to analyze adhesive function and morphogenesis. Methods 2003 30:11.

227   Kreidberg JA: Functions of alpha3beta1 integrin. Curr Opin Cell Biol 2000;12:548-553.

228   Zhang ZG, Bothe I, Hirche F, Zweers M, Gullberg D, Pfitzer G, Krieg T, Eckes B, Aumailley M: Interactions of primary fibroblasts and keratinocytes with extracellular matrix proteins: Contribution of alpha2beta1 integrin. J Cell Sci 2006;119:1886-1895.

229   Takada Y, Murphy E, Pil P, Chen C, Ginsberg MH, Hemler ME: Molecular cloning and expression of the cDNA for alpha 3 subunit of human alpha 3 beta 1 (vla-3), an integrin receptor for fibronectin, laminin, and collagen. J Cell Biol 1991;115:257-266.

230   Wolfenson H, Lavelin I, Geiger B: Dynamic regulation of the structure and functions of integrin adhesions. Dev Cell 2013;24:447-458.

231   Mitra SK, Hanson DA, Schlaepfer DD: Focal adhesion kinase: In command and control of cell motility. Nat Rev Mol Cell Biol 2005;6:56-68.

232   Kinoshita K, Aono Y, Azuma M, Kishi J, Takezaki A, Kishi M, Makino H, Okazaki H, Uehara H, Izumi K, Sone S, Nishioka Y: Antifibrotic effects of focal adhesion kinase inhibitor in bleomycin-induced pulmonary fibrosis in mice. Am J Respir Cell Mol Biol 2013;49:536-543.

233   Bruce Alberts AJ, Julian Lewis, Martin Raff, Keith Roberts, Peter Walter Molecular biology of the cell, fourth edition. . New York, New York: Garland Science, 2002.

234   Bao W, Stromblad S: Use of an immobilized monoclonal antibody to examine integrin alpha5beta1 signaling independent of cell spreading. Biol Proced Online 2002;4:81-87.

235   Leavesley DI, Schwartz MA, Rosenfeld M, Cheresh DA: Integrin beta 1- and beta 3-mediated endothelial cell migration is triggered through distinct signaling mechanisms. J Cell Biol 1993;121:163-170.

236   Wary KK, Dans M, Mariotti A, Giancotti FG: Biochemical analysis of integrin-mediated SHC signaling. Methods Mol Biol 1999;129:35-49.

237   Chakraborti S, Mandal M, Das S, Mandal A, Chakraborti T: Regulation of matrix metalloproteinases: An overview. Mol Cell Biochem 2003;253:269-285.

238   Muromachi K, Kamio N, Narita T, Annen-Kamio M, Sugiya H, Matsushima K: MMP-3 provokes CTGF/CCN2 production independently of protease activity and dependently on dynamin-related endocytosis, which contributes to human dental pulp cell migration. J Cell Biochem 2012;113:1348-1358.

239   Taylor JL, Hattle JM, Dreitz SA, Troudt JM, Izzo LS, Basaraba RJ, Orme IM, Matrisian LM, Izzo AA: Role for matrix metalloproteinase 9 in granuloma formation during pulmonary *Mycobacterium tuberculosis* infection. Infect Immun 2006;74:6135-6144.

240   Volkman HE, Pozos TC, Zheng J, Davis JM, Rawls JF, Ramakrishnan L: Tuberculous granuloma induction via interaction of a bacterial secreted protein with host epithelium. Science 2010;327:466-469.

241   Iyer V, Pumiglia K, DiPersio CM: Alpha3beta1 integrin regulates MMP-9 mRNA stability in immortalized keratinocytes: A novel mechanism of integrin-mediated mmp gene expression. J Cell Sci 2005;118:1185-1195.

242   Meng XN, Jin Y, Yu Y, Bai J, Liu GY, Zhu J, Zhao YZ, Wang Z, Chen F, Lee KY, Fu SB: Characterisation of fibronectin-mediated fak signalling pathways in lung cancer cell migration and invasion. Br J Cancer 2009;101:327-334.

243   Rohani MG, Pilcher BK, Chen P, Parks WC: Cdc42 inhibits erk-mediated collagenase-1 (MMP-1) expression in collagen-activated human keratinocytes. J Invest Dermatol 2013

244   Deroanne CF, Hamelryckx D, Ho TT, Lambert CA, Catroux P, Lapiere CM, Nusgens BV: Cdc42 downregulates MMP-1 expression by inhibiting the erk1/2 pathway. J Cell Sci 2005;118:1173-1183.

245   Singh S, Saraiva L, Elkington PT, Friedland JS: Regulation of matrix metalloproteinase-1, -3, and -9 in *Mycobacterium tuberculosis*-dependent respiratory networks by the rapamycin-sensitive PI3K/p70S6K cascade. FASEB J 2013

246   Murphy G, Nagase H: Localizing matrix metalloproteinase activities in the pericellular environment. The FEBS journal 2011;278:2-15.

247   Parks WC: What is the alpha2beta1 integrin doing in the epidermis? J Invest Dermatol 2007;127:264-266.

248   Sondag CM, Combs CK: Adhesion of monocytes to type i collagen stimulates an APP-dependent proinflammatory signaling response and release of abeta1-40. J Neuroinflammation 2010;7:22.

249   Ammon C, Meyer SP, Schwarzfischer L, Krause SW, Andreesen R, Kreutz M: Comparative analysis of integrin expression on monocyte-derived macrophages and monocyte-derived dendritic cells. Immunology 2000;100:364-369.

250   Shi C, Zhang X, Chen Z, Sulaiman K, Feinberg MW, Ballantyne CM, Jain MK, Simon DI: Integrin engagement regulates monocyte differentiation through the forkhead transcription factor FOXP1. J Clin Invest 2004;114:408-418.

251   Bargatze RF, Jutila MA, Butcher EC: Distinct roles of L-selectin and integrins alpha 4 beta 7 and LFA-1 in lymphocyte homing to peyer's patch-hev in situ: The multistep model confirmed and refined. Immunity 1995;3:99-108.

252   Fan ST, Edgington TS: Coupling of the adhesive receptor CD11b/CD18 to functional enhancement of effector macrophage tissue factor response. J Clin Invest 1991;87:50-57.

253   Rezzonico R, Chicheportiche R, Imbert V, Dayer JM: Engagement of CD11b and CD11c beta2 integrin by antibodies or soluble CD23 induces IL-1beta production

on primary human monocytes through mitogen-activated protein kinase-dependent pathways. Blood 2000;95:3868-3877.

254   Sitrin RG, Pan PM, Srikanth S, Todd RF, 3rd: Fibrinogen activates NF-kappa B transcription factors in mononuclear phagocytes. J Immunol 1998;161:1462-1470.

255   Shi C, Zhang X, Chen Z, Robinson MK, Simon DI: Leukocyte integrin MAC-1 recruits toll/interleukin-1 receptor superfamily signaling intermediates to modulate NF-kappaB activity. Circ Res 2001;89:859-865.

256   Bianchi E, Denti S, Granata A, Bossi G, Geginat J, Villa A, Rogge L, Pardi R: Integrin LFA-1 interacts with the transcriptional co-activator JAB1 to modulate AP-1 activity. Nature 2000;404:617-621.

257   Weerasinghe D, McHugh KP, Ross FP, Brown EJ, Gisler RH, Imhof BA: A role for the alphavbeta3 integrin in the transmigration of monocytes. J Cell Biol 1998;142:595-607.

258   Rolli M, Fransvea E, Pilch J, Saven A, Felding-Habermann B: Activated integrin alphavbeta3 cooperates with metalloproteinase MMP-9 in regulating migration of metastatic breast cancer cells. Proc Natl Acad Sci U S A 2003;100:9482-9487.

259   Hofmann UB, Westphal JR, Van Kraats AA, Ruiter DJ, Van Muijen GN: Expression of integrin alpha(v)beta(3) correlates with activation of membrane-type matrix metalloproteinase-1 (MT1-MMP) and matrix metalloproteinase-2 (mmp-2) in human melanoma cells in vitro and in vivo. Int J Cancer 2000;87:12-19.

260   Karadag A, Ogbureke KU, Fedarko NS, Fisher LW: Bone sialoprotein, matrix metalloproteinase 2, and alpha(v)beta3 integrin in osteotropic cancer cell invasion. J Natl Cancer Inst 2004;96:956-965.

261   Zhao Y, Bachelier R, Treilleux I, Pujuguet P, Peyruchaud O, Baron R, Clement-Lacroix P, Clezardin P: Tumor alphavbeta3 integrin is a therapeutic target for breast cancer bone metastases. Cancer Res 2007;67:5821-5830.

262   Stromblad S, Becker JC, Yebra M, Brooks PC, Cheresh DA: Suppression of p53 activity and p21WAF1/CIP1 expression by vascular cell integrin alphavbeta3 during angiogenesis. J Clin Invest 1996;98:426-433.

263   Batra J, Robinson J, Soares AS, Fields AP, Radisky DC, Radisky ES: Matrix metalloproteinase-10 (MMP-10) interaction with tissue inhibitors of metalloproteinases TIMP-1 and TIMP-2: Binding studies and crystal structure. J Biol Chem 2012;287:15935-15946.

264   Al Shammari B, Shiomi T, Tezera L, Bielecka MK, Workman V, Sathyamoorthy T, Mauri F, Jayasinghe SN, Robertson BD, D'Armiento J, Friedland JS, Elkington PT: The extracellular matrix regulates granuloma necrosis in tuberculosis. J Infect Dis 2015

265   de Fougerolles AR, Chi-Rosso G, Bajardi A, Gotwals P, Green CD, Koteliansky VE: Global expression analysis of extracellular matrix-integrin interactions in monocytes. Immunity 2000;13:749-758.

266   Hermann P, Armant M, Brown E, Rubio M, Ishihara H, Ulrich D, Caspary RG, Lindberg FP, Armitage R, Maliszewski C, Delespesse G, Sarfati M: The vitronectin receptor and its associated CD47 molecule mediates proinflammatory cytokine synthesis in human monocytes by interaction with soluble CD23. J Cell Biol 1999;144:767-775.

267   Clay H, Davis JM, Beery D, Huttenlocher A, Lyons SE, Ramakrishnan L: Dichotomous role of the macrophage in early *Mycobacterium marinum* infection of the zebrafish. Cell host & microbe 2007;2:29-39.

268   Mayer-Barber KD, Andrade BB, Oland SD, Amaral EP, Barber DL, Gonzales J, Derrick SC, Shi R, Kumar NP, Wei W, Yuan X, Zhang G, Cai Y, Babu S, Catalfamo M, Salazar AM, Via LE, Barry CE, 3rd, Sher A: Host-directed therapy of tuberculosis based on interleukin-1 and type I interferon crosstalk. Nature 2014;511:99-103.

269   Wang Y, Jin S, Sonobe Y, Cheng Y, Horiuchi H, Parajuli B, Kawanokuchi J, Mizuno T, Takeuchi H, Suzumura A: Interleukin-1beta induces blood-brain barrier disruption by downregulating sonic hedgehog in astrocytes. PLoS One 2014;9:e110024.

270   Pulzova L, Bhide MR, Andrej K: Pathogen translocation across the blood-brain barrier. FEMS Immunol Med Microbiol 2009;57:203-213.

271   Nguyen L, Pieters J: The trojan horse: Survival tactics of pathogenic mycobacteria in macrophages. Trends Cell Biol 2005;15:269-276.

272   Be NA, Bishai WR, Jain SK: Role of *Mycobacterium tuberculosis* pknd in the pathogenesis of central nervous system tuberculosis. BMC Microbiol 2012;12:7.

273   Tukachinsky H, Kuzmickas RP, Jao CY, Liu J, Salic A: Dispatched and scube mediate the efficient secretion of the cholesterol-modified hedgehog ligand. Cell reports 2012;2:308-320.

274   Zheng M, Wei J, Tang Y, Yang C, Wei Y, Yin X, Liu Q: Apoe-deficient promotes blood-brain barrier disruption in experimental autoimmune encephalomyelitis via alteration of MMP-9. J Mol Neurosci 2014;54:282-290.

275   Kamat PK, Swarnkar S, Rai S, Kumar V, Tyagi N: Astrocyte mediated mmp-9 activation in the synapse dysfunction: An implication in alzheimer disease. Therapeutic targets for neurological diseases 2014;1

276   Ricci S, Grandgirard D, Wenzel M, Braccini T, Salvatore P, Oggioni MR, Leib SL, Koedel U: Inhibition of matrix metalloproteinases attenuates brain damage in experimental meningococcal meningitis. BMC Infect Dis 2014;14:3853.

277   van der Flier M, Hoppenreijs S, van Rensburg AJ, Ruyken M, Kolk AH, Springer P, Hoepelman AI, Geelen SP, Kimpen JL, Schoeman JF: Vascular endothelial growth factor and blood-brain barrier disruption in tuberculous meningitis. Pediatr Infect Dis J 2004;23:608-613.

278   Zimmermann DR, Dours-Zimmermann MT: Extracellular matrix of the central nervous system: From neglect to challenge. Histochem Cell Biol 2008;130:635-653.

279   Papatriantafyllou M: Neuroimmunology: A CNS guard as prickly as a hedgehog. Nat Rev Immunol 2012;12:4.

280   Jakobs P, Exner S, Schurmann S, Pickhinke U, Bandari S, Ortmann C, Kupich S, Schulz P, Hansen U, Seidler DG, Grobe K: Scube2 enhances proteolytic shh processing from the surface of shh-producing cells. J Cell Sci 2014;127:1726-1737.

281   Wu BT, Su YH, Tsai MT, Wasserman SM, Topper JN, Yang RB: A novel secreted, cell-surface glycoprotein containing multiple epidermal growth factor-like repeats and one CUB domain is highly expressed in primary osteoblasts and bones. J Biol Chem 2004;279:37485-37490.

282   Wu YY, Peck K, Chang YL, Pan SH, Cheng YF, Lin JC, Yang RB, Hong TM, Yang PC: Scube3 is an endogenous TGF-beta receptor ligand and regulates the epithelial-mesenchymal transition in lung cancer. Oncogene 2011;30:3682-3693.

283   Cheng CJ, Lin YC, Tsai MT, Chen CS, Hsieh MC, Chen CL, Yang RB: Scube2 suppresses breast tumor cell proliferation and confers a favorable prognosis in invasive breast cancer. Cancer Res 2009;69:3634-3641.

284   Cooper AM: Cell-mediated immune responses in tuberculosis, ed 2009/03/24. 2009.

285   O'Garra A, Redford PS, McNab FW, Bloom CI, Wilkinson RJ, Berry MP: The immune response in tuberculosis. Annu Rev Immunol 2013;31:475-527.

286   Kubler A, Luna B, Larsson C, Ammerman NC, Andrade BB, Orandle M, Bock KW, Xu Z, Bagci U, Molura DJ, Marshall J, Burns J, Winglee K, Ahidjo BA, Cheung LS, Klunk M, Jain SK, Kumar NP, Babu S, Sher A, Friedland JS, Elkington PT, Bishai WR: *Mycobacterium tuberculosis* dysregulates mmp/timp balance to drive rapid cavitation and unrestrained bacterial proliferation. J Pathol 2015;235:431-444.

287   Be NA, Klinkenberg LG, Bishai WR, Karakousis PC, Jain SK: Strain-dependent cns dissemination in guinea pigs after *Mycobacterium tuberculosis* aerosol challenge. Tuberculosis (Edinb) 2011;91:386-389.

288   van Well GT, Wieland CW, Florquin S, Roord JJ, van der Poll T, van Furth AM: A new murine model to study the pathogenesis of tuberculous meningitis. J Infect Dis 2007;195:694-697.

289   FDA USA. FDA news release, 2012.

Appendix I: Publications, presentations and awards

Papers under submission

Brilha S, *et al*. α2β1-mediated adhesion of human bronchial epithelium to collagen matrix modulates TB-induced MMP-1 expression to promote epithelial wound repair.

Brilha S, Porter JC, Friedland JS. Integrin signalling regulates secretion of collagenases and stromeolysins by *Mycobacterium tuberculosis* infected monocytes.

Brilha S, Ong CWM, Friedland JS. *Mycobacterium tuberculosis* causes disruption of the blood-brain barrier with downregulation of the Hedgehog pathway.

Belton M, **Brilha S**, Manavaki R, *et al*. Hypoxia and HIF-1α-dependent MMP-1 secretion in human pulmonary tuberculosis.

Papers accepted for publication

Ong CWM, Elkington P, **Brilha S,** *et al.* Neutrophil-derived MMP-8 drives AMPK - dependent matrix destruction in human pulmonary tuberculosis.

Oral presentations in scientific meetings

Brilha S, Ong CWM, Friedland JS. *The blood-brain barrier is disrupted by matrix metalloproteinases in tuberculous meningitis*. 18th British Infection Association Scientific Meeting; London, 21/05/2015.

Brilha S, Ong CWM, Friedland JS. Matrix Metalloproteinases cause blood-brain barrier disruption in central nervous system tuberculosis. 12th International congress of Neuroimmunology; Mainz, 9-13/11/2014.

Sutre AF, Santos J, **Brilha S**, Badura R, Valadas E, Antunes F. Latent tuberculosis infection in Lisbon, Portugal. 22nd ECCMID; London 31/03-3/04/2012.

Poster presentations in scientific meetings

Brilha S, Wysoczanski R, Porter JC, Friedland JS. The Extracellular environment regulates Matrix Metalloproteinase secretion in pulmonary Tuberculosis. The British Society of Immunology Annual Congress. Brighton 1-4/12/2014

Brilha S, Porter JC, Zecchini HI, Friedland JS. Integrin alpha2beta1 modulates MMP-1 expression in Tuberculosis. 15th International Congress Immunology, Milan, 22-27/08/2013.

Brilha S, Porter JC, Zecchini HI, Friedland JS. Respiratory epithelial cell adhesion to type I collagen modulates MMP-1 expression in Tuberculosis. Imperial College London Young Scientist Day; 07/2013.

Brilha S, Friedland JS. Respiratory epithelial cell adhesion to type I collagen downregulates MMP-1 expression in TB. 3rd European Congress of Immunology; Glasgow, 5-8/09/2012.

Awards

Travel award from the British Society of Immunology for attendance of the BSI Annual Congress. Brighton, 2014.

Travel award from the European Federation of Immunological Societies for attendance of the 15th International Congress Immunology; Milan, 2013.